Dissertations   **Theses and Dissertations**

2015

The MIR-17-92 Cluster Contributes to MLL Leukemia Development Through the Repression of the Meis1 Competitor Pknox1

Yousaf Anwar Mian
Loyola University Chicago

Follow this and additional works at: https://ecommons.luc.edu/luc_diss

Part of the Molecular Biology Commons

LOYOLA UNIVERSITY CHICAGO

THE MIR-17-92 CLUSTER CONTRIBUTES TO MLL LEUKEMIA DEVELOPMENT

THROUGH THE REPRESSION OF THE MEIS1 COMPETITOR PKNOX1

A DISSERTATION SUBMITTED TO

THE FACULTY OF THE GRADUATE SCHOOL

IN CANDIDACY FOR THE DEGREE OF

DOCTOR OF PHILOSOPHY

PROGRAM IN MOLECULAR BIOLOGY

BY

YOUSAF ANWAR MIAN

CHICAGO, IL

DECEMBER 2015

ACKNOWLEDGEMENTS

I would like to thank everyone who supported and encouraged me throughout my graduate school career. First and foremost, I would like to thank my mentor, Dr. Nancy Zeleznik-Le, Ph.D., who accepted me into her lab and has taken the time to train me. Nancy's mentorship and guidance was crucial for my success in graduate school and enabled me to learn. I especially appreciate the patience and optimism that Nancy showed throughout my years in the lab and my dissertation writing process. I would further like to thank the lab members of the Zeleznik-Le lab. Laurie Risner, Noah Birch, Alyson Lokken, Sonia Brockway, Adam Marek, Shubin Zhang, and Nick Achille have been wonderful labmates and friends. They have shared their knowledge of experimental techniques, served as sounding boards for ideas, and made the lab a wonderful place to work and study.

I would additionally like to thank my dissertation committee for their comments, ideas, and expertise in this project. Dr. Manuel Diaz, M.D., Dr. Jiwang Zhang, M.D., Ph.D., Dr. Charles Hemenway, M.D., Ph.D., and Dr. Jianjun Chen, Ph.D. have provided extremely valuable insight into the design of good experiments and the scientific process. Their areas of expertise and depth of knowledge have proven critical in understanding the finer points of my project.

I would further like to thank the Molecular Biology Program and the Graduate school of Loyola University Chicago for a affording me the opportunity to study

To my family.

TABLE OF CONTENTS

LIST OF TABLES

LIST OF FIGURES

ABSTRACT

Mixed lineage leukemias have a relatively poor prognosis and arise as a result of translocations between the *MLL* gene and one of multiple partner genes. Downstream targets of MLL are aberrantly upregulated and include the developmentally important *HOX* genes and *MEIS1,* as well as multiple miRNAs, including the *miR-17-92* cluster and *miR-196b*. Here I utilize custom anti-miRNA oligonucleotides to examine the contribution of specific miRNAs to MLL leukemias both as individual miRNAs and in cooperation with other miRNAs. Combinatorial treatment with antagomirs against *miR-17* and *miR-19a* of the *miR-17-92* cluster dramatically reduces colony forming ability of MLL-fusion containing cell lines but not non-MLL AML controls.

Further, I validated *PKNOX1* as a target of both *miR-17* and *miR-19a*. MEIS1 and PKNOX1 are TALE domain proteins that participate in ternary complexes with HOX and PBX proteins. Here I examine the competitive relationship between PKNOX1 and MEIS1 in PBX-containing complex formation and determine the antagonistic role of PKNOX1 to leukemia in a murine *MLL-AF9* model. Collectively, these data implicate the *miR-17-92* cluster as part of a regulatory mechanism necessary to maintain *MEIS1/HOXA9* -mediated transformation in MLL leukemia. This approach represents a paradigm where targeting multiple non-homologous miRNAs may be utilized as a novel therapeutic regimen.

CHAPTER 1

INTRODUCTION

MLL leukemias develop as the result of a balanced translocation involving the *MLL* gene located at the 11q23 locus and one of over 70 fusion partners [1]. The resulting leukemias develop as either acute myeloid leukemia, acute lymphocytic leukemia, or a mixed lineage leukemia and have a poorer prognosis than many non-MLL leukemias [2, 3]. MLL leukemias possess a chimeric fusion protein which aberrantly upregulates expression of target genes, including *HOXA9* and *MEIS1* [4, 5]. *HOXA9* and *MEIS1* are essential for MLL leukemia [5-7]. The poorer prognosis associated with MLL leukemia gives reason to better understand it, and undertake studies to clarify the mechanisms by which it operates.

MiRNAs are small noncoding RNAs of approximately 22 nucleotides which function through repression of target mRNAs [8, 9]. Currently, over 2500 miRNAs have been identified in humans and are thought to contribute to the regulation of up to half of all transcribed genes [10]. Previous studies by our lab and others found that multiple miRNAs, including *miR-196b*, and the miRNAs of the *miR-17-92* cluster, are overexpressed in MLL leukemias relative to other acute myeloid leukemias [11, 12]. These miRNAs present an attractive target for therapeutic intervention in MLL leukemias due to their critical roles in regulation of important target genes. Recent work has been

undertaken to develop modified nucleic acids for the inhibition of miRNAs [8, 13, 14]. Antagomirs and other anti-miRNA technologies have been tested *in vitro* and *in vivo* to this effect [8, 13, 14].

This dissertation examines the role of miRNAs disregulated in MLL leukemias through two aims. My first aim is to determine the necessity of miRNAs to the development of leukemia, both individually and in combination. I hypothesized that one or more miRNA upregulated in MLL leukemia are essential to leukemia function. To examine the contribution of miRNAs to leukemia, I have inhibited miRNA function using custom oligonucleotides termed 'antagomirs.' I examined the changes in colony forming ability as a surrogate for leukemogenesis in human cell lines with MLL translocations and in *MLL-AF9* transduced murine bone marrow utilizing individual antagomir treatments. Further, I have performed colony assays in human cell lines (MOLM-13 MV4-11, RS4;11) accompanied by analysis of cell cycle and cell growth in liquid culture.

My second aim is to determine the potential downstream targets of miRNAs disregulated in MLL leukemia. I have hypothesized that miRNAs contribute to MLL leukemia through downregulation of *PKNOX1* (a.k.a. *PREP1*), a TALE domain protein closely related to the essential MLL target gene *MEIS1*. I have additionally hypothesized that miRNA mediated disruption of the balance between PKNOX1 and MEIS1 contributes to MLL leukemia. To examine the relationship between miRNA levels and *PKNOX1*, I have performed luciferase assays and have further examined the change in PKNOX1 protein levels upon antagomir treatment in human cell lines. To determine the

competitive role between PKNOX1 and MEIS1, I have further examined the role of

PKNOX1 in MLL leukemia through both colony assays and liquid culture experiments.

CHAPTER 2

LITERATURE REVIEW

MLL leukemia background

The Mixed Lineage Leukemia (*MLL*, a.k.a. *ALL-1*, *HRX*, *KMT2A*) gene is located at the chromosomal position of 11q23 and has been identified as recurrent site of chromosomal translocations in leukemia [15]. Leukemias arising from *MLL* translocations may result in either Acute Lymphoid Leukemia (ALL) or Acute Myeloid Leukemia (AML) (reviewed in [2, 3]). These leukemias may additionally be bi-phenotypic or mixed lineage leukemias, as defined by the presence of mixed surface markers (reviewed in [2, 3]).

Both ALL and AML are relatively heterogeneous as characterized by cytogenetic abnormalities, and possess numerous cytogenetic abnormalities of which MLL related leukemias represent a significant fraction. ALLs possess cytogenetic abnormalities, including t(12;21) encoding *TEL-AML1*; t(8;14), t(2;8) and t(8;22) encoding *MYC-related* translocations; t(1;19) encoding *E2A-PBX*; t(9;22) translocations encoding *BCR-ABL*; and 11q23 translocations encoding MLL rearrangements [16]. AMLs also display numerous cytogenetic abnormalities, as well as cytogenetically normal karyotypes, which account for half of all AMLs. Several commonly occurring cytogenetic abnormalities within AML produce fusion genes involving members of the core binding factor heterodimeric transcription factor complex which is comprised of AML1 (RUNX1) and

CBFB [17]. The balanced translocation t(8;21)(q22;q22) generates a chimeric protein *AML1-ETO* (*RUNX1-RUNX1T1*), while abnormalities of chromosome 16, including inv(16) (p13;q22) and t(16;16)(p13;q22) affect the core binding factor beta subunit (CBFB) [17]. The balanced translocation of t(15;17)(q22;q12) is another commonly observed cytogenetic abnormality associated with AML, encoding a fusion proteins known as PML-RARα and resulting specifically in Acute Promyelocytic Leukemia (APL) [17].

AMLs are classified according to the French-American-British (FAB) classification system, with MLL translocation leukemias predominantly resulting in M5a (Monoblastic, poorly differentiated) and M5b (Monoblastic, differentiated) leukemias, with 38.5% and 21.2%, respectively [18]. MLL leukemias further result in M4 (Myelomonocytic) leukemias (21.2%) [18]. ALL leukemias may be classified by FAB classification system (L1-L3), but are more commonly classified by immunophenotype under the World Health Organization guidelines. Within these guidelines, *MLL* rearrangements are present in both T-cell ALLs and B-cell ALLs [19].

MLL leukemias are responsible for 7-10% of all ALLs and 5-8% of all AMLs [2]. Within infant leukemias, affecting children <1 year old, MLL leukemias account for 70% of infant ALLs and 35-50% of infant AMLs [3]. Additionally, *MLL* translocations are often observed in therapy associated leukemia, which presents almost exclusively as AML, representing approximately 10% of all leukemias, often developing after treatment with Topoisomerase 2 inhibitors [3]. *MLL* rearrangements also represent approximately 3% of *de novo* leukemias [18]. Prognosis for *MLL* rearranged leukemias is poor, with 5

year overall survival rates of ~10 %, and a median survival of 9 months after diagnosis [18].

Wild-type MLL

Human *MLL* is an ortholog the Drosophila gene *Trithorax* (*Trx*) which acts in opposition the polycomb group by maintaining the expression of target genes (reviewed in [20]). The *MLL* gene encodes a 3969 amino acid (~430 kDa) multi-domain regulator of transcription encoded on chromosome band 11q23 (reviewed in [20]). Located toward the N-terminus of MLL, between amino acids 170-310, the AT-Hooks of MLL recognize cruciform DNA and facilitate the binding of the MLL complex to DNA [21]. MLL possesses a repression domain located between amino acids 1101-1400 [21]. The MLL repression domain recruits factors associated with repression of target genes, including: BMI-1 and HPC2 of the Polycomb group, the histone deacetylases HDAC1 and HDAC2, and CtBP [22]. Within the repression domain, the MLL CXXC domain is defined by eight cysteine residues which coordinate 2 zinc ions to mediate interaction with unmethylated cytosine-containing CG dinucleotides within CpG islands [23]. Previous studies by our lab have shown that the MLL CXXC domain protects unmethylated CpG islands from DNA methylation through direct binding to DNA in the promoter regions of target genes and subsequently maintains the target gene expression [24]. The MLL CXXC-DNA relationship is essential to the leukemogenic capacity of MLL fusions. Disruption of this relationship by mutations in the CXXC domain decreases colony forming ability of an *MLL-AF9* construct when transduced into murine bone marrow progenitor cells [23]. MLL additionally possesses 4 PHD (plant homeodomain) fingers

that mediate protein-protein interactions, as well as an atypical bromodomain, located between PHD fingers 3 and 4. Of the 4 PHD fingers, PHD finger 3 has been shown to bind to bind to H3K4 modified by di- and tri- methylation [25] and also the cyclophylin Cyp33 [26]. However, PHD finger 3 binding of methylated H3K4 and Cyp33 are mutually exclusive, suggesting that PHD finger 3 may function as a key regulatory domain of MLL [27]. MLL possesses an H3K4 histone methyltransferase SET (Su(var)3-9,ehanancer of zeste, trithorax) domain located at the C-terminal end [4, 28]. H3K4 methylation is associated with transcriptional activation [29]. The MLL protein domain schematic is illustrated in Figure 1.

Upon transcription and translation, the full length MLL protein is cleaved in two places by TASPASE1, a threonine aspartase protease; at amino acids 2719 and 2730, to excise a 12 amino acid polypeptide and form a 320 kDa N-terminal fragment (MLL-N) and 180 kDa C-terminal fragment (MLL-C) [30, 31]. The cleaved MLL proteins associate together in MLL-containing complexes involved in the regulation of transcription [31]. Association between MLL-N and MLL-C occurs through noncovalent binding between the FYRN and FYRC domains (FY-Rich C-terminal) and (FY-Rich N-terminal) of MLL-N and MLL-C, respectively [31].

In addition to self-association between the N- and C-terminal proteins, MLL recruits >29 additional complex components [28]. Menin (Multiple endocrine neoplasia type 1) is a DNA binding protein, originally characterized as a tumor suppressor [32]. Menin associates with the N-terminus of MLL-N, where an RXRFP interaction domain located at the amino-terminal end of MLL binds to Menin (MEN1) [33, 34]. LEDGF

(lens epithelium derived growth factor), in turn, associates with Menin [35]. C-Myb has also been shown to associate with MLL through interaction with Menin [36]. Collectively, these proteins interact with DNA in cooperation with the AT-Hooks and CXXC domain of MLL [2]. Interaction with both Menin and LEDGF are required for MLL regulation of target genes [33, 35] and loss of the N-terminal domain of MLL abrogates the leukemogenic activity of the MLL fusion protein [34].

MLL-C facilitates numerous protein-protein interactions with several additional factors to the complex, including: WDR5 [37], ASH2L [38], RBBP5 [39], and CBP [40]. ASH2L and RBBP5 dimerize and bind to the C-terminus of MLL, stabilizing the active conformation of the MLL SET domain [39]. CBP is a histone acetyltransferase that acetylates histones, among other substrates [41]. WDR5 recognizes H3K4 without discriminating between unmethylated, mono-, di-, or tri- methylation and positions the H3K4 residue for methylation by the MLL SET domain [37, 42]. WDR5 has additionally been implicated in the binding of non-coding RNA *HOTTIP* [43] in the regulation of the *HOXA* cluster (schematic of MLL complex illustrated in Figure 1).

Previous studies have characterized *Mll* function through the development of a murine hypomorphic model, which is commonly referred to as an *Mll* knockout model. *Mll (-/-)* mice are embryonic lethal and embryos display developmental defects including brachial arch dysplasia and aberrations in segmental boundaries [44, 45]. Examination of the expression of known target genes, including *Hoxa7* and *Hoxc9*, in *Mll (-/-)* embryos, implicate MLL in the maintenance, but not initiation of expression of genes. *Mll (-/-)* embryos were able to initiate expression of these target genes, but were unable to

maintain expression past 8.5-9 dpc [44]. Knockout studies additionally showed a hematopoietic phenotype, with *Mll (-/-)* embryos displaying a defect in yolk sac hematopoiesis [46].

<div align="center">**MLL fusions**</div>

MLL fusions arise as the result of chromosome translocations which result in an in-frame joining of the *MLL* gene to a partner gene. MLL fusions most often occur as a result of incorrect non-homologous end joining from double stranded DNA break repair [47]. Chromosomal breakage occurs within a defined 8.3 kb region of the *MLL* gene called the Breakpoint Cluster Region (BCR). Currently, 79 partner genes have been identified as fusion partners in MLL translocations [1]. Despite the myriad of MLL fusion partners, >85 % of MLL fusions occur with only 6 partners [1]. These most common fusion partners are AF4 (38%), AF9 (18%), ENL (13%), AF10 (8%), ELL (4%), AF6 (4%) [1]. The occurrence of fusion partners is distinctly different between MLL AMLs and MLL ALLs, with AF4 being the most common fusion partner in MLL ALL (60%) and AF9 being the most common fusion within MLL AML (29%)[1].

MLL fusion proteins are functionally distinct from wild type MLL. In MLL-fusions proteins, the AT-Hooks and the MLL CXXC domain is retained within the fusion protein. However, while wild type MLL-C recruits additional factors involved in the maintenance of expression of target genes, loss of the MLL-C and replacement with a fusion partner alters the recruitment of cofactors. Many of the resulting fusions enable the recruitment of factors including DOT1L and the super elongation complex (SEC).

DOT1L is a histone methyltransferase that targets H3K79 for methylation as an

activating chromatin mark occurring along transcriptionally active genes (reviewed in [48]). H3K79 methylation usually corresponds to transcription of associated genes [49]. MLL leukemias display aberrant H3K79 methylation along known MLL-targeted genetic regions, including the *HOXA* loci [50, 51]. DOT1L has been shown to be necessary for transformation of murine bone marrow by MLL fusions, with *Dot1l* deletion resulting in a loss of colony forming ability and an increase in apoptosis [52]. Subsequent studies have shown that selective inhibition of DOT1L catalytic function effectively blocks H3K79 methylation and inhibits proliferation and promotes apoptosis and differentiation of MLL rearranged cell lines [53].

Both MLL and MLL fusions recruit the RNA Polymerase 2- interacting Polymerase Associated Factor complex (PAFc) through interaction between MLL repression domain and the PAFc subunit PAF1 [54]. Interaction with the PAF complex is required for proper recruitment of MLL to the *Hoxa9* locus and the transformation by MLL fusions [54]. Several common fusion partners are components the super elongating complex (SEC) that enables transcriptional elongation by releasing RNA Polymerase 2 from transcriptional pausing at the transcriptional elongation control checkpoint (TECC). (Function of SEC extensively reviewed in [55-57]). The SEC is comprised of several subunits, including: AF9 (ALL1 fused gene from chromosome 9) or its homolog ENL (eleven nineteen leukemia), ELL (eleven nineteen Lys-rich leukemia) family protein, AFF1/4, EAF1/2, and the kinase P-TEFb (Pol 2 transcription elongation factor comprised of cyclin T1 or T2 and Cdk9) [57]. Of these complex components, several are MLL fusion partners, including: AF4, AF9, AF10, ENL, and ELL [1, 3]. Functionally, P-TEFb

Figure 1. MLL domains and complexes
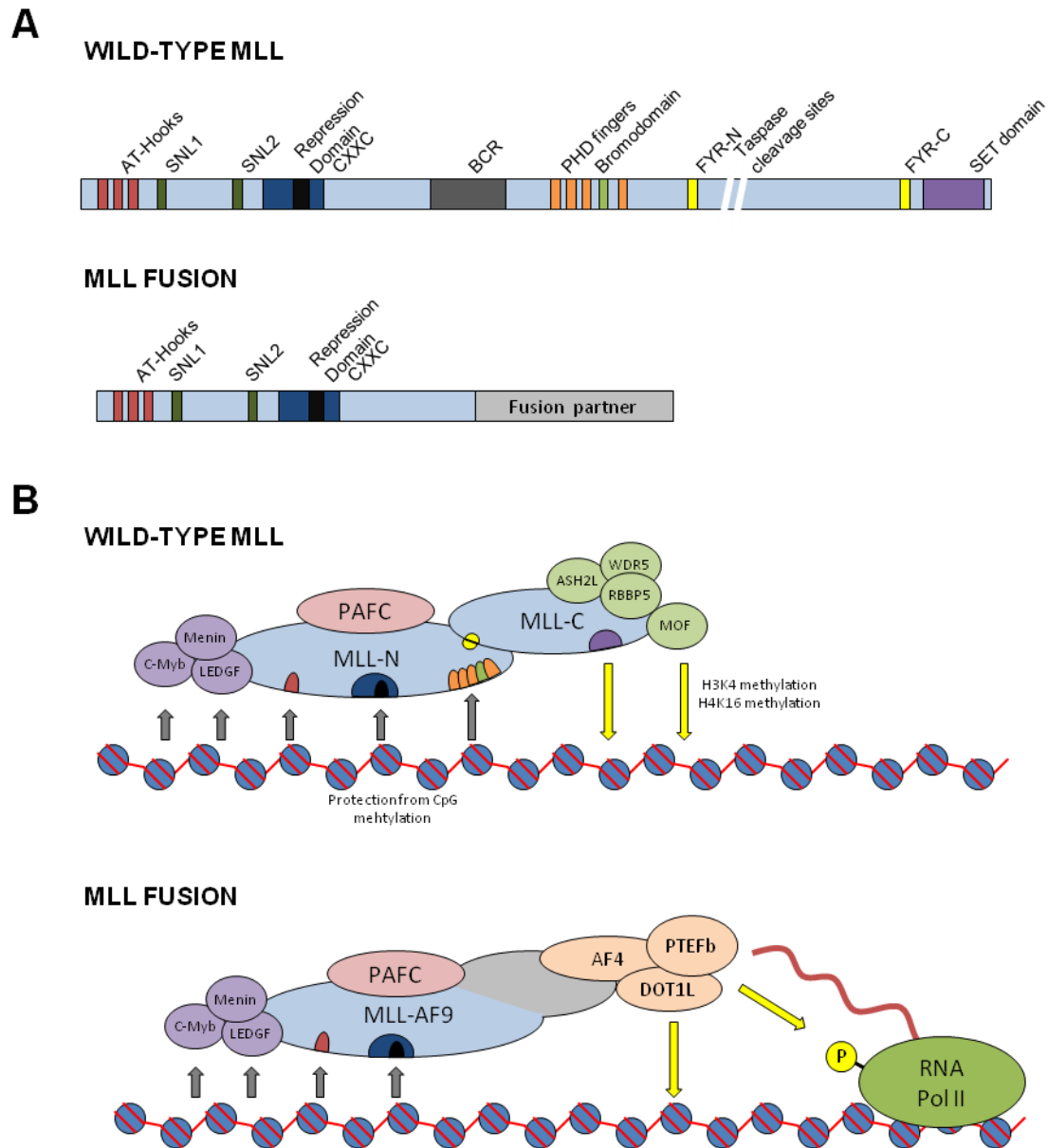
A) Schematic depiction of MLL protein domains for both wild-type MLL (top) and MLL fusion (bottom) proteins. Adapted from Krivstov *et al*. [58]. B) Cartoon depiction of MLL interaction with proteins and chromatin for wild-type MLL (top) and MLL fusion (bottom). Adapted from Krivstov *et al*.[58] and Slany et al. [3].

phosphorylates RNA Polymerase 2 at serine 2, which allows release of RNA Pol 2 from a pause site [55] (schematic illustrated in Figure 1).

Additional, but less frequent fusions have been documented which include fusion partners that facilitate dimerization of MLL fusion proteins, including AF1p and GAS7 [59]. These fusion partners are cytoplasmic proteins that possess homo-oligomerizing coiled-coiled domains which are sufficient to allow for leukemic transformation by these MLL fusion proteins [59]. Examination of a pharmacologically dimerizable MLL, MLL-FKBP, indicates that MLL amino-terminal dimers bind to the CpG islands of the *Hoxa9* locus and upregulate critical MLL target genes including *Hoxa7*, *Hoxa9*, and *Mies1* [60]. In addition to chromosomal translocations, MLL also undergoes partial tandem duplications (*MLL* PTD) accounting for 4% of MLL leukemias [1]. *MLL* PTDs contain duplication of exons 5-11, allowing for MLL to dimerize and subsequently misregulate target genes [58].

MLL target genes

Several studies have sought to define the genes targeted by MLL and MLL fusions by examining the global disregulation of genes in MLL fusion leukemias [61-65]. Examination of MLL occupancy sites indicates that MLL associates with RNA Polymerase 2 across the entire gene for a subset of transcriptionally active target genes, and dissociates upon downregulation, consistent with MLL's function in transcriptional maintenance [61]. Armstrong *et al.* examined the gene expression signature of MLL leukemia patients compared to non-MLL ALL and AML leukemias [62]. They found that MLL leukemias regulated a gene set distinct from either ALL or AML that was rich

with highly expressed *HOX* genes [62]. Examination of the binding of MLL-ENL and comparison of MLL-ENL binding with MLL wild-type binding, indicates that MLL fusions bind to a subset genes regulated by wild type MLL [63]. MLL-ENL bound to 223 genes with significant increase in mRNA expression of 12 genes, including *Hoxa9* and *Meis1* [63]. A separate study performed by Li *et al.* examined the deregulation of genes in leukemias possessing *MLL-ENL* and *MLL-ELL* translocation [64]. 88 genes were found to be disregulated in both human and murine leukemia models, including *Hox* genes and the *miR-17-92* cluster [64]. Critically, changes in gene expression were conserved between human and mouse [64]. Collectively, these studies corroborate earlier findings that MLL functions to maintain gene expression, particularly at *Hox* genes. However, they also implicate MLL in the maintenance of expression of other target genes including the *miR-17-92* cluster.

HOX genes

HOX genes are the most well studied downstream targets of MLL. MLL and MLL fusions directly regulate posterior *HOX* genes, as well as the HOX partner MEIS1, resulting in an aberrant maintenance of the expression in MLL leukemias [4, 5]. Both *HOXA9* and *MEIS1* and direct downstream targets of MLL [4, 5]. Previous studies have shown that *HOXA9* is essential to the development of MLL leukemias [5-7]. *Hoxa9* deficient murine bone marrow cells cannot be transformed with MLL fusions *in vitro* [6], while depletion of *HOXA9* in human cell lines harboring *MLL* translocations blocks proliferation and induces apoptosis [7].

HOX genes encode transcription factors critical to body patterning, development,

and hematopoiesis [66]. Mammals possess 39 *HOX* genes organized in 4 paralogous clusters (*HOXA – HOXD*) at 4 different genetic loci, with *HOXA*, *HOXB*, *HOXC*, and *HOXD* located on 7p15, 12q21, 12q13, and 2q31, respectively (reviewed in [67]). Each cluster is similarly organized with the lower numbered *HOX* genes located towards the 3' end of the cluster and higher numbered *HOX* genes located at the 5' end. *HOX* genes are illustrated in Figure 2. *HOX* gene expression is important for determining the spatial identity and segmentation in development, with *HOX* genes expressed collinearly from lower to higher number along the anterior-posterior axis, with the lower numbered *HOX* genes expressed toward the anterior and the higher numbered *HOX* genes expressed towards the posterior (reviewed in [67, 68]). Temporal control of *HOX* gene expression is also controlled collinearly with lower numbered *HOX* genes being expressed earlier in development than their higher numbered counterparts (reviewed in [67, 68]). Disregulation and mutation of *HOX* genes results in limb malformations and developmental diseases, including cancers (reviewed in [67]). Critical to understanding the development of AML, the *NUP98-HOXA9* fusion drives AML development [69]. Further, a study of 6817 genes in acute leukemia identified *HOXA9* expression as a negative prognostic indicator for AML [70].

HOX proteins contain a 60 amino acid homeodomain consisting of 3 alpha helices, with DNA helix 3 contacting DNA [67]. The homeodomain interacts with target DNA sequences through the DNA helix 3. HOX proteins additionally possess a short amino acid sequence (YPWM) which interacts with the homeodomain of a PBX partner gene [71].

Figure 2. *HOX* gene clusters
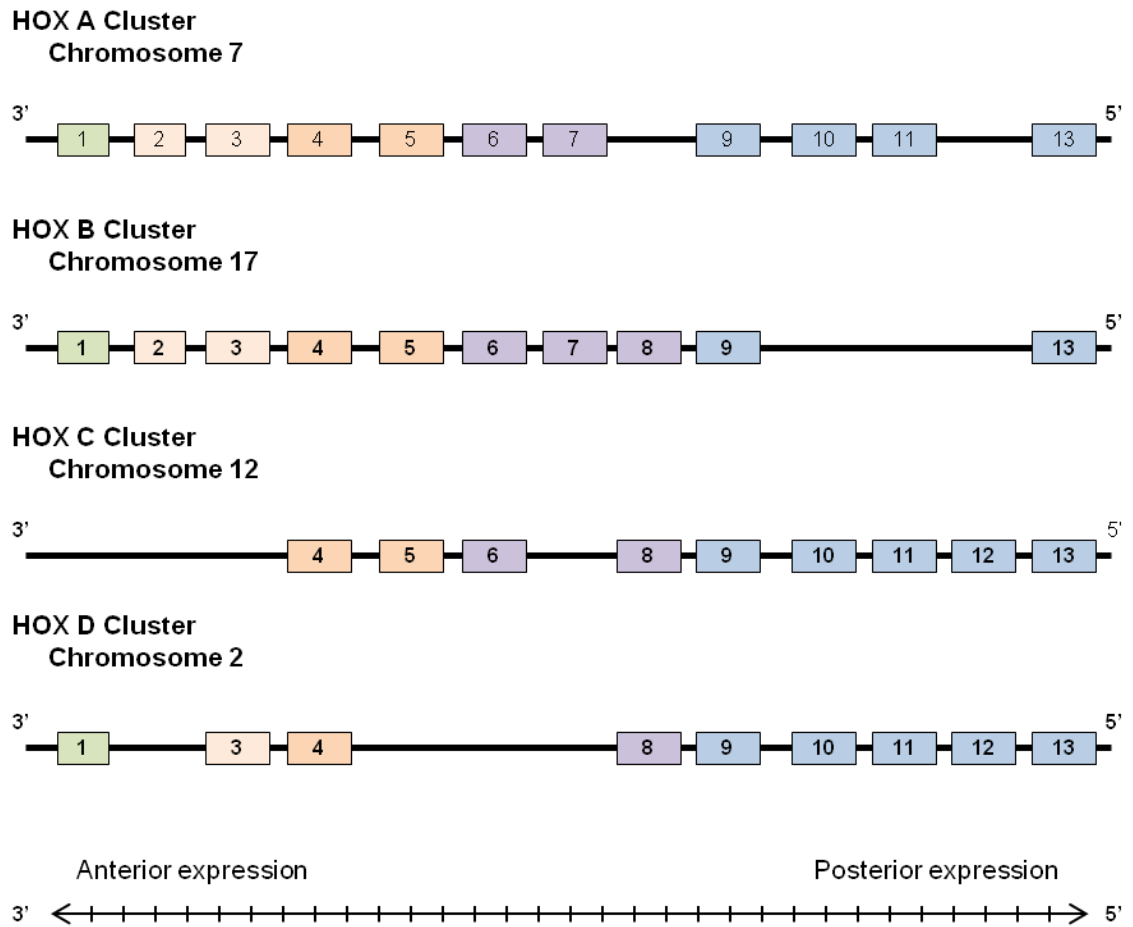
Schematic depiction of *HOX* gene clusters in human. *HOX* genes are organized into 4 paralogous clusters lettered A-D. *HOX* gene expression occurs in a co-linear fashion with Anterior expression occurring from *HOX* genes located towards the 3' end of the *HOX* clusters and posterior expression occurring from *HOX* genes located towards the 5' end of the *HOX* clusters. Adapted from Argiropoulos and Humphries [66].

HOX-TALE complexes

HOX proteins function in complexes formed with TALE domain containing partner proteins, primarily MEIS proteins, PBX proteins, PKNOX (PREP) proteins. The TALE (Three Amino acid Loop Extension) family of proteins were identified and characterized as having an atypical homeodomain with 3 amino acids positioned between the first and second helices of the homeodomain [72, 73]. This TALE possessing homeodomain is highly conserved and present in all family members and subfamilies of the larger TALE family [72, 73]. The TALE family is subdivided into the several families, including: PBC, MEINOX, IRO, TGIF, and MKX families [72, 73]. MEINOX and PBC family members are critical cofactors of HOX genes in leukemia.

The PBC family consists of the 4 PBX homologs (PBX1, PBX2, PBX3, PBX4) in both mouse and human [72]. Additional functional forms of PBX are formed by splice variants of PBX1 (PBX1A, PBX1B) and PBX3 (PBX3A, PBX3B) (reviewed in [74]). Common to all members of the TALE family of proteins, the PBC family possesses and homeodomain with a three amino acid loop extension. PBC family members additionally possess a "bipartite" PBC domain divided into PBC-A and PBC-B, N-terminal to the homeodomain, which function in protein-protein interactions (reviewed in [74]). High conservation is observed in both the homeodomain and the PBC domains.

The MEINOX family (originally categorized as the MEIS family) consists of 3 MEIS proteins (MEIS1, MEIS2, MEIS3) and 2 PKNOX proteins (PKNOX1, PKNOX2) in both human and mouse [72, 73]. Members of the MEINOX family possess the TALE domain containing homeodomain which is highly conserved between MEIS and PKNOX

subfamilies [72, 73]. Additionally, both MEIS and PKNOX families share high homology in the bipartite MEIS domain, consisting of a MEIS-A and MEIS-B and utilized for protein-protein interactions (reviewed in [74]). However, there is divergence in the presence or absence of nuclear localization signals, as well as the C-terminal region [74].

While *HOXA9* and *MEIS1* are often discussed as the critical downstream effectors of MLL leukemias and are used to generate AML independently of MLL involvement, these proteins are able to participate in a diverse combination of protein complexes. MEINOX proteins are capable of forming binary MEINOX-PBX complexes through interaction of the MEIS-A and MEIS-B domains of MEIS1/PKNOX1 with the PBC-A and PBC-B of PBX partners [75, 76]. MEINOX-PBX complexes form in the presence or absence of DNA, indicating that interaction is not DNA dependent [75]. This interaction does not occlude or otherwise interfere with the PBX component's homeodomain. In addition to interactions with MEINOX family proteins, PBX proteins are capable of forming stable HOX-PBX dimers with HOX protein partners (reviewed in [71]). HOX-PBX interactions are mediated by the Tryptophan of the HOX protein's YPWM motif binding to the homeodomain of the PBX partner (reviewed in [71]). Notably, HOX-PBX interactions do not utilized the PBC-A or PBC-B domains required in PBX-MEINOX interactions.

Numerous studies document the formation of ternary complexes containing a HOX component, a MEINOX component, and a PBC component [77-81]. HOX-PBX-MEIS protein complexes may contain PKNOX1 (also known as PREP1) as an alternative

to MEIS1 as protein-protein interactions within the ternary complexes are mediated through MEINOX-PBX interaction [82]. PKNOX1 and MEIS1 are highly homologous in the domains required for both PBX interaction and DNA binding and interact with the same surface on PBX1 [76].

AbdB-like HOX proteins, encoding HOX9-13, are uniquely capable of directly interacting with MEIS1 [83-85]. This interaction is not conserved across the MEINOX family as it requires residues located within the C-terminal domain of MEIS1 that are not conserved in PKONX1 [84]. Thus, only MEIS1, and not PKNOX proteins, directly bind to with HOX partners. TALE domain complexes are illustrated in Figure 3.

Functional roles of TALE proteins

While numerous studies have utilized PBX1 to study the protein-protein interactions of the PBX family of proteins, an increasing body of evidence has implicated PBX3 as the critical PBX protein in MLL leukemia. Recently, *PBX3* upregulation has been identified as part of a 4 gene signature associated with poorer prognosis in MLL leukemias [86]. Though *PBX3* is highly upregulated, its homologs, *PBX1* and *PBX2*, are down regulated [87]. Functionally, inhibition of the PBX-HOX interaction through an 18-mer peptide in cell lines harboring MLL-related translocations results in decreased proliferation and apoptosis [87].

Meis1 was initially identified as a viral insertion site in BHX2 mice in the development of leukemia [88]. The gene for human *MEIS1* was cloned and identified as a homoebox-containing gene located at chromosome 2p13-p14 [89]. Along with *HOXA7* and *HOXA9*, *MEIS1* overexpression was implicated in the development of AML [90].

Figure 3. TALE domain proteins and complexes
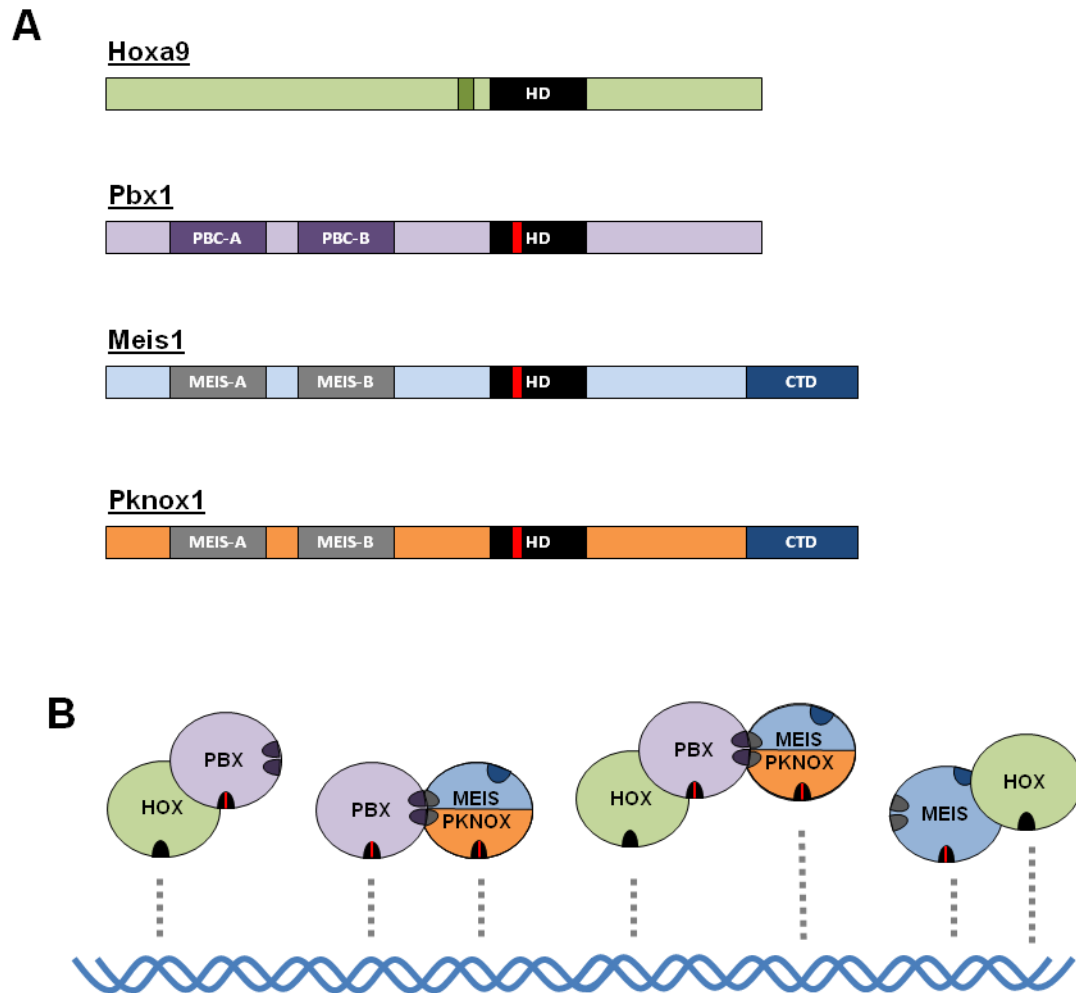
A) Schematic depiction of HOX protein families. HOX family members are depicted in green. PBX family members are depicted in purple. MEIS1 is depicted in blue. PKNOX1 is depicted in orange. Homeodomains are shown in black, while TALE domains are shown with a red stripe located within the Homeodomain. PBC domains are shown in dark purple, while MEIS domains are shown in gray. Adapted from Ladam, *et al.* [71] Longobardi, *et al.* [74] B) Cartoon depiction of different HOX-TALE complexes and their DNA interactions. Coloring of proteins and protein domains are matched to schematics in panel A.

Numerous studies have indicated that *Meis1* is essential to the development of MLL leukemia. In fetal liver cells, *Meis1 (-/-)* cells are incapable of serial replating ability after transformation with *MLL* fusion-expressing retrovirus [91]. Moreover, the level of *Meis1* expression correlates to the latency of leukemia development in murine models [91]. Knockdown of *Meis1* using a lentiviral shRNA results in a decrease in proliferation and an increase in survival *in vivo* [92].

The leukemogenic capacity of *Meis1* requires several domains to generate leukemia when infected into murine bone marrow along with *Hoxa9*. Meis1 oncogenic activity requires both the Pbx interacting motif and the C-terminal region [93]. Specific deletion of the C-terminal domain in Meis1 ablates transforming capacity of Meis1, while replacement with a strongly activating VP16 activation domain allows Meis1 to retain leukemogenic capabilities [94]. The retention of leukemogenic capability in a chimeric *Meis1-VP16* mutant indicates that *Meis1* generates leukemia through activation of target genes. The oncogenic activity of Meis1 is located in the C-terminal domain which differs from that of Pknox1 [93-95]. *Meis1* cooperates with *Hoxa9* in transformation*; whereas* co-expression of *Pknox1* with *Hoxa9* lacks this effect [94]. However, chimeric Pknox1 proteins which replace the Pknox1 C-terminal domain with the Meis1 C-terminus can restore acceleration of leukemia development [94].

The MEIS1 C-terminal domain is responsible for numerous protein-protein interactions including interaction with HOX proteins in binary complexes. Several lines of evidence, however, implicate ternary complexes as the critical leukemogenic complexes. Deletion of the Pbx-interacting domains of Meis1 abrogated its leukemogenic

potential when co-infected with a *Hoxa9*-expressing virus [93]. *PBX3* is upregulated in MLL leukemia and disruption of the HOX-PBX interaction through a small peptide inhibitor promoted apoptosis and decreased expression of known HOX-MEIS targets in an MLL leukemia cell line [87]. Collectively, these findings suggest that HOX-MEIS activity requires PBX participation in a ternary complex.

Numerous HOXA9-MEIS1 target genes have been identified. Most prominently, MEIS1 regulates FMS-like tyrosine kinase 3 (*FLT3)* in AML [93]. *FLT3* encodes a receptor tyrosine kinase expressed in hematopoietic stem and progenitor cells whose signaling pathway regulates proliferation, apoptosis, and differentiation (FLT3 function reviewed in [96]. Activating mutations, such as *FLT3* internal tandem duplications have been identified as a causative genetic lesion in cytogenetically normal AML. Within infant MLL leukemias *FLT3* expression is often elevated and corresponds to a worse prognosis. However, transduction of murine bone marrow with *Meis1* and *Hoxa9* generates leukemia in both *Flt3 (+/+)* and *Flt3 (-/-)* cells, indicating that *Flt3* is dispensable for the *Meis1-Hoxa9* viral overexpression-generated leukemia [97].

c-Myb was additionally identified as a target for upregulation by Hoxa9-Meis leukemogenesis after being identified in an array analyzing genetic disregulation of *Hoxa9-Meis1* transformed murine bone marrow [98]. Inhibition of *c-Myb* through either a dominant negative mutant or siRNA ablated the leukemogenic capability of *MLL-ENL*, indicating that *c-Myb* function is essential for *MLL* transformation [98]. Subsequent studies showed c-Myb directly interacts with MLL complexes through binding to Menin, suggesting a regulatory feedback mechanism whereby *Hoxa9-Meis1* activity influences

MLL complex composition.

Additional documented HoxA9-Meis1 targets include: *gata1* [99], *Trib2* [100], *Ccl* [100], and *cyclin D3* [101]. An Illumina-based ChIP-Seq examination of Hoxa9 and Meis1 binding sites indicated that Hoxa9 and/or Meis1 bind to 825 genomic regions, with approximately 200 genomic regions bound by both [102]. Hoxa9 binding is enriched at enhancers, and coincides with binding by additional lineage restricted transcription factors including PU.1, C/EBP, CREB, STAT, and RUNX1 [102].

PKNOX1 (also known as PREP1) was identified as a homeodomain containing protein and the gene subsequently localized to the human chromosome 21q22.3 and mouse chromosome 17B/C [103, 104]. Pknox1 was initially characterized as a Pbx binding partner [105]. Functional characterization of Pknox1 indicated that it is a binding partner of Pbx1 in both the presence and absence of DNA [106, 107]. Upon binding to DNA, Pknox1 contributes to the specificity of complex binding through recognition of a TGACAG motif [107]. *Pknox1* expression correlates inversely with *Meis1* expression during mouse hematopoiesis, as indicated in publicly available datasets (Figure 4). *Pknox1* is expressed at low levels in more immature cells and increases in expression during differentiation, while *Meis1* expression is highest in immature cells and decreases during differentiation.

Deletion of *Pknox1* in a mouse is embryonic lethal early in development (day 7.5) (Blasi lab, unpublished, discussed in [108]). A hypomorphic *Pknox1* mutation, generated by an insertion into the 5' UTR of the *Pknox1* transcript results in decreases in *Pknox1* mRNA and protein levels, with *Pknox1 (i/i)* mutants expressing <10% relative to wt.

Hypomorphic *Pknox1* mutants display high rates of embryonic lethality with deaths occurring between 17.5 dpc and birth. Embryos exhibited multiple developmental defects, including reduced angiogenesis, eye development abnormalities, and severe anemia [108]. Mice which survive to birth exhibit T-cell developmental defects and develop lymphomas [109]. Further, a decrease in Pbx1 and Meis1 levels were observed in a *Pknox1* hypomorph, attributed to a loss of stabilizing effect that derived from interaction with Pknox1 [108]. The stabilization effect of Pknox1 on partner proteins may be governed with the nuclear import [110] .

Further characterization of *Pknox1* hypomorphic mutants in an *Eµ-myc* model of lymphomagenesis implicate *Pknox1* as a tumor suppressor [109]. Loss of Pknox1 in cells homozygous for a hypomorphic mutation *Pknox1 (i/i)* or heterozygous for a knockout *Pknox1(+/-)* result in an increase in tumor volume, an acceleration of lymphoma development, and decreased survival [109].

Pknox1 and Meis1 are highly homologous in their homeodomains and their Pbx interacting motifs, but do not share much homology in the C-terminus [94]. Chimeric Pknox1 proteins with the Meis1 C-terminus appended to the C-terminus of Pknox1 are able to generate leukemia when transfected into murine bone marrow, along with Hoxa9 [94]. Further, chimeric Pknox1-VP16 mutants are similarly able to generate leukemia [94]. These studies suggest that the C-terminus of Pknox1 lacks the gene activating capabilities of Meis1. Recent ChIP-seq analysis of Meis1, Pknox1, and Pbx1/2/3 occupancies performed during murine embryo development in conjunction with analysis of gene expression have further suggested that Pknox1- and Meis1-containing complexes

Figure 4. *Pknox1* and *Meis1* expression during hematopoiesis
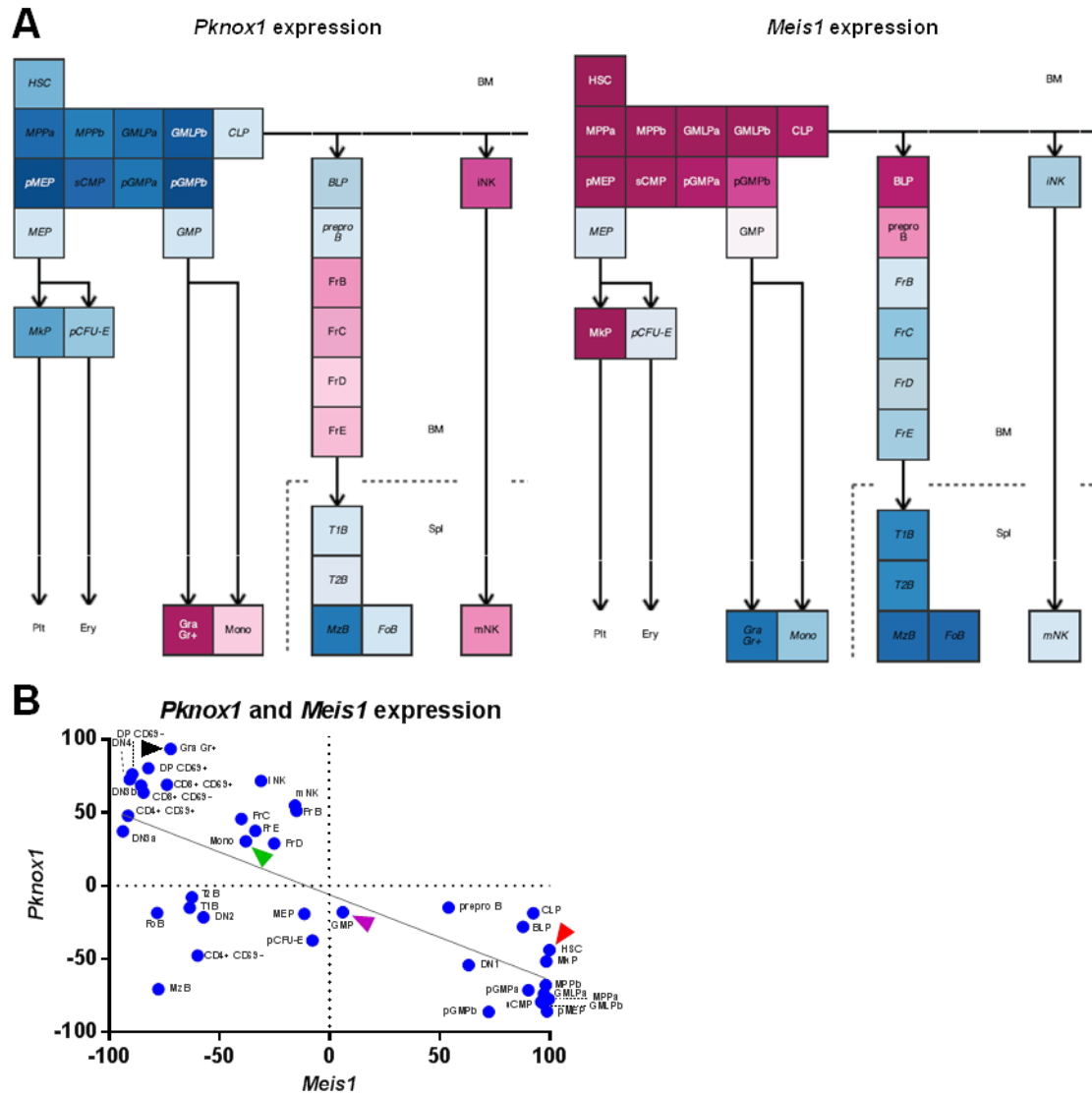
A) mRNA expression patterns from compiled microarray studies in mouse hematopoiesis for *Pknox1* (left) and *Meis1* (right) as depicted by GEXC database indicating mRNA upregulation (red) or downregulation (blue). B) Normalized values for *Pknox1* and *Meis1* expression levels from panel A in mouse hematopoiesis. All stages in differentiation indicated with blue dots. Arrows indicate HSC (red), GMP (purple), Granulocyte (black), and Monocyte (green).

often have antagonistic roles in the regulation of common target genes [111]. Both

Pknox1 and Meis1 are capable of interacting with Pbx proteins or in Hox-Meinox-Pbx

ternary complexes. ChIP-seq data characterizing the occupancies of Meis, Pbx1/2/3, and

Pknox1 in murine embryonic development indicate the diversity of co-occupancies of

TALE domain proteins *in vitro* [111]. Intriguingly, these studies have found that while

both Meis1 and Pknox1 can participate in ternary complexes *in vitro*, co-occupancies of

Meis1 and Pknox1 do not equally coincide with other complex components (e.g. Hoxc9

and/or Pbx1/2/3). Meis1 peaks often coincide with Hox peaks in the absence of Pbx1,

while Pknox1 peaks coincide with Pbx1 in the absence of Meis1 [111]. Consistent with

previous biochemical studies, this indicates that Meis1 may interact directly with Hox

partners. However, Meinox-Pbx dimers were primarily comprised of Pknox1 bound to a

Pbx component.

Recently, additional studies performed by the Blasi group published 2 papers

clarifying the competitive role of Pknox1 and Meis1 in Hox-Meinox-Pbx complexes in a

mouse model. In examining the colony forming ability of mouse embryonic fibroblasts

(MEFs), they found that *Meis1* transforms in a *Pknox1 (i/i)* background, while exogenous

expression of *Pknox1* ablates *Meis1*-mediated transformation [112]. Further, Pknox1

indirectly regulates the stability of Meis1 through binding to Pbx1, as unbound Meis1 is

degraded [112]. Examination of the Pknox1 - Meis1 relationship in bone marrow cells

indicates that *Pknox1* functions as a tumor suppressor in hematopoietic cells [113].

Exogenous over expression of *Pknox1* inhibits the capability of *Hoxa9* and *Meis1* to

transform hematopoietic stem cells; *Hoxa9* and *Meis1* transformation is accelerated in a

Pknox1 (i/i) background [113]. These studies, however, do not address the competitive

relationship of PKNOX1 and MEIS1 in an MLL leukemia model.

miRNA Biogenesis and function

MiRNAs are small non-coding RNAs (~22 nt) that post-transcriptionally

downregulate the expression of mRNA targets and are among the many genes regulated

by MLL (reviewed in [8, 9]). miRNAs were initially identified and characterized in *C.*

elegans with the discovery of *lin-4* [114]. While *lin-4* has no homologs in human or

mouse, subsequent studies identified *let-7*, a gene regulating the developmental timing of

the *C.elegans* L4/Adult switch by down-regulating the developmental timing switch *lin-*

41 [115]. *Let-7* is conserved in human and mouse [116]. According to the most recent

catalog of miRNAs, miRBase 21, as predicted by deep sequencing, 2588 miRNAs are

known to exist in human and 1915 are known in mouse [10].

miRNAs are located in genomically fragile hot-spots that are often subject to

DNA damage [117]. More than 50% of miRNAs are located in polycistronic clusters

where a single transcript gives rise to more than one mature miRNA [117]. miRNAs

arise from a diverse array of primary-miRNA transcripts. Most miRNAs arise from

capped and poly-adenylated primary-miRNA transcripts transcribed by RNA Polymerase

2 [118]. However, several studies have shown the production of miRNAs from

transcripts transcribed by RNA Polymerase 3 [119]. MiRNAs may arise from either

exonic or intronic sequences of both coding and non-coding RNAs, as well as 3' UTRs

[120, 121].

Mature miRNAs are generated through sequential processing events. Within the

primary-miRNA transcript, the miRNAs form thermodynamically stable hairpins of ~70 nt that are cleaved within the nucleus by DROSHA, a type III RNAse, with assistance from the RNA binding protein DGCR8/PASHA, which guides the positioning of the RNAse onto the pri-miRNA [122-124]. The resulting hairpin, designated as a pre-miRNA, is subsequently exported to the cytoplasm by Exportin-5, a RAN-GTPase nuclear exporting protein [125]. The pre-miRNA is loaded onto Dicer, which cleaves the hairpin into 2 strands of ~22 nt, leaving 2 nucleotide overhangs at the ends of each strand to produce a mature miRNA duplex [126].

The mature miRNA duplex is loaded into an Argonaute containing complex, consisting of Dicer, TRBP, and an Argonaute component [127]. Humans possess four argonaute genes (AGO1/2/3/4), which are defined by common domains including a PAZ and PIWI domains [128]. Together, these domains form a "bilobal" structure engaged in binding to both the miRNA and the target mRNA. For each mature miRNA duplex, only one strand is incorporated as a miRNA into the RISC complex while the opposite strand is rapidly degraded, with strand selection being determined by the stability of the cleaved 5' end of each strand of the miRNA duplex [129, 130]. The Argonaute component additionally associates with GW182 to form the core of the RISC complex.

The most critical nucleotides of the mature miRNA are nucleotides 2-7, which are termed the "seed region" of the miRNA [131]. These nucleotides must be complementary to the target mRNA, with some exceptions allowing for G:U wobble, in order for the RISC-miRNA complex to effectively downregulate the target mRNA [132, 133]. Within the RISC complex, the miRNA is situated within the complex so that the

miRNA seed region is projected outward toward the targeted mRNA [134]. The RISC complex then scans target mRNAs for complementarity, with miRNA targeting focused on the 3' UTR of the target mRNA. Perfectly matched miRNA:mRNA pairing results in a cleavage event in Argonaute 2-containing complexes whereby the target mRNA is cleaved opposite the miRNA by the "slicer" activity present in Ago2 [135]. In both perfectly matched and imperfectly matched pairings, the RISC complex recruits additional factors to the mRNA to de-cap and degrade the mRNA transcript [136]. In this manner, all targeted mRNAs are reduced upon recognition and binding by miRNA containing RISC complexes. miRNA mediated degradation of target mRNAs occurs in the cytoplasm within subcellular structures known as P-Bodies (aka GW bodies) which consist of miRISC complexes and decapping and deadenylation factors [137].

Recognition of the target mRNA is primarily mediated by the 'seed' region of the miRNA [131], and may be predicted using computer matching algorithms that seek to identify complementarities between the miRNA and target mRNA (review of target prediction algorithms in [132, 133, 138]). Numerous publicly available algorithms have been developed, including (but not limited to): TargetScan [131], MiRanda [139], Diana-microT [140], RNA22 [141], and miRWalk [142]. While most miRNA target prediction algorithms require a match between the seed region and the putative target mRNA [138], targeting models require different spans of matching complementarity within the seed region and several allow for a less stringent matching with a G:U wobble in the seed region [132]. miRNA biogenesis is illustrated in Figure 5.

Figure 5. miRNA biogenesis
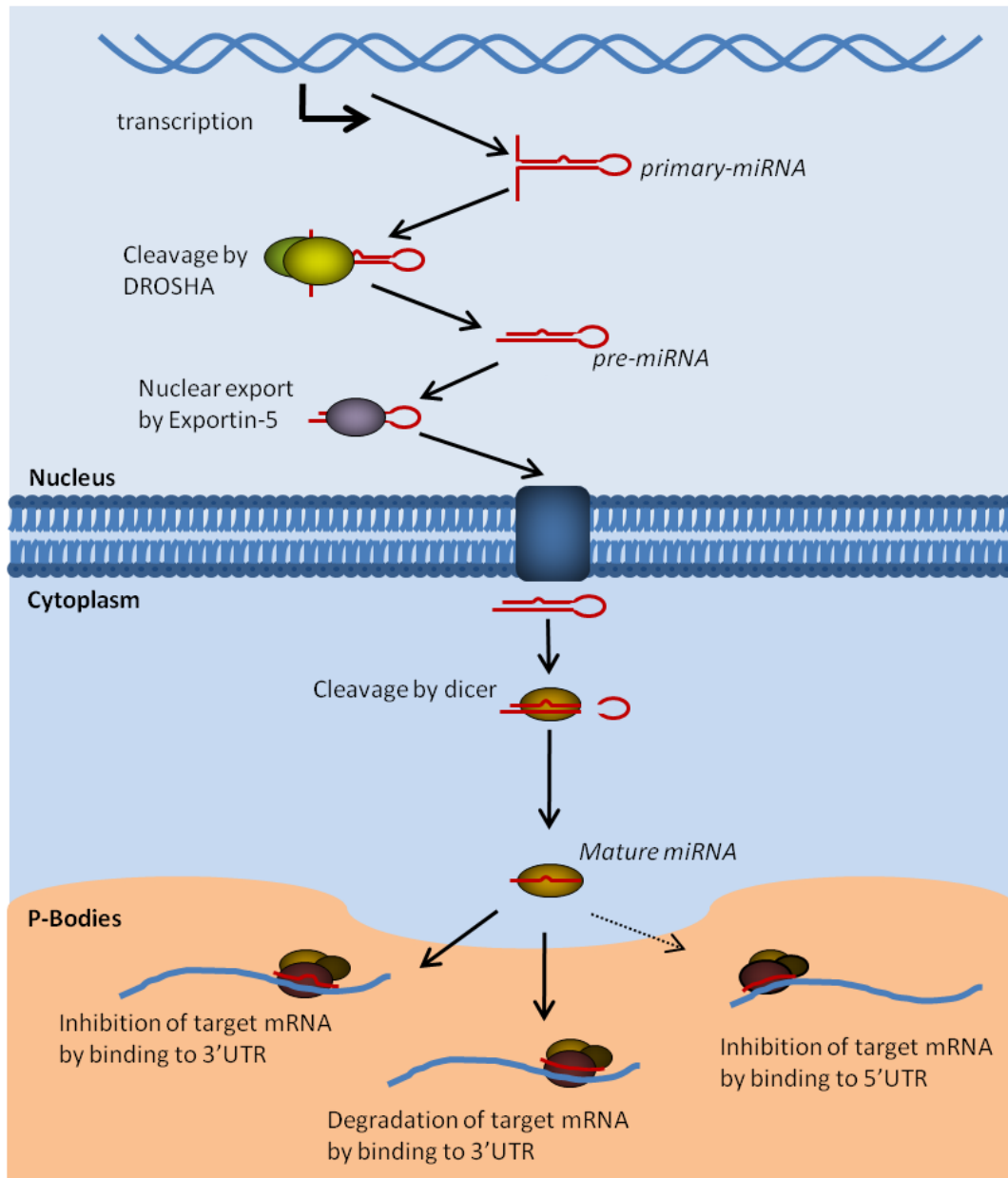
Canonical miRNA biogenesis pathway. miRNAs are generated as a result of transcription by RNA Polymerase and sequential cleavage steps. Mature miRNAs are incorporated into a RISC complex. Adapted from Mian and Zeleznik-Le [8].

Further advances in the understanding of miRNA will likely change the targeting prediction for miRNAs, and our understanding of miRNA function. It has been accepted that miRNAs may target the 5'UTR of mRNA target transcripts as well as the 3'UTR for downregulation by the RISC complex [143]. Meanwhile several groups have explored alternate novel mechanisms of miRNA activity such as miRNA upregulation of target transcripts, whereby miRNA binding to the target mRNA may occlude a binding site targeted by a repressive factor and thereby protect the transcript from downregulation. The primary example of this form of regulation is the relationship between *miR-10* and TOP motifs [144]. Additionally, a bioinformatic analysis of miRNA binding has suggested that miRNA may simultaneously bind to both the 5'UTR and 3'UTR of a target mRNA [145]. However, this phenomenon has yet to be functionally demonstrated, and may be impeded by steric hindrance. Examination of miRNA:mRNA through RISC-complex pulldowns, coupled with target mRNA sequencing (HITS-CLIP) has been used to document the interactions of miRNAs in neuronal cells. Strikingly, this study found many instances of miRNA:mRNA interaction in the absence of matched seed region[146]. Further study is required to fully examine the functional interaction of miRNAs with targeted transcripts.

In addition to dysregulation of specific miRNAs, the miRNA biogenesis pathway has been implicated as a potential target of dysregulation in various cancer models. Schmittgen *et al.* found that downregulation of Dicer occurred in a several cancer models, resulting in global miRNA downregulation [147].

miRNA disregulation in leukemia

MiRNA dysregulation has been implicated in numerous forms of cancer, including leukemia. Considerable effort has been applied toward discerning the disregulation of miRNAs within leukemias to determine how miRNA disregulation corresponds to lineage, cytogenetic abnormality, and clinical prognosis (reviewed in [8]). Further effort has been applied to discerning the signature of miRNA disregulation within leukemias (illustrated Table 1).

Acute leukemias are divided into lymphoid and myeloid lineages, with different gene expression patterns. To examine the potential difference in miRNA expression between lineages, a study by the Chen group examined the miRNA expression between ALL and AML leukemias with common cytogenetic abnormalities including MLL related translocations in both the AML and ALL subsets, and identified 27 miRNAs differentially expressed between AML and ALL [148]. The 4 most discriminatory were: *miR-128a* and *miR-128b* upregulated in ALL and *let-7* and *miR-223* downregulated in ALL. Interestingly, MLL related leukemias clustered with their lymphoid or myeloid counterparts, and not together. Several AMLs and ALLs with the same MLL-ENL translocation clustered with their lymphoid and myeloid counterparts, suggesting that these miRNAs are regulated by factors other than MLL.

Further examination of the miRNA expression differences between ALL and AML, were performed using 85 leukemia patient samples with either ALL or AML and identified a signature of 16 miRNAs differentially expressed between ALL and AML [149]. This signature identified 9 miRNAs upregulated (*miR-128a*, *miR-128b*, *miR-155*,

miR-146a, *miR-150*, *miR-17*, *miR-20a*, *miR-29a/c*, and *miR-29b*) and 7 miRNAs

downregulated (*miR-223*, *miR-196b*, *miR-221, miR-222*, *miR-23a*, *miR-27a/b*, and *let-7*)

in ALL relative to AML. This study also identified miRNAs whose expression positively

or negatively correlated with overall survival for ALL (*miR-221* was associated with

improved survival, while *miR-146a*, *miR-181a/c* were associated with poorer survival)

and AML patients (*miR-25* was associated with improved survival, while *miR-26*, *miR-29b*, *miR-146a*, and *miR-196b* were associated with poorer survival).

Numerous studies have examined the expression of miRNAs in both ALL and

AML, looking for patterns of miRNA dysregulation corresponding to molecular subtype

and prognosis. Studies of miRNA dysregulation in ALL have examined the differential

expression of miRNAs within ALL, including those harboring MLL translocations. One

study performed by Zanette *et al.* examined the miRNA expression profiles of

lymphocytic leukemias utilizing a Taqman system designed to asses miRNA levels for

164 commonly expressed miRNAs [150]. ALL samples were pooled and compared to

both B-CLL and CD19+ B-Cells. Pooled ALL samples identified a miRNA signature

differentiating ALL from CD19+ B-Cells. The 5 most highly upregulated miRNAs were

miR-128b, *miR-204*, *miR-218*, *miR-331*, and *miR-181*; while the 5 most downregulated

miRNAs were *miR-135b*, *miR-132*, *miR-199*, *miR-139*, and *miR-150* [150]. In addition to

the most highly upregulated miRNAs, the authors also detected elevated expression of

miRNAs of the *miR-17-92* cluster, as well as the *miR-17* family member *miR-106a* [150].

Schotte *et al.* examined miRNA expression in MLL and non-MLL precursor B-ALLs

(including *TEL-AML1*, *BCR-ABL*, *E2A-PBX1*, hyperdiploid leukemias, and B-ALLs

lacking known genetic abnormalities) [151]. ALLs had a genetic signature or 19 miRNAs differentially expressed between ALL and CD34+ cells, with 14 upregulated miRNAs (*miR-128a, -142-3p, 142-5p, -150, -151-5p, -181a, -181b, -181c, -193, -30e-5p, -34b, -365, -582, -708*) and 5 downregulated miRNAs (*miR-100, -125b, -99a, -196b, let-7e*). MLL ALLs had a miRNA expression pattern that was distinct from non-MLL precursor B-ALLs with 1 miRNA upregulated (*miR-196b*) and 7 miRNAs downregulated (*miR-193, -151-5p, -30e-5p, -34b, -582, -708, let-7e*) (Table 1). Strikingly, *miR-196b* was expressed 560-fold higher than in B-ALLs lacking known genetic abnormalities [151].

Numerous studies have examined miRNA dysregulation of AML through high throughput methodologies, attempting to characterize differential miRNA expression between different cytogenetic abnormalities [152-156] and among cytogenetically normal AML [155, 157-159]. Jongen-Lavrencic *et al.* utilized a multiplex qRT-PCR assay system to characterize miRNA dysregulation of AMLs with common cytogenetic abnormalities and molecular abnormalities [153]. Unsupervised clustering analysis indicated 22 clusters of similar miRNA expression, which in turn corresponded to cytogentic subgroups (i.e. cytogenetic abnormalities) and molecular subgroups (i.e. commonly observed mutations observed within cytogenetically normal AMLs). MLL leukemias showed upregulation of *miR-9* and *miR-429* and downregulation of *miR-213* and *miR-146a* relative to all non-MLL AMLs. Dixon-McIver, *et al.* analyzed 157 miRNAs from 100 AML patients via a multiplex qRT-PCR platform [154]. Normal bone marrow vs. AML showed a signature of 17 upregulated miRNAs (*miR-27a*, *miR-30d*, *miR-142-5p*, *miR-155*, *miR-181a/b/c*, *miR-195*, *miR-221*, *miR-222*, *miR-324-5p*, *miR-326*,

miR-328, *miR-331*, *miR-340*, *miR-374*, and *let-7*) and 16 downregulated miRNAs (*miR-9**, *miR-15b*, *miR-26a*, *miR-30a-3p*, *miR-34c*, *miR-103*, *miR-147*, *miR-151*, *miR-182*, *miR-184*, *miR-199a*, *miR-302b**, *miR-302d*, *miR-325*, *miR-367*, *miR-372*).   MLL leukemias clustered together with monocytic leukemias. Garzon *et al.* examined the differential miRNA expression patterns by microarray and qPCR validation with respect to both cytogenetic abnormality and prognosis [155]. Examination of miRNA levels in AML samples revealed a signature of 26 miRNAs downregulated and none upregulated relative to miRNA expression in CD34+ cells from normal bone marrow donors. Further, elevated *miR-191* or *miR-199* expression were negatively correlated to event-free and overall survival. Within AML samples, MLL leukemias were identified by a signature of 8 upregulated miRNAs and 14 downregulated miRNAs relative to non-MLL patients. Variance within the MLL translocated samples was further present with 16 miRNAs upregulated in *MLL-AF6* relative to *MLL-AF9*, indicating an increased level of complexity governing MLL miRNA regulation. A high throughput bead based study by Jianjun Chen's group examined the differential miRNA expression between several common cytogentically abnormal AMLs, including Core Binding Factor translocations, *PML-RARα* translocations, and MLL translocations [152]. The *miR-17-92* cluster was strongly upregulated in MLL leukemias relative to non-MLL AMLs. Several miRNAs from within the *HOX* cluster, *miR-196b*, *miR-10a*, and *miR-10b* are upregulated in MLL leukemias. *MiR-124a* and *j-miR-2* were also upregulated. Several miRNAs were down regulated in MLL leukemias relative to non MLL leukemias including the *miR-181* family (*miR-181a/b/c/d*), *miR-126/miR-126**, *miR-130a*, *miR-146a*, *miR-224*, *miR-368*,

TABLE 1. miRNAs differentially expressed in acute leukemias

Subject	Compared	Upregulated	Downregulated	Reference
t(11q23) ALL	AML	*miR-128a, - 128b,-130, -151, -210, j-miR-1*	*miR-223, -125a, -221, -222, -23a, -23b, -24, -27a, -27b, -199b, -26a, -335, -21, -22, -424, -451, let-7a, let-7b, let-7c, let-7e*	Mi, *et al.*[148]
ALL	AML	*miR-128a, miR-128b, miR-155, miR-146a, miR-150, miR-17, miR-20a, miR-29a/c, and miR-29b*	*miR-223, miR-196b, miR-221, miR-222, miR-23a, miR-27a/b, and let-7*	Wang, *et al.* [149]
inv(16)	other AMLs	*miR-424, -199b, -365, -335, -511, -193a*	*miR-192, -296, -155, -148a, -218, -135b, -196b, -196a, -432, -135a, -10a, -10b, -127, -let-7b*	Jongen-Lavrencic, *et al.* [153]
t(8;21) AML	other AMLs	*miR-126**	*miR -19a, -221, -107, -188, -338, -342, -20b, -187, -501, -339, -210, -502, -182, -500, -152, -135a, -148a, -125b, -100, -99a, -1, -133a, -133b, -224, -9, -10a, - 10b, -196a, -196b, let-7b, let-7c*	Jongen-Lavrencic, *et al.* [153]
t(15;17) AML	other AMLs	*miR-130a, -130b, -335, -148a, -222, -146a, -181d, -193a, -450, -213, -199, -409-5p, -181b, -496, -181a, -424, -497, -154, -125b, -365, -369-5p, -99a, -203, -433, -323, -494, -100, -370, -432, -224, -127, -452, -299-5p, -376a, -134, -485-5p, -382, -379, -193b*	*miR-196a, -196b, -151,-10b, let-7c*	Jongen-Lavrencic, *et al.* [153]
t(11q23) AML	other AMLs	*miR-9, -429*	*miR-213, -146a*	Jongen-Lavrencic, *et al.* [153]
NPM1 mutated AML	other AMLs	*miR-10a, -10b, -135a, -196b, -196a, -152, let-7b*	*miR-99b, 323, -143, -146a, -497, -320 -511, -450, -151, -494, -193b, -365, -203, -335, -130a, -485-5p, -126*, -299-5p, -433, -451, -134, -370, -379, -432, -224, -382, -376a, -424, -127*	Jongen-Lavrencic, *et al.* [153]
FLT3 mutated AML	other AMLs	*miR-511, -155, -10b, -135a*	*miR-30a-3p, -203, -130a, -214, -338, -143, -145, -182*	Jongen-Lavrencic, *et al.* [153]
ALL	CD19+ normal	*miR-128b, -204, -218, -331, -181b, -204, -148, -210, -218, -296, -381, 17-3p, -17-5p, -19a, -20, -92*	*miR-135b, -132, -199, -139, -150*	Zanette, *et al.* [150]

ALL	normal CD34+	*miR-128a, -142-3p, 142-5p, -150, -151-5p, -181a, -181b, -181c, -193, -30e-5p, -34b, -365, -582, -708*	*miR-100, -125b, -99a, -196b, let-7e*	Schotte, *et al.* [151]
t(11q23) ALL	other ALL	*miR-196b*	*miR-193, -151-5p, -30e-5p, -34b, -582, -708, let-7e*	Schotte, *et al.* [151]
AML	normal CD34+	NA	*miR-126, -130a, -135, -93, -146, -106b, -224, 125a, -92, -106a, -95, -155, -25, -96, -124a, -18, -20, -7d, -26a, -222, -101, -338, -371, -199b, -29b, -301*	Garzon, *et al.[155]*
t(11q23) AML	other AMLs	*miR-326, -219, -194, -301, -324, -339, -99b, 328*	*miR-34b, -15a, -29c, -372, -30a, -29b, -30e, -196a, let-7f, -102, -331, -229, -193*	Garzon, *et al.[155]*
FLT3 mutated AML	FLT3 wt	*miR-155, -10a, -10b*	NA	Garzon, *et al.[155]*
NPM1 mutated AML	NPM1 unmutated AML	*miR-10a, -10b, -100, -21, -16a, -16b, -19b, -18a, -29c, -29a, -16-1, -29b, -24, -20, -17, -369, - 19a, -106, -16-2, -195, -102, -152, -9, -142, -378, -98, -374, -15a, 155, let-7a-3, let-7f, let-7c, let-7a-2, let-7a-1, let-7g, let-7d*	*miR-22, -192, -128a, -383, -373, -324, -127, -373, -324, -127, -373*, -139, -193b, -145, -498, -135a, -299, -429, -493, -326, -204, -198, 486*	Garzon, *et al.* [159]
FLT3 mutated AML	FLT3 wt	*miR-155, -302a, -133a*	NA	Garzon, *et al.* [159]
t(11q23) AML	Other AMLs	*miR-27a, miR-30d, miR-142-5p, miR-155, miR-181a/b/c, miR-195, miR-221, miR-222, miR-324-5p, miR-326, miR-328, miR-331, miR-340, miR-374, and let-7*	*miR-9*, miR-15b, miR-26a, miR-30a-3p, miR-34c, miR-103, miR-147, miR-151, miR-182, miR-184, miR-199a, miR-302b*, miR-302d, miR-325, miR-367, miR-372*	Dixon-McIver, *et al.* [154]
t(8;21), inv(16), t(16;16) AML	other AMLs	*miR-126/126*, -130a*	*miR-196b, -17-5p, -17-3p, -18a, -19a, 19b, 20a, 92*	Li, *et al.* [152]
t(15;17) AML	other AMLs	*miR-181a, -181b, -181c, -181d, -100, -125b, -224, -368, -382, -424*	*miR-126/126*, -422b, -10a, -150, -124a, -17-5p, -20a, j-miR-2*	Li, *et al.* [152]
t(11q23) AML	other AMLs	*miR-10a, -10b, -124a, -196b, -17-5p, -17-3p, -18a, -19a, -19b, -20a, -92, j-miR-2*	*miR-126/126*, -130a, -146a, -181a, -181b, -181c, -181d, -224, -368, -382, -424*	Li, *et al.* [152]
t(11q23) AML	Other AMLs	*miR-21*	*miR-26a, miR-30c, miR-30d, miR-100, miR-125b, miR-126-3p, miR-143, miR-146a, miR-146b-5p, miR-181a, miR-181b, miR-181d, miR-221, miR-222, and let-7*	Dashkey, *et al.* [156]

miRNA dysregulation was cataloged for miRNAs dysregulated in acute leukemias. Adapted from Mian and Zeleznik-Le [8].

miR-424. Dashkey *et al.* examined 102 samples from childhood and adolescent AMLs by microarray across multiple cytogenetic abnormalities, including: *CBF* translocations, *PML-RARα* translocations, and *MLL* rearrangements [156]. MLL leukemias showed a unique signature relative to non MLL leukemias of 15 downregulated miRNAs (*miR-26a*, *miR-30c*, *miR-30d*, *miR-100*, *miR-125b*, *miR-126-3p*, *miR-143*, *miR-146a*, *miR-146b-5p*, *miR-181a*, *miR-181b*, *miR-181d*, *miR-221*, *miR-222*, and *let-7*) and a single upregulated miRNA (*miR-21*).

Collectively, these studies of miRNA signatures of AMLs with different cytogenetic abnormalities present very different pictures, with some overlap in results. These differences can be attributed to different comparison groups and different platforms. However, the role of several miRNAs were verified by detailed functional studies verifying dysregulation of miRNAs.

HOX **associated miRNAs**

5 miRNAs are located within the *HOX* clusters in mammals, including *miR-10a*, *miR-10b*, and *miR-196a-1*, *miR-196a-2*, and *miR-196b* [160]. Several of these miRNAs have been shown to be upregulated in MLL AML relative to non-MLL AMLs [152]. *miR-196b* has several homologs located at other loci within the *HOX* clusters. *Mir-196a-1* and *miR-196a-2* are located upstream from *HOXB9* and *HOXC9*, respectively (Figure 6). Within the *miR-196 family*, *miR-196a* and *miR-196b* differ only at nucleotide 12 with *miR-196a* encoding an adenine and *miR-196b* encoding a uracil [161]. Both *miR-196a-1* and *miR-196a-2* are identical in their mature miRNA sequence (Figure 6).

MiR-196b is located within the *HOXA9* locus and is evolutionarily conserved

throughout mammals [11]. The *pri-miR-196* transcript is a non-coding transcript that is expressed from an alternate *AB* exon of *HOXA9* that is directly regulated by MLL and is highly upregulated in MLL AMLs relative to other non-MLL AMLs [11, 152]. Previous work from our lab has shown that inhibition of *miR-196b* through 'antagomir' inhibitors abrogates the leukemogenic capacity of *MLL-AF9* transduced bone marrow, while transduction of *miR-196b* enhances colony forming ability of murine bone marrow progenitor cells [11]. Studies of *miR-196b* in ALL have revealed that *miR-196* expression levels correlate with *HOXA9* expression and *miR-196b* is upregulated in ALLs where the *HOXA* cluster is often highly expressed [162]. *miR-196b* was implicated in the downregulation of *HOXA9* and *MEIS1* in MLL leukemia [163]. Overexpression of *miR-196b* in a murine model transformed with *MLL-AF9* results in a delay in onset of AML, implicating *miR-196b* can function as a tumor suppressor. Secondary transplantation, however, result in an accelerated onset of leukemia, indicating the dualistic role of *miR-196b* in targeting both oncogenes and tumor suppressors [163].

miR-196 was initially characterized as regulator of *HOXB8* despite a G:U wobble mismatch located within the seed region matching site of the *HOXB8* MRE [161]. In addition to regulating *HOXB8*, *miR-196a* and *miR-196b* are predicted to regulate several additional *HOX* genes, including *HOXC8*, *HOXD8*, and *HOXA7* (Figure 6).

Numerous studies have implicated *miR-196* in development and hematopoiesis. During embryonic development, *miR-196* downregulates *Hoxb8*, which induces expression of *Sonic hedgehog* (*Shh*) to promote the development of nascent limb buds [164]. In embryonic chicken development, *miR-196b* regulation of *Hoxb8* governs

Figure 6. *HOX* associated miRNAs
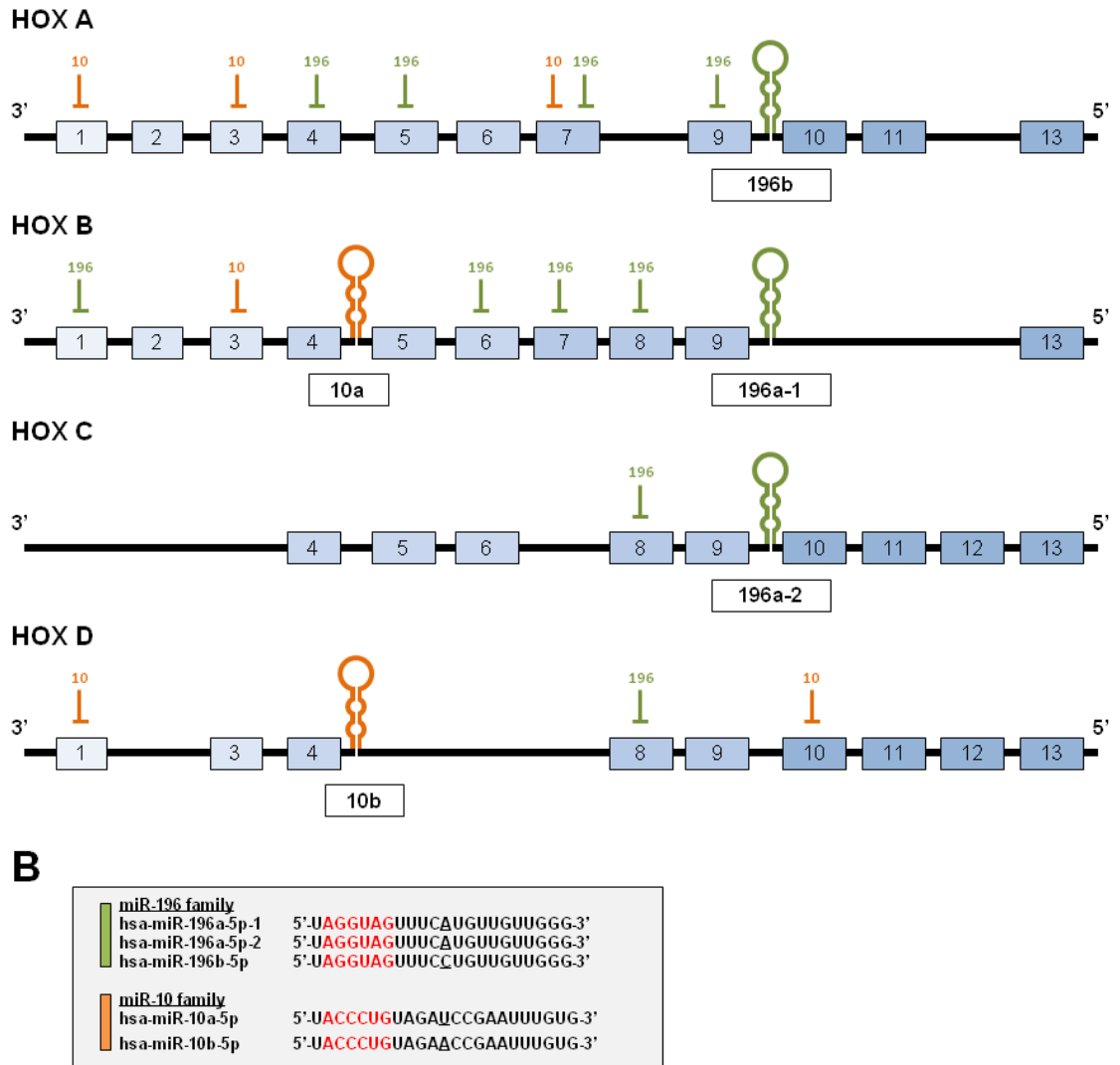
A) Schematic depiction of *HOX* associated *miRNA*s in human. miRNAs are indicated by stem loop structures drawn onto *HOX* clusters. miRNA regulatory relationships with *HOX* genes are indicated on chart. Adapted from Yekta et. al. [160]. B) *miRNA* sequences from the *miR-10* and *miR-196* families grouped by family and color coded with the *miR-196* family indicated in green and the *miR-10* family in orange. Seed region indicated in red. Underlined sequences indicate non conserved bases.

vertebrate segmental identity, with specific knockdown of *miR-196* resulting in skeletal abnormalities in the last cervical vertebra [165].

miR-196b is dysregulated in a number of additional cancer models, as both an oncogene and tumor suppressor; including glioblastoma multiforme [166], cervical cancer [167], and chronic myeloid leukemias [168]. In glioblastoma, high *miR-196b* expression levels are correlated to lower overall survival with increased cellular proliferation, implicating *miR-196b* as a potential oncogene [166]. However, in cervical cancer and chronic myeloid leukemia, *miR-196b* has been shown to function as a tumor suppressor, regulating *HOXB7* in cervical cancer [167], and *BCR-ABL* and *HOXA9* in CML [168].

In addition to *miR-196b*, *miR-10a* also arises from within the *HOX* gene clusters and has been found to be upregulated in MLL leukemias [152]. The *miR-10* family is comprised of two *HOX* cluster located miRNAs. *miR-10a* is located downstream of *HOXB4*, while *miR-10b* is located downstream of *HOXD4* [169]. *miR-10a* and *miR-10b* differ only in nucleotide 12, with *miR-10a* encoding a uracil and *miR-10b* encoding an adenine [169]. *miR-10* family members have been implicated in both canonical miRNA function through RISC-mediated mRNA downregulation as well as non-canonical function. For example, *miR-10b* downregulates *HOXD10* in breast cancer through the canonical miRNA:RISC mechanism, leading to a decrease in *HOXD10* mRNA stability and an increase in tumor metastasis [170]. However, *miR-10a* has been shown to bind to TOP motif containing mRNA transcripts, immediately downstream of the TOP motif, resulting in increased expression of these target mRNAs [144]. TOP (terminal

oligopyrimidine tract) sequences consist of a short tract of 4-15 pyrimidine residues located adjacent to the 5' cap within the 5'UTR of an mRNA, and have a regulatory function as a binding site for translational repressors [171]. The role of *miR-10a* in regulating the translation of these mRNAs is unusual in that: 1) it does not entail perfect seed matching between *miR-10a* and the target, and 2) binding of *miR-10a* results in an increase in translation rather than a decrease [144].

miR-17-92 cluster

The *miR-17-92* cluster (also known as *oncomir-1*) consists of 6 miRNAs co-expressed from a single transcript (*miR-17*, *miR-18a*, *miR-19a*, *miR-20a*, *miR-19b-1*, and *miR-92* located on band q31 of chromosome 13 in humans [172, 173] . The *miR-17-92* cluster has several homologous miRNA clusters including the *miR-106a* cluster and the *miR-106b* cluster located on chromosome X band q26 and chromosome 7 band q22, respectively (Figure 7). The *miR-17-92* cluster arises from an intron of a pri-miRNA transcript that is non-coding. However, the homologous *miR-106a* primary miRNA transcript has not been identified [174]. The *miR-106b* cluster arises from an intron of the *MCM7* mRNA transcript, which encodes a protein, mini chromosome maintenance 7, and includes only 3 different miRNA encoding hairpins [174].

Numerous studies have implicated the *miR-17-92* cluster in cancers, cell cycle control, and development (extensively reviewed in [173, 175]). Knockout of the *miR-17-92* cluster and its homologous clusters in mouse models produced several distinct phenotypes. *miR-17-92 (-/-)* embryos are smaller than their wild type counterparts, and *miR-17-92* knockout mice die shortly after birth, with lung hypoplasia [176]. In these

studies, bone marrow transplantation experiments implicated the *miR-17-92* cluster in B cell development [176].

The *miR-17-92* cluster was initially identified as a target of Myc regulation [177]. However, recent studies have indicated that additional regulatory factors also control *miR-17-92* expression. Examination of endogenous E2F binding indicates that E2F1, E2F2, and E2F3 bind to the *miR-17-92* promoter and increase transcription of the *miR-17-92* host gene [178]. Further studies, indicate that p53 suppresses *miR-17-92* expression through direct transcriptional regulation under hypoxic conditions [179]. Examination of the *miR-17-92* cluster in MLL leukemia has identified a direct regulatory relationship by both wild-type MLL and MLL fusion proteins [12]. Both wild type and fusion MLL proteins localize to the promoter of the *miR-17-92* host gene, as indicated by chromatin immunoprecipitation assays [12]. Cell lines with *MLL* translocations showed an increase in MLL binding to the *miR-17-92* promoter, increased H3 acetylation, and H3K4 trimethylation as compared to those without *MLL* translocations [12]. Further, examination of miRNA expression profiles in AML with common translocations indicate that the *miR-17-92* cluster is upregulated in MLL AMLs relative to non-MLL AMLs [152]. The *miR-17-92* cluster and its homologous miRNA clusters, encode four families of miRNA categorized by homology in the seed region (miRNA sequences are reviewed in [172, 173]). Homologous miRNAs are generally accepted to have overlapping functions and target sequences, as a result of commonalities within the seed region. For example, *miR-17* and *-20a* share the same seed sequence which is critical for target recognition (reviewed in [174]).

Figure 7. *miR-17-92* **cluster and related miRNAs**
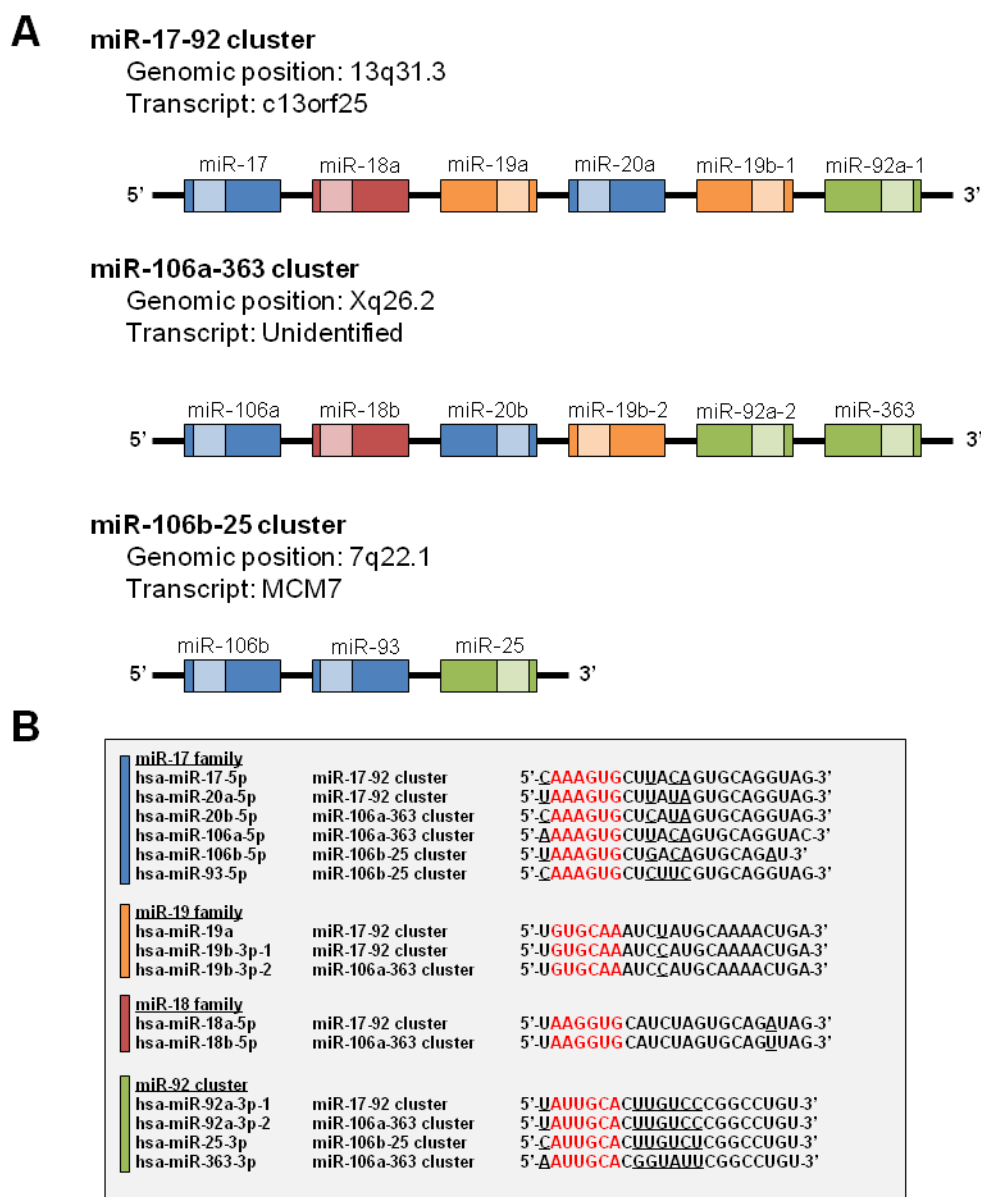
A) Organization of the miRNAs within the *miR-17-92* cluster (top), *miR-106a-363* cluster (middle), and *miR-106b-25* cluster (bottom). Light colored box indicates the arm (5p or 3p) which produces the predominant mature miRNA. miRNA families are grouped by color with the *miR-17* family indicated in blue, *miR-19* family in orange, *miR-18a* family in red, and the *miR-92* family in green. B) miRNA sequences from the *miR-17-92* cluster and paralogous clusters. miRNAs organized by family. Seed region indicated in red. Underlined sequences indicate non conserved bases.

The *miR-17* family is comprised of *miR-17* and *miR-20a* of the *miR-17-92* cluster; *miR-106a* and *miR-20b* of the *miR-106a-363* cluster, and *miR-106b* and *miR-93* of the *miR-106b-25* cluster. MiRNAs of the *miR-17* family have a common seed sequence of AAAGUG, and share a great deal of homology throughout non-seed nucleotides as well, often differing at only one or two nucleotides (Figure 7). Within the *miR-17-92* cluster, *miR-17* and *miR-20a* differ at nucleotides 1 and 12, with *miR-17* possessing cytosines in these positions, and *miR-20a* possessing uracils. The *miR-17* family, which is comprised of *miR-17* and *miR-20a*, is one of the most studied miRNA families, with numerous defined targets, including (but not limited to): *AIB1* [180], *HSP27* [181], and *TGFβ* [182]. Critically, the *miR-17* family has been implicated in cell cycle progression, through regulation of several components the G1/S checkpoint. *MiR-17* downregulates the negative checkpoint regulator *CDKN1A (p21)* [183]. Further examination of the *miR-17* homolog *miR-106a*, indicated that *miR-106* also directly targets *CDKN1A (p21)* [184].Conversely, *miR-17* also downregulates the expression of *E2F1*, and in doing so prevents the cell from dying due to double strand breaks that would otherwise occur as a result of unrestricted growth [177, 185]. In addition to *E2F1*, *miR-20a* regulates several other E2F family members, including *E2F2* and *E2F3* [178]. Recent work has identified a feedback loop whereby the *miR-17-92* cluster downregulates E2Fs which regulate the *miR-17-92* cluster. Within hematopoiesis, *miR-17*, *20a*, and*106a* have been implicated as regulators of monocytopoiesis through downregulation of AML1, which functions to positively regulate the M-CSF receptor and negatively regulate the *miR-17-92* and *miR-106a-363* clusters [186]. Introduction of exogenous miRNAs from the *miR-17* family

into cord blood CD34+ progenitor cells cultured under a monocytic differentiation protocol resulted in an increase in blast cells and inhibition of monocytic differentiation while inhibition of miRNAs from the *miR-17* family results in decreased proliferation and increased differentiation [186].

The *miR-19* family is comprised of 2 separate 23 nucleotide miRNAs, *miR-19a* and *miR-19b-1*, and have a common seed sequence of GUGCAA (Figure 7). *MiR-19a* and *miR- 19b* differ in only a single nucleotide at position 11; *miR-19a* has an uracil, while *miR-19b* has a cytosine. Located outside of the seed region, these nucleotides are involved in stabilization of the miRNA:mRNA interaction, but are not essential for targeting the miRNA to the transcript. Numerous *miR-19* targets have been identified, including (but not limited to): *TNFα* [187, 188], *BCL2L11* [189], and *PTEN* [190]. Of these targets, *PTEN* is often cited as a critical downstream target of the *miR-19* family. The regulatory relationship between *miR-19* and *PTEN* was initially described using an Eμ-myc model of lymphoma, where overexpression of *miR-19b* resulted in decreased *PTEN* levels and increased cell survival [190].

miR-18a is additionally located within the *miR-17-92* cluster, while its homolog *miR-18b* is within the *miR-106a-363* cluster. *MiR-18a* differs from *miR-18b* at a single nucleotide with a uracil instead of a cytosine, and both share a common seed sequence of AAGGUG (Figure 7). *MiR-18a* is one of the least well studied miRNAs of the *miR-17-92* cluster. However, several mRNAs have been identified as *miR-18a* targets, including (but not limited to): *PIAS3* [191], *CTGF* [192], and *SMAD4* [182].. Intriguingly, *miR-18a* was found to inhibit the global function of miRNAs through targeting of the *Dicer*

mRNA [193]. In a cardiovascular model, *miR-18*, along with *miR-19*, has been implicated in the regulation of angiogenesis via downregulation of the pro-angiogenic factors *CTGF* and *Tsp1* [192]. *MiR-18a* regulates function of the *TGF-β* signaling pathway through downregulation of the downstream effector *SMAD4* [182].

The *miR-92* family is represented by *miR-92a-1* within the *miR-17-92* cluster; *miR-92a-2* and *miR-363* within the *miR-106a-363* cluster; and *miR-25* within the *miR-106b-25* cluster (Figure 7). Numerous *miR-92* targets have been identified including (but not limited to): *Integrin-5a* [194], *VHL* [195], and *PHLPP2* [196]. Critically, *miR-92* has been implicated in regulating apoptosis through regulation of *BCL2L11 (Bim)* [197].

Several mRNAs have been validated as targets of multiple non-family miRNAs from the *miR-17-92* cluster, suggesting that miRNAs may act cooperatively to regulate targets. For example, *PTEN* is downregulated by *miR-17*, *miR-19*, and *miR-18a* through miRNA binding to unrelated MREs within the 3'UTR [190, 198, 199]. The pro-apoptotic *BCL2* family member *BCL2L11* (*Bim*) is an additional target of cooperation for miRNAs of the *miR-17-92* cluster, regulated by both *miR-19* [189] and *miR-92* [197]. Despite the extensive work published on validating targets of the *miR-17-92* cluster, few studies have examined the contributions of this cluster to MLL leukemia or validated the potential mechanism by which the *miR-17-92* cluster acts in MLL leukemia. Enforced overexpression of *miR-17-19b* increases the colony forming ability of *MLL-ELL* transformed bone marrow [12]. Further, overexpression of the *miR-17-92* cluster results in downregulation of 363 potential target genes, indicating that dysregulation of the *miR-17-92* cluster has broad implications in target mRNA regulation [12]. Within MLL

leukemia, *miR-17* regulates *CDKN1A* (*p21*) expression [183]. Overexpression of *miR-17-19b* accelerated the onset of *MLL-AF10* leukemia in a murine model, which was phenocopied by shRNA knockdown of *CDKN1A* (*p21*). The growing number of validated targets for each miRNA suggests that miRNAs are not limited to single targets, and that other, as yet non-validated targets, likely contribute to the disease process.

Antisense oligonucleotide technologies

Findings highlighting the importance of miRNAs in cancer, as well as other diseases, have drawn attention to the potential therapeutic value of modulating miRNA function, either by replacing lost/downregulated miRNAs or inhibiting amplified/overexpressed miRNAs. To this end, multiple different technologies have emerged to modulate miRNA levels utilizing synthetically manufactured oligos (history of oligonucleotide therapeutics reviewed in [8, 13, 14]).

As miRNAs function to post-transcriptionally regulate transcription, replacement of lost miRNA function may be achieved using anti-sense oligonucleotides (ASOs) complementary to sequences found in target mRNAs and function in both RISC-dependent and RISC-independent functions. RISC-independent mechanisms of ASO function target specific mRNAs with perfectly matched complementary oligonucleotides (oligos), and recruit the endogenously expressed RNAse H to cleave the mRNA:ASO duplex (reviewed in [8, 200]). Alternatively, RISC-dependent replacements of miRNA function can be attained through introducing either a shRNA, siRNA, or miRNA analogue (reviewed in [201]).

Numerous chemical modifications have been developed for use in oligos (Figure

8). The chemical modifications utilized for anti-miRNA oligonucleotides (AMOs) were developed from those used for synthetic siRNAs and mRNA targeting ASOs, and utilize the same modifications. AMOs directed against miRNAs function through stable binding to miRNAs. AMO downregulation of miRNAs occurs through irreversible binding and sequestration of target miRNAs [202]. Thus their most valuable attributes are a high thermodynamic stability, compatibility with binding to RISC associated miRNAs, and resistance to nuclease degradation (discussed in [13, 203]). Inhibition of miRNA function is dependent on chemically modified anti-sense oligonucleotides (ASOs) that are complementary to the target miRNAs and inhibit miRNA activity through thermodynamically stable Watson-Crick base pairing to target miRNAs (reviewed in [13]). The simplest ASOs may employ either unmodified RNA or DNA nucleotides complementary to the target miRNA. However, unmodified oligos are poor candidates for therapeutic use due to immune response activation, rapid oligo degradation, poor cellular uptake, and limited bioavailability of ASOs (reviewed in [13, 200, 203]). To improve bioavailability, nuclease resistance, and miRNA:AMO duplex stability; numerous chemical modifications have been developed for ASOs, including modification of the phosphodiester backbone and modification of the ribose sugars.

Modifications of the non-bridging oxygen of the phosphate group linking the ribose sugars of the backbone, include methylphosphonates, phosphorothioates, and boranophosphonates (reviewed in [14, 201, 203]). Modification of the non-bridging oxygen introduces chirality to the phosphate, and each modification results in a racemic mixture of both stereoisoforms of the of the phosphodiester linkage [203], increasing

levels of nuclease incorporation result in increasing nuclease resistance.

Phosphorothioate modifications consist of the addition of a sulfur in place of one of the non-bridging oxygen molecules of a phosphate within the oligo backbone. A phosphorothioate modification confers resistance against RNAse degradation, at a slight cost of binding affinity (~0.25° C/modification)[13], and thus may require additional modifications to offset decrease in binding affinity. Further, *in vivo* examination of siRNAs indicates that inclusion of phosphorothioate modifications modestly improved serum stability of siRNAs, and produces similar biodistribution of siRNAs among organs [204]. Phosphorothioate modifications are nuclease resistant, thus conferring a level of resistance to degradation [205], but are compatible with RNAse H, and thus suitable for use in ASO designs [14, 205].

Numerous modifications alter the ribose sugar at the 2' position, directly binding either the 2' carbon or modifying the attached hydroxyl group, including: 2'- O-Methyl (2'-O-Me), 2'-O-methoxyethyl (2'-O-MOE), 2'-Flouro (2'-F), 2'-Deoxy-2'-fluoro-β-D-arabino (FANA), N3'-P5' phosphoramidates (NPs), and locked nucleic acids (LNA) (reviewed in [13, 200, 201]). The sugars of nucleotides exist in multiple different "pucker" conformations, which are described by the angles of the C2 and C3 tetrahedral bonds of the furanose ring [203]. The principle stable sugar conformations employ either a C3-endo, C2-exo conformation (a.k.a. North conformation, N-type conformation) or a C3-exo, C2'-endo conformation (a.k.a. South conformation, S-type conformation) [206]. Pucker conformation, in turn, alters the bond lengths of the sugar and phosphate bonds of nucleic acids, altering the thermodynamic stability of base pairing [207].

2'- O-Methyl (2'-O-Me) modifications have been widely utilized in ASO development. As with other modifications to the 2' position of the ribose sugars, 2'-O-Me modifications improve the binding affinity of the oligo by forcing the ribose sugars into a C3-endo conformation, resulting in an increase in thermodynamic binding stability of 2-3 °C/nucleotide [203]. Examination of chemically modified siRNAs has indicated that incorporation of 2'-O-Me modifications confers resistance to immune activation [208]. 2'-O-Me modified oligos were applied to AMOs targeting miRNAs incorporated in a RISC complex in 2004. Two independent studies examined the use of uniformly modified 2'-O-Me oligonucleotides to block the function of siRNAs associated with the RISC complex in *C. elegans* [209] and human cell lines [210], and found the modified oligonucleotides to be capable of inhibiting the function of siRNAs and miRNAs within RNA-protein complexes. The 2'-O-methoxyethyl (2'-O-MOE) modification is another commonly used 2'-alkyl ribose modification, altering ribose sugar conformation to result in an increase in thermodynamic binding stability of 2 °C/nucleotide [203].

Locked Nucleic Acids (LNAs) are a 2'-O, 4'-C-methylene-β-D-ribofuranosyl modified version of a ribose (consisting of a methylene bridge between the 2'-hydroxyl group and 4' carbon of the ribose sugar), and were initially synthesized in 1998 [211, 212]. As with other 2' ribose modifications, LNA modifications lock the ribose sugar into a C3 endo conformation and thermodynamically stabilizes binding to target nucleotides [213, 214]. Incorporation of locked nucleic acids additionally affects the pucker conformation of adjacent nucleotides [215]. LNAs increase the binding affinity of nucleotides in a sequence dependent manner with an increase in thermodynamic stability

that is partially dependent on adjacent nucleotides [216, 217], and results in a change in

binding affinity of 1.5-6 °C/nucleotide [13]. In addition to improving the thermodynamic

stability of binding with a target, incorporation of LNA modifications increase resistance

to nuclease mediated degradation [218]. Further, LNAs are incompatible with RNAse H

function but compatible with RISC activity function [219]. However, LNA

simultaneously increase hepatic toxicity [220]. Several additional modifications are

currently under development based on this chemistry, including amino-LNAs, thio-

LNAs, α-L-ribo-LNAs, and β-D-xylo-LNAs [213].

Chemical modifications appended to the ends of the oligo have been used to alter

the distribution and serum half-life of antisense oligos. Addition of a cholesterol to the 3'

end of an oligonucleotide was initially described in the context of a siRNA targeting the

ApoB mRNA transcript [221]. Cholesterol transport within the serum is mediated by

binding to albumin, high density lipoprotein (HDL), and low density lipoprotein (LDL)

[222, 223]. In addition to the cholesterol tag, several modified lipids (of varying lengths)

have been employed as tags conjugated to the 3' end of siRNAs, including: myristoyl,

lithocolic-oleyl, docosanyl, lauroyl, stearoyl, palmitoyl, oleoyl, and linoleoyl tags [224].

Modification of siRNAs by different lipophilic conjugates altered the biodistribution of

siRNAs *in vivo* [224]. Uptake method *in vivo* relies on the human homolog to the *C*

elegans transmembrane receptor Sid1 as well as the SR-B1 receptor [224].

Oligonucleotide chemical modifications are modular and may be applied across

the oligo or only at specific residues, resulting in 'mixmers," consisting of combinations

of multiple different chemical modifications and variation in the length of antisense

oligonucleotides suited to different functions. Numerous chimeric mixtures of oligonucleotide modifications have been employed for specifically targeting miRNAs, including: 2'-O-MOE/PS [225], 2'-O-MOE/LNA/PS [226], 2'-O-Me/LNA/PS [227], LNA/2'-O-Me [228], 2'-O-MOE/2'-F [229]. While numerous studies have utilized AMOs of the same length as the target miRNA, additional studies have utilized AMOs shorter than the target, focusing on developing the minimally required oligos so as to minimize toxicity and non-specific binding while maintaining target affinity. For example, an 8-mer oligonucleotide, comprised of LNAs with a complete phosphorothioate backbone, targeting the seed region of *miR-33*, provided efficient knockdown of both *miR-33a* and *miR-33b in vivo* in mouse and primate [230, 231].

Among the different ASO patterns of modifications, 'antagomirs' were empirically developed as a specific pattern of multiple modifications consisting of: 2'-O-Me modifications across all ribose sugars of the oligo, phosphorothioate bonds at the first two and the last four phosphodiester linkages, and a cholesterol tag at the 3' end of the oligo [232, 233]. These ASOs were initially characterized as a potential therapeutic intervention to inhibit miRNAs *in vivo* [232, 233]. Krutzfeldt, *et al.* tested several potential antagomir designs with different modification patterns. They observed a decrease in knockdown efficiency for oligos containing phosphorothioate modifications of all phosphodiester bonds, relative to oligos with phosphorothioate modifications at the first 2 and last 4 phosphodiester bonds [232], and thus limited use to these specific residues to block RNAse function while minimizing negative effects.

Figure 8. Antisense oligonucleotide modifications and patterns
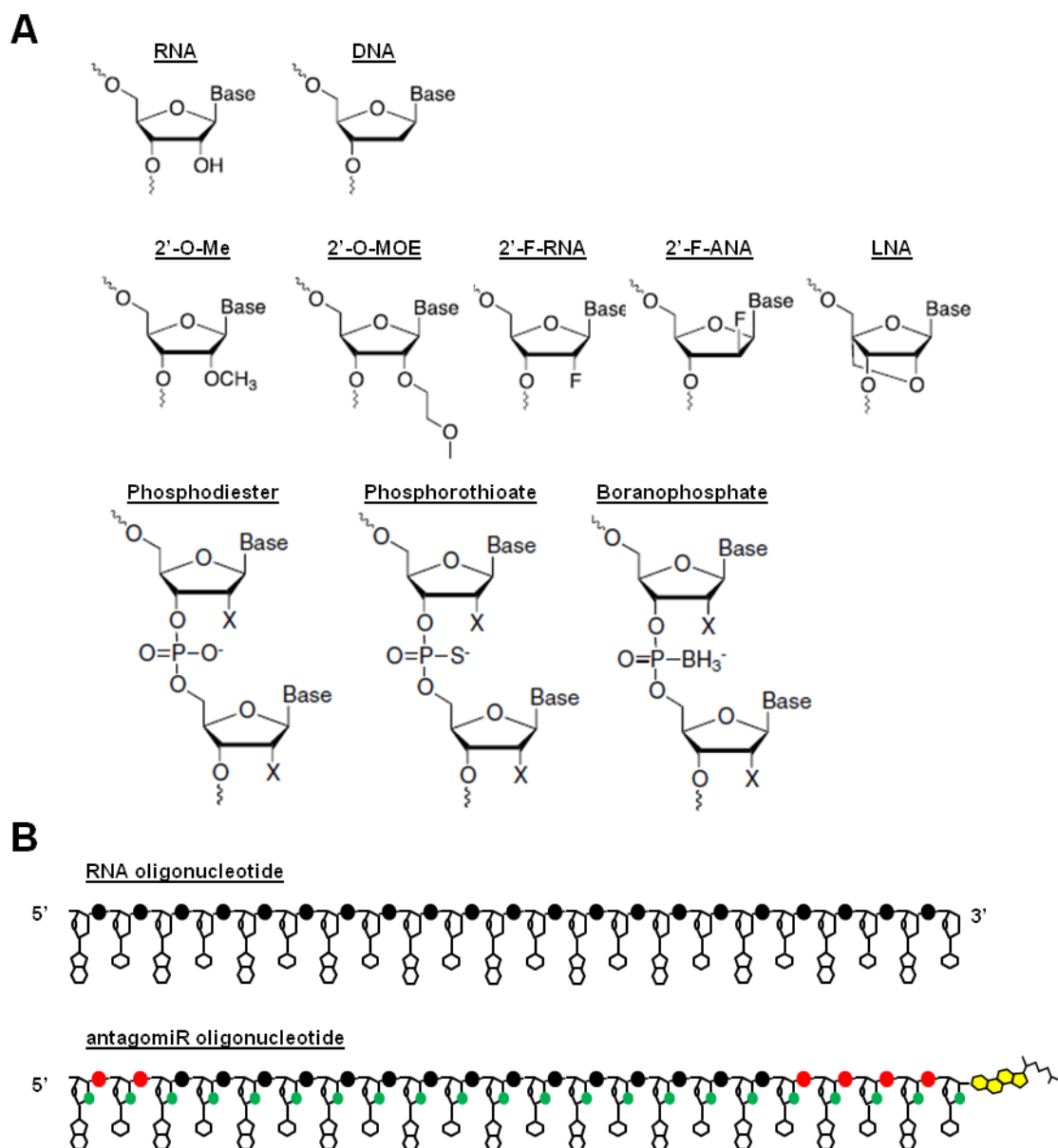
Canonical miRNA biogenesis pathway. A) Selected modifications for anti-sense oligonucleotides. Adapted from DeLeavey, *et al.* [203]. B) Depiction of an unaltered oligo nucleotide (top) and a modified oligonucleotide with 'antagomir' modifications (bottom). Phosphorothioate modifications depicted with red circles, 2'-O-Me modifications depicted in green, and cholesterol in yellow.

Further, in examining the specificity of antagomirs and the potential effects of single or multiple mismatches between the antagomir and the targeted miRNA, Krutzfeldt, *et. al.* observed that a single mismatch at key residues abrogated miRNA knockdown [232]. Examination of the subcellular location of fluorescently labeled antagomirs indicated that antagomir modified oligonucleotides localized within punctate structures located in the cytoplasm, but did not co-localize alongside the P-body marker GW182 [232]. Examination of target miRNAs upon antagomir treatment indicate consistent knockdown of target miRNAs throughout examined tissues [233].

Several groups have utilized the antagomir pattern of modifications to inhibit miRNA function *in vitro* and *in vivo*. Previous work from our group, performed in collaboration with the Grimes lab, utilized an *anti-miR-196b* antagomir *in vitro* colony assay, to test the necessity of *miR-196b* to the clonogenic capacity of *MLL-AF9* transduced bone marrow progenitor cells [11]. Studies by the Grimes lab have utilized antagomir oligonucleotides against *miR-21* and *miR-196b* to examine the contribution of miRNAs in AML *in vivo* [234, 235].

In my dissertation research, I examine targeting miRNAs upregulated in MLL leukemia both individually and in combinations as a potential therapeutic approach. I find that combinatorial antagomirs function as a potent anti-leukemia treatment *in vitro*. I further examine the regulatory role of miRNAs in modulating the expression of PKNOX1 and its availability for inclusion in HOX-PBX complexes. This establishes one potential mechanism by which miRNA inhibition disrupts the leukemogenic potential of MLL fusion proteins in leukemia.

CHAPTER 3

MATERIALS AND METHODS

Cell lines and culture conditions

Human leukemia cell lines were obtained from DSMZ and cultured according to manufacturer's instructions. MOLM-13 was derived from the peripheral blood of a patient undergoing a relapse of M5 AML leukemia and harbors t(9;11) translocation resulting in an *MLL-AF9* fusion [236]. The THP1 cell line also harbors an t(9;11) translocation, and is derived from a patient with a monocytic AML [237]. In addition to cell lines with MLL-AF9 gene fusions, I also examined several cell lines with t(4;11) translocations resulting in *MLL-AF4* gene fusions. RS4;11 is an *MLL-AF4* expressing cell line derived from the bone marrow of a patient with a biphenotypic leukemia, expressing characteristics of both B-cells and monocytes [238]. The MV4-11 cell line also possesses an *MLL-AF4* gene fusion, and was derived from the bone marrow of a patient with a childhood leukemia [239]. I additionally utilized U937 and HL60 as non-MLL cell line controls. U937 cells were derived from a patient with histiocytic lymphoma [240], while HL60 cells were derived from a patient with Acute myeloid leukemia and harbors a c-Myc amplification [241]. Experiments performed in adherent cell lines utilized HEK293T cells, originally derived from human embryonic kidney and transformed with the SV40 T antigen [242].

MOLM-13 (*MLL-AF9*), and RS4;11 (*MLL-AF4*) were maintained at

concentrations between $1X10^5$ cells/mL and $1X10^6$ cells/mL in RPMI with 10% Fetal

Bovine Serum and 1% Penicillin/Streptomycin (Pen/Strep). MV4-11 (*MLL-AF9*) and

K562 (*BCR-ABL*) was maintained at concentrations between $1X10^5$ cells/mL and $1X10^6$

cells/mL in IMDM with 10% FBS and 1% Pen/Strep. Adherent cell lines were cultured

HEK293T, Rat1A, NIH-3T3 cells were cultured in DMEM with 10% FBS and 1%

Pen/Strep. *MLL-AF9* transformed bone marrow was cultured in liquid culture at

concentrations between $3X10^5$ cells/mL and $1X10^6$ cells/mLin RPMI with 10% fetal

bovine serum and 1% Pen/Strep. Cells were supplemented with IL-3 (10 ng/mL), IL-6

(10 ng/mL), and SCF (100 ng/mL) cytokines. All cells were kept at 37˚ C with 5% CO_2.

HEK293T cells were transfected using CalPhos Mammalian transfection system

(ClonTech, Mountain View, CA, Cat #631312) per manufacturer's instructions.

Constructs

MSCV-MLL-AF9 [23] MIGR1 [23], *MSCV-Meis1-pgk-EGFP* [94], and *pKOF2-Prep1-GFP* [94] retroviral constructs were described previously. Briefly, the *MSCV-MLL-AF9* retroviral construct contains a human *MLL-AF9* fusion gene within the Murine

Stem Cell Virus system and can be utilized to introduce and express genes of interest in

hematopoietic stem cells. The *MSCV-Meis1-pgk-EGFP* expresses a murine *Meis1* within

the *MSCV* retrovirus with a gene encoding a fluorescent protein, *EGFP*, expressed from a

separate promoter [94]. The *pKOF2-Prep1-GFP* encodes the full length of *Pknox1* (also

known as *Prep1*) cloned into a modified MSCV vector, with GFP expressed from a

separate promoter [94, 243].

Bone marrow isolation, enrichment, and infection for generation of *MLL-AF9*

transformed bone marrow was performed as previously described [244]. Additional

infection with *MIGR1* or *pKOF2-Prep1-GFP* was performed on *MLL-AF9* bone marrow

cell that had been cultured in methylcellulose for 4 weeks.

pRL-TK (Promega, Madison, WI, Cat# E2241), *MSCV-PIG* [190], and *MSCV-*

PIG- miR-17-19b [190] have been described previously. The *pRL-TK* construct encodes

Renilla luciferase driven by the *HSV-1* Thymodine Kinase promoter, and serves as a

commonly used experimental control in luciferase due to: 1) the ability to readily

distinguish between *Renilla* and Firefly luminescence, and 2) the constancy of expression

of the luciferase enzyme under the *TK* promoter. Exogenous miRNA expression was

attained through transfection with the *MSCV-PIG- miR-17-19b* plasmid (received as a

generous gift from Dr. Jianjun Chen, University of Cincinnati). *MSCV-PIG- miR-17-19b*

was constructed by cloning a fragment of the *miR-17-92* cluster containing the miRNA

hairpins from *miR-17* to *miR-19b-1*, within the *MSCV* (Mouse Stem Cell Virus) retroviral

backbone [190]. The construct additionally contains a *PIG* cassette, encoding *Puro-*

IRES-GFP for use in selection [190]. *MSCV-PIG*, which lacks any fragment o the *miR-*

17-92 cluster was used as a control.

Luciferase constructs were generated by cloning the 3' UTR from *Pknox1* in the

pmiR-Report system (ThermoFisher Scientific, Cat#AM5795). The *pmiR-Report* system

encodes a firefly luciferase gene driven by CMV promoter within the *pmiR* backbone. A

multiple cloning site is located downstream of the luciferase to allow cloning of a 3'UTR.

Mutations to the miRNA binding sites were generated using the Stratagene Multi-site

directed mutagenesis kit (Stratagene, La Jolla, Cat# 200514). Details of cloning

techniques and strategies described elsewhere in the Materials and Methods section.

Antagomir modifications and treatment

Antagomirs were synthesized by the Dharmacon division of Thermo (Lafayette, CO) following the pattern of modifications outlined previously [232, 233]. Antagomirs were designed as small oligonucleotides (oligos) complementary to the targeted miRNA. All nucleotides contained 2'-O-methyl modifications on the ribose sugar. For all oligos, the first 2 and last 4 phosphodiester linkages were replaced with a phosphorothioate linkage. The 3' ends of all oligos possess a cholesterol group. Fluorescent antagomirs possess an additional DY547 fluorescent label at the 5' end.

Antagomir treatments were performed according to 3 different protocols (specified in text). For superficial treatment with antagomirs, cells were counted and resuspended in fresh culture medium at 2X treatment concentrations (100k cells/mL). Cells were then added to an equal volume containing antagomirs and 10X PBS in media at 2X the concentration of the final solution. Superficial antagomir treatment with pre-incubation has been previously utilized by our lab and others [11, 234, 235]. For pre-incubation, cells were incubated in 100 µL of culture media, with antagomir at 10X the final treatment concentration, along with 10X PBS to compensate for antagomir volume, on ice for 30 mins and followed by at room temperature for 5 mins. The cell-antagomir mixture was then diluted tenfold with culture media (for liquid culture experiments) or with . Herein, I refer to this treatment as the "superficial treatment with pre-incubation" to distinguish it from simple superficial treatments that do not require any pre-incubations.

Table 2. Sequences and modifications of antagomirs

antagomir	antagomir sequence (5'→3')
anti-Ce-mir-67	mU*mC*mUmAmCmUmCmUmUmUmCmUmAmGmGmAmGm GmUmU*mG*mU*mG*mA-Chl
anti-Ce-mir-67-DY547	DY547*mU*mCmUmAmCmUmCmUmUmUmCmUmAmGmGm AmGmGmUmU*mG*mU*mG*mA-Chl
anti-mir-196b	mC*mC*mCmAmAmCmAmAmCmAmGmGmAmAmAmCmUm A*mC*mC*mU*mA-Chl
anti-mir-10a	mC*mA*mCmAmAmAmUmUmCmGmGmAmUmCmUmAmCm AmG*mG*mG*mU*mA-Chl
anti-mir-191	mC*mA*mGmCmUmGmCmUmUmUmGmGmGmAmUmUm CmC*mG*mU*mU*mG-Chl
anti-mir-93*	mC*mG*mGmGmAmAmGmUmGmCmUmAmGmCmUmCmAm G*mC*mA*mG*mU-Chl
anti-mir-17	mC*mU*mAmCmCmUmGmCmAmCmUmGmUmAmAmGmCm AmC*mU*mU*mU*mG-Chl
anti-mir-18a	mC*mU*mAmUmCmUmGmCmAmCmUmAmGmAmUmGmCm AmC*mC*mU*mU*mA-Chl
anti-mir-19a	mU*mC*mAmGmUmUmUmUmGmCmAmUmAmGmAmUmUm UmG*mC*mA*mC*mA-Chl
anti-mir-19b-1	mU*mC*mAmGmUmUmUmUmGmCmAmUmGmGmAmUmUm UmG*mC*mA*mC*mA-Chl
anti-mir-20a	mC*mU*mAmCmCmUmGmCmAmCmUmAmUmAmAmGmCm AmC*mU*mU*mU*mA-Chl
anti-mir-92a-1	mA*mC*mAmGmGmCmCmGmGmGmAmCmAmAmGmUmGm C*mA*mA*mU*mA-Chl

Antagomir sequences are depicted above. Stars (*) indicate phosphorothioate
modifications to phosphodiester linkages. Lower-case m preceding nucleotide letter
indicates 2'-O-Me modifications to the furanose ring.

For Lipofectamine 2000[TM] treatment with antagomirs, cells were counted and

resuspended in serum-free media. Lipofectamine complexes were generated under sterile

conditions according to the manufacturer's protocol maximal dosage for RNAi/RNA

delivery (20 pmol or antagomiR). Cells were subsequently treated for 48 hrs with

lipofectamine-antagomir complexes per the manufacturer's instructions.

Preparation of retrovirus

Virus was generated from relevant retroviral constructs using Phoenix Eco packaging cells supplemented with packaging vector. Plasmids were generated by maxiprep according to manufacturer's instructions. DNA was quantified with a Nanodrop 2000™ and transfected into Phoenix Eco cells by Calcium Phosphate transfection (ClonTech, Mountain View, CA, Cat# 631312) according to manufacturer's protocol. Briefly, five 10 cm dishes were plated at $3x10^6$ cells/ plate. Twenty four hours later, media was changed. Transfection mix was prepared by adding DNA to H_20 to $CaPO_4$. DNA was added in the following amounts: 22.5 µg of ecotropic viral plasmid (*MSCV-MLL-AF9*, *MIGR1*, or *pKOF2-Prep1-GFP*)/plate and 2.5 µg packaging vector (*pCL-Eco*)/plate. The mixture was briefly vortexed to mix and added dropwise to 2X HBS while gently vortexing the HBS. Complexes were left to form for 20 minutes in the sterile hood, after which the DNA complex solution was added dropwise to PhoenixEco cells across the plates. Cells were incubated at 32˚C for 2 days. Supernatant was collected each day and fresh media was added. Supernatant was stored at 4 degrees until viral concentration.

To improve infection efficiency, *MSCV-MLL-AF9* virus was concentrated using Centricon Plus-70 Centrifugal Filters (Millipore, Billerica, MA, Cat# UFC710008). Briefly, concentration columns were primed by centrifugation of sterile H_2O at 3000 rpm. 70 mL of viral supernatant was added to the filter unit and centrifuged at 1645 rpm for 3 hours. To elute viral particles, filter units were inverted and spun at 1645 rpm for an

additional 10 minutes. Eluant was collected and total volume was adjusted to 7 mL using

RPMI. Virus was aliquoted to 750 µl/tube and snap frozen on dry ice. Aliquots of virus

were stored at -80˚ C for later use.

Efficacy of *MLL-AF9* virus generation was tested by infection in Rat1A cells.

Infectivity of viral aliquots was confirmed through infection titer of Rat1A cells. 8.5×10^4

Rat1A cells were plated in 6-well plates and cultured overnight at 37C in DMEM + 10%

FBS + 1% P/S. The following day, cells were infected with virus diluted at multiple

concentrations between $1:10^3$ to $1:10^6$ in DMEM+10% FBS + 16 µg/mL Polybrene.

Media was aspirated from cells and virus dilutions were added to plates for 4 hours at

37°C. After 4 hours of treatment, 1 mL of additional media was added to each well and

plates were reincubated for an additional 20 hrs. Cells were cultured in fresh media for

48 hrs and then continuously cultured in the presence of G418 for 12days. Colony

formation was visualized by removing media and briefly staining plates with methylene

blue. Colonies were counted and multiplied by dilution factor to determine the cfu/mL

virus.

pKOF2-Prep1-GFP and *MIGR1* do not have a G418 resistance cassette and are

thus unable to be subjected to viral titrations by this methodology. To measure quality

viral particle generation, I infected Rat1A cells with 1:10 and 1:100 dilutions of virus and

tested for GFP positivity using FACS analysis on a LSR-FORTESSA (BD BioSciences,

Franklin Lakes, NJ).

Isolation and purification of bone marrow stem/progenitor cells

Analysis of *MLL-AF9* in a murine model was performed using murine bone

marrow stem and progenitor cells transformed with *MLL-AF9*-expressing retrovirus. Murine bone marrow was collected and transformed consistent with previous experiments performed by our lab. Briefly, C57BL/6 mice were euthanized with gaseous CO_2 and immediately dissected under sterile conditions to remove legs. Tibia and Femur bones from both hind legs were isolated and epiphyses were removed. Bone marrow was collected in 2% FBS supplemented media by flushing diaphyses with 1 mL media through a 25G needle. Cell aggregates were dispersed and a single cell suspension was generated by additional passing through a 1 mL syringe and 25G needle. Collected cells were washed in chilled PBS supplemented with 2% FBS. To obtain a population of white blood cells, red blood cells were lysed by incubating in red blood cell lysis buffer (155 mM NH_4Cl, 11.9 mM $NaHCO_3$, 100 nM EDTA) for 5 mins on ice.

Bone marrow was enriched for c-Kit+ (CD117) stem and progenitor cells using EasySep Positive selection kit (Stemcell Technologies, Vancouver, BC, Cat# 18056) according to the manufacturer's protocol. EasySep purification utilizes antibodies directed against surface markers used to characterize sub-populations of cells.

Briefly, bone marrow was suspended in PBS+2%FBS at a concentration of ($1x10^7$ cells/mL). 70 µL of CD117-PE labeling reagent was added and incubated in the hood for 15 mins. 70 µL of PE selection cocktail was added and solution was incubated for an additional 10 mins. 50 µL of magnetic nanoparticles were added and mixture was incubated for 10 mins. Cells were purified by washing 3 times in PBS+5%FBS. To wash cells, tubes containing magnetically labeled cells were placed into magnet for 5 mins. After 5 mins, tubes were gently inverted to decant supernatant. Tubes were then removed

from magnet and an additional 500 µL of PBS was added to each tube. After c-kit

positive selection, cells were counted and were activated overnight in RPMI+10%FBS

supplemented with cytokines.

Infection of bone marrow cells

Retroviral infection was performed to introduce a human *MLL-AF9* fusion to

murine c-kit+ progenitor cells for AML transformation. After c-kit+ selection, cells were

activated overnight in a 96 well plate in RPMI+10%FBS supplemented with cytokines

(10 ng/mL each of IL-6, IL-3, and 100 ng/mL SCF).

Spinoculations were prepared in 1 mL volumes as follows: one 750 µL aliquot of

virus, 7.5 µL HEPES, 1 µL polybrene (4 µg/ul), 30 µL cells (at 1×10^6 cells/mL). For viral

infection, cells were centrifuged at 3000 rpm for 4 hrs at 33° C on 2 successive days.

Between spinoculations, each sample was rested overnight in 100 µL of RPMI + 10%

FBS supplemented with cytokines (10 ng/mL each of IL-6, IL-3, and 100 ng/mL SCF) in

96 well plates. Cells were put into methylcellulose colony assays immediately after the

second day of infection.

Murine methylcellulose colony assay

Murine cells were plated in H3234 Methocult supplemented with IL-3 (10

ng/mL), IL-6 (10 ng/mL), and SCF (100 ng/mL) cytokines. Murine cells were plated at

concentrations between 10k cells/plate and 500 cells/plate, depending on growth the

previous week and on anticipated colony number.

Cells were put into methylcellulose colony assays immediately after the second

day of infection. For antagomir treatments, appropriate cell volumes were added to a 5

mL FACS tube containing a antagomirs, 10X PBS to compensate for antagomir volume, and RPMI+10% FBS totaling 100 µL. Cells were incubated on ice for 30 mins and at room temperature for 5 mins as specified by the Grimes lab protocol. After incubation, cells were immediately transferred to a 1.5 mL microcentrifuge tube containing antagomirs (2.3 µL for 100 nM treatment and 4.6 µL for 200 nM treatments), cytokines (IL-3, IL-6, and SCF totaling 9.9 µL), G418 (82.5 µL for the first week) and media to 600 µL. This mixture was added to thawed methylcellulose aliquots (2.7 µL each), and mixed via vortexing. 1.1 mL of the resulting mixture was added to culture dishes using a 3 mL syringe with a blunt end needle.

The initial round of plating for colony assay additionally included G418 at 10 ng/mL to select for successfully infected cells. All platings were set up in duplicate. Colonies were counted at day 7 on a Leica DMIL inverted microscope and photographed using a Cannon PowerShot SD1000, at 7.1 MP. Cells were collected under sterile conditions by washing each plate with 2 mL PBS 3 times and collecting into a 50 mL Falcon tube containing 30 mL of PBS. Cells were centrifuged for 10 minutes at 1500 rpm in a floor centrifuge. PBS was aspirated, and cells were resuspended in 0 .5 – 5 mL of fresh PBS. Cells were counted by hemocytometer and total cell number was calculated for each colony assay. For weeks 1-3, cells were re-treated with antagomir according to the protocol described above. At week 4, all remaining cells were collected for RNA.

Slides were prepared for inspection of cellular morphology. 2.5×10^4 cells were centrifuged onto positively charged slides at 1000 rpm for 4 minutes on a Thermo Cytospin 4 (Thermo Scientific, Cat# 3120110). Slides were air dried and stained with

Hema 3 Wright Giemsa stain (Fisher Scientific, Waltham, MA, Cat# 23-122-929, 23-122-937, 23-122-952) for 15 seconds with each stain. Slides were visualized on an Evos imagecore microscope (Life Technologies, Carlsbad, CA).

Cloning and screening strategy

Luciferase reporter constructs were generated by cloning the 3'UTR of *PKNOX1* into the pmiR-Report system (obtained from Dr. Jianjun Chen, University of Cincinnati). Wild-type reporter construct was cloned from human genomic DNA as described below.

PKNOX1 3'UTR was amplified using forward and reverse primers (Integrated DNA Technologies, Skokie, IL) indicated in Table 3. The 3'UTR for *PKNOX1* is transcribed from within a single exon of *PKNOX1*. Thus, PCR amplification could be performed on genomic DNA without potential inclusion of intronic sequence. PCR was performed utilizing a high-fidelity recombinant polymerase, Phusion Taq (NEB, Ipswich, MA, Cat# M0530) according to manufacturer's guidelines. Amplification reactions were set up as follows: 1 µL (100 ng) human genomic DNA template, 2.5 µL (0.25 µM) Forward Primer, 2.5 µL (0.25 µM) Reverse primer, 5 µL 10X PCR Buffer, 1 µL dNTPs, 0.5 µL Taq, and 32.5 µL water to volume. Amplification reactions were performed in a ThermoHybaid PCRExpress PCR block. Cycling parameters were set as follows: 5 mins at 95˚ C, and 35 cycles at 95˚C for 30 sec, 65˚C for 30 sec, and 68˚C for 5 mins, and 68˚C for 5 mins.

The amplification product was electrophoresed on 1 % agarose gels and the appropriately sized band (3.5 kb) was excised and purified by Qiaex II gel extraction kit (Qiagen, Hilden, Germany, Cat# 20021). The resulting PCR amplicon was sequentially

digested with MluI and SpeI in parallel with the pmiR-Report vector. Ligations were set up at a 1:3 vector:insert ratio using the NEB ligation kit (NEB, Ipswich, MA, Cat# M0202). Ligation was set up as follows: 1 µL vector (25 ng), 12.1 µL insert (75 ng), 1 µL T4 DNA Ligase, 2 µL ligation buffer, water to 20 ul. Ligations were incubated overnight at 16˚C.

Ligation mix was transformed into chemically competent DH5a *E. coli*. Briefly, chemically competent bacterial cells were thawed on ice for 10 mins and added to a pre-chilled 14 mL round bottom polypropylene tube with 1 µL of ligation mix. Mixture was sequentially incubated on ice for 30 mins, at 42˚C for 45 seconds, and ice for 5 mins. 900 µL of pre-warmed SOC media was added and cultures were incubated with rotation (225 rpm) at 37˚C for 1 hour. Bacterial cells were plated on Ampicillin-LB plates. Potential positive transformants were picked and grown in 2 mL LB-AMP. 1.5 mL was used for a column free miniprep. Plasmid was digested with cloning enzymes (MluI and SpeI) to test for the presence of insert. If insert is present, it will be apparent on a gel after digestion.

Table 3. Primers for cloning luciferase constructs

Amplicon	Primer sequence (5'→3')	
PKNOX1	Forward:	GGACTAGTCCTGGTCTTGGAGAACAGTGACT
	Reverse:	CGACGCGTCGCTTTGATAAATCAATTGCTTCAC

Primers for cloning the 3'UTR of *PKNOX1*

Site directed mutagenesis and screening strategy

Specific mutations were generated to remove the individual miRNA binding sites

from the *PKNOX1* 3'UTR. To make multiple mutations simultaneously, I used the

Stratagene Multi-Site Directed mutagenesis kit (Stratagene, La Jolla, CA, Cat #200514).

Multiple primers directed against the same strand of DNA may be added to the reaction

simultaneously. As the extended strand meets the next downstream primer, a ligase

present in the enzyme mix seals the nick in the DNA, allowing for multiple primer-

mediated mutations to be incorporated simultaneously. The resulting single stranded

product is suitable for transformation. The *PKNOX1* 3'UTR possesses 6 putative binding

sites for miRNAs from the *miR-17-92* cluster. Because of proximity of the sites to be

mutated and the decreased efficiency of introducing too many mutations simultaneously,

site directed mutagenesis was pursued in two separate multi-site directed mutagenesis

rounds. *pmiR-Report-Pknox1* 3'UTR (wt) was used as a template for initial mutagenesis,

with primers designed to mutate either MRE1, MRE5, MRE6 or MRE2, MRE3, MRE4.

Compound mutation of the *miR-17* family MREs was generated by subjecting a plasmid

with only MRE1 to additional mutagenesis using the primer for MRE4. Compound

mutation of all putative MREs was achieved by subjecting a compound mutant (MRE1,

MRE5, and MRE6) to additional mutagenesis (for MRE2, MRE3, and MRE4). Primers

and mutations are depicted in Table 4.

Mutations to ablate miRNA binding were made by changing multiple nucleotides

within the seed match of the mRNA. To facilitate a screening strategy of restriction

mapping, seed match sites were converted to restriction enzyme sites recognized by

enzymes that would only cut once in the wild type plasmid.

Site directed mutagenesis reactions were set up according to the manufacturer's instructions. Both rounds of mutations utilized the same reaction mix proportions. Reactions were set as follows: 1 µL template (100 ng), 1 µL of primer 1 (100 ng), 1 µL of primer 1 (100 ng), X µL of primer 3 (100 ng), 1 µL of enzyme, 2.5 µL of 10X reaction mix, 1 µL dNTPs mix, 1 µL multi-enzyme mix, and ddH20 to 25 µl. Amplification reactions were performed in a ThermoHybaid PCRExpress PCR block. Cycling parameters were set as follows: 5 mins at 95° C, and 40 cycles at 95°C for 30 sec, 55°C for 30 sec, and 65°C for 10 mins. Resulting PCR products were cleared of template plasmid by DpnI digestion. DpnI only digests methylated DNA. DNA methylation occurs in bacteria, but not in PCR amplification. Restriction digestion of DNA with DpnI would eliminate only the template bacteria, but not the resulting mutants, which were generated via PCR. 1 µL of DpnI was added to each reaction mix and incubated for 15 minutes at 37°C. 1 µL of resulting mix was transformed into XL-10 Gold competent cells, per manufacturer's instructions (Competent cells provided with kit).

To screen for positive mutants, transformant colonies were picked and grown in 2 mL LB with ampicillin. 1.5 mL was subsequently purified by column-less miniprep. Plasmids were digested using HindIII or MluI. Incorporation of any mutations by site directed mutagenesis would result in an increasingly fragmented digestion pattern, with compound mutants incorporating all mutations producing a very fragmented product.

Table 4. Primers for mutagenesis of *PKNOX1* 3'UTR

Target	Primer sequence (5'→3')
PKNOX1 MRE1 (Δ19ab)	GCAGGAGCAGAACCGCACCTGACTTTTTGGAG*AAGCTT*CAGCAAACATTTTACACAGTTTTATTTCTAA
PKNOX1 MRE2 (Δ17,20)	TTTCTAATATGTTTTATATGTAGATATAGAAGAGTG*ACGCG*TTGTATTTCATAGTAAGCTTAAAGCGCGTCTTTGCC
PKNOX1 MRE3 (Δ18)	CAGCATGTTTGAGGTCAGTTGG*ACGCG*TAAAACACCTGTTCTCCAGCCC
PKNOX1 MRE4 (Δ17,20)	GCCTGTGTGAGGTAGCAGTGGG*ACGCG*TTCATTGAGACAAACTCCAGGG '
PKNOX1 MRE5 (Δ92)	CCCAGGCTGGAGGGCAATGG*AAGCT*TCTCAGCTCACTGCAACCTC
PKNOX1 MRE6 (Δ92)	CCCAGGCTGGAGGGCAATGG*AAGCT*TCTCAGCTCACTGCAACCTC
vector internal	GCACCCCAGGCTTTACACTTTATGCTTCCGGCT

The above table depicts the primers utilized for mutagenesis. All primers from the same strand. miRNA Response element in red. Unaltered nucleotides within the seed region in blue. Restriction sites in Orange or Green. Purine to pyrimidine changes (and vise versa in bold. Nucleotide changes italicized.

Putative positives were regrown and plasmids were prepared with miniprep kit to provide

a cleaner plasmid prep suitable for sequencing. Plasmids were then sent to ATCC for

sequencing using both pmiR Forward and pmiR Reverse plasmids. Internal sequence of

the *PKNOX1* 3'UTR was out of range of end primers and was sequenced utilizing internal

primers specific to the *PKNOX1* 3'UTR: PKNOX1 seq1 and PKNOX1 seq2 (Table 5).

Table 5. Primers for sequencing *PKNOX1* luciferase construct

Target	Primer sequence (5'→3')
pmiR Forward	CCCTTGAACCTCCTCGTTCGACC
pmiR Reverse	GAGACGTGCTACTTCCATTTGTC
PKNOX1 seq1	TGAAATGGTAGCCAGTGACCCGTT
PKNOX1 seq2	AATGGTGCAATCTCAGCTCACTGC

The above table indicates the primers utilized for sequencing of pmiR-Report constructs

RNA isolation and cDNA synthesis

RNA was extracted from cells treated with antagomirs for 72 hrs in liquid culture

using Sigma TRI Reagent (Sigma Aldrich, St. Louis, Cat# T9424) according to

manufacturer's instructions. Briefly, cell pellets were collected in a 1.5 mL

microcentrifuge tube and spun down at 3000 rpm. Cells were resuspended in .5 mL - 1

mL of TRI reagent under a fume hood (according to cell number) Once mixture was

homogenous, cells were frozen and stored at -80˚ C for later use.

RNA collection was performed under RNAse free conditions using filter tips. All

workspaces and pipettes were cleaned with RNAse Zap (Life Technologies, Carlsbad,

Cat# AM9782) prior to use. RNA samples were thawed and processed according to TRI

reagent standard protocol. Briefly, 200 µL of chloroform was added per mL of TRI

reagent used. Mixture was inverted vigorously 15 times to mix samples. Samples were

separated by centrifugation at 13000 rpm at 4˚C in a microcentrifuge. The aqueous layer

was removed and added to a microcentrifuge tube containing 560 µL Isopropanol/mL

TRI reagent used. After a 15 minute incubation, RNA was precipitated by centrifugation.

Pellet was washed once in 70% ethanol and air dried. Pellets were resuspended in

nuclease free H$_2$0 and dissolved at 65˚C for 1 hour. Resulting RNA mix was subsequently handled on ice in an RNAse free environment.

cDNA synthesis was performed using 10 ng of total RNA using Applied Biosystems miRNA Reverse Transcription kit (Life Technologies, Carlsbad Cat# 4366596) according to manufacturer's protocol. RNA was quantified and quality was assessed using a Nanodrop 2000. RNA was normalized to a concentration of 100 ng/μL and subsequently diluted to a working concentration. 10 ng of RNA was used per reverse transcription (RT) reaction. For each sample, separate RT reactions were performed for each RNA or control to be quantified. To control for potential discrepancies in RNA level/quality between tubes, a master mix was made for each sample with all components except the RT primers. The appropriate master mix was then added to the RT tube with the appropriate RT primer. Reverse transcription reactions were performed in a Thermo Hybaid PCR Express Cycler using the following cycling parameters: 16° C for 30 mins, 42° C for 30 mins, 85° C for 5 mins, 4° C hold.

Quantitative real-time polymerase chain reaction

To determine relative miRNA levels, quantitative real-time PCR was performed on an Applied Biosystems 7300 cycler using Applied Biosystems Taqman assays for *hsa-miR-17-5p*, *hsa-miR-19a*, *hsa-miR-196b*, or *RNU6*.

Quantitative real-time PCR was performed in technical triplicates. Master mixes were prepared for each reaction in excess of 3 fold the amount required for complete reaction. TaqMan small RNA assay kits were utilized for *hsa-miR-17*, *hsa-miR-19a*, *hsa-miR-196b*, and *RNU6*. Each reaction consisted of 1 μL TaqMan Small RNA Assay

(20X), 10 μL TaqMan Universal PCR Master Mix II, 7.67 μL RNAse free H20, and 1.33 μL of cDNA product. PCR reactions were prepared in the dark. Plates were spun down for 2 mins at 1000 rpm to collect sample at bottom of plate.

Cycling parameters for qPCR were defined by the kit manufacturer. Briefly, cycling condition were as follows: 50˚C for 2 minutes, 95˚C for 10 mins, and 40 cycles of 95˚C for 15 seconds, 60˚C for 1 minute. "No template" controls were run to verify that contamination was not present. Data was analyzed using the Delta Delta Ct ($2^{-\Delta\Delta Ct}$) method with *RNU6* serving as a control [245].

Human methylcellulose colony assays

Methylcellulose colony assays for human cell lines were performed using H4100 Methocult methylcellulose (Stemcell, Vancouver, Cat# 04100) supplemented with a final serum concentration of 10% FBS. Methylcellulose colony assays were performed in 12-well plates.

To ensure consistent results, human cell lines were maintained at >90% viability for at least 3 days prior to use in any methylcellulose assay. Immediately prior to treatment, cells were counted and resuspended at a concentration of $1X10^5$ cells/mL. Because each cell line has a different clonogenic potential, each cell line was plated in methylcellulose at different concentrations (numbers given for treatment in 12-well plate): MOLM-13 (100 cells/well), MV4-11 (1000 cells/well), RS4;11 (250 cells/well), HL-60 (250 cells/well), U937 (250 cells/well). Antagomir treatment concentrations were empirically determined for the MLL fusion-containing cell lines and were set to 1-2 μM).

Non-MLL cell lines were treated at 2 µM to be equivalent to highest treatment
concentrations.

Appropriate cell numbers were then added to a 1.5 mL microcentrifuge tube
containing antagomirs (1.65 µL for 1 µM treatment, and 3.3 µL for 2 µM treatment).,
10X PBS to compensate for antagomiR volumes, and media +10% FBS to a final volume
of 550 µL . The resulting solution was then gently pipetted into a FACS tube containing
(1.1 mL) methylcellulose and mixed by briefly by vortexing. 550 µL of the final
cell/antagomir/methylcellulose mixture was added to each well in a 12-well plate in
duplicates. Individual colonies were counted on Leica DMIL inverted microscope and
photographed using a Cannon PowerShot SD1000, at 7.1 MP after 7-8 days in culture for
MV4-11, MOLM-13, RS4;11 and K562. THP1 colonies were cultured for 14-15 days.
Combinatorial treatments were counted on a Leica DMIL inverted microscope and
photographed using a Nikon camera.

To collect cells, 1 mL of PBS was added to each well to diluted methylcellulose.
Methylcellulose was gently rinsed from the plate and subsequently washed 2 times with
PBS. Each duplicate experiment was resuspended in a total of 12 mL PBS. Cells were
spun down and resuspended in PBS (.1-2mL) for counting, collecting for slides,
collecting for FACS, etc. Colonies were viewed under a Nikon microscope and imaged
with Olympus DP21 imaging system at 100X.

Cell proliferation Assay

To asses cell proliferation I used the Cell-Titer-Glo assay (Promega, Madison,
Cat# G7570). This assay measures cell number indirectly by measuring the ATP content

in a luminescent assay. Because ATP content remains constant across live cells,

quantification of ATP may be used to indirectly quantify the total number of live cells.

Cells were counted and resuspended at 100k cells/mL in culture medium under sterile

culture conditions. Cells were added to a mixture of antagomirs, 10X PBS, and culture

media to yield a final concentration of 50k cells/mL, 1-2 µM antagomirs (specified in

figure legends), and 10X PBS to compensate for antagomir volumes. Cells were plated in

96-well plates in triplicate with 100 µL of cell/antagomiR mixture per well in 3

independent experiments. Cell viability was assessed after 4 days of antagomir treatment

using Promega Cell-Titer-Glo kit (Promega, Madison, Cat# G7570) according to

manufacturer's instructions. Briefly, cells in 96 well plates were gently resuspended by

pipetting up and down. 15 µL of cells were subsequently added to 85 µL of media in a

white opaque plate, 100 µL of Cell Titer Glo reagent was thawed at room temperature in

the dark and subsequently added to the cell –media mixture.

Luminescence was measured on a Glomax 96 microplate luminometer using the

default program setting. Integration time was set at 0.5 seconds/well for all samples.

Averages of 3 triplicates were averaged for each sample tested. Remaining cells were

collected for cell cycle analysis.

Murine *MLL-AF9* transformed bone marrow cells were examined for cell viability

in culture after infection with either *MIGR1*, *MSCV-Meis1-pgk-EGFP*, or *MSCV-pKOF2-*

Prep1-GFP. Similarly to human cell lines, viability was assessed using Cell-Titer-Glo

assay (Promega, Madison, G7570). GFP+ cells were plated at 50k cells/mL in 100 µL in

96 well plates. At given time points, 15 µL of cells were removed from media and

subsequently added to 85 µL of media in a white opaque plate, 100 µL of Cell Titer Glo reagent was thawed at room temperature in the dark and added to cell–media mixture. Luminescence was measured on Glomax 96 microplate luminometer using the protocol utilized for human cell lines.

<div align="center">**Cell cycle analysis**</div>

To determine cell cycle distribution, cells were fixed and stained with propidium iodide (PI) and analyzed via FACS. Propidium iodide (PI) is a fluorescent DNA intercalating agent that readily enters fixed cells and can subsequently be used to quantify the amount of DNA in a particular cell. Because DNA is synthesized during replication, the quantity of DNA can be used to indicate whether a cell is actively cycling.

To determine cell cycle distribution upon antagomir treatment, all three replicates from each sample of the previous cell viability were collected and pooled in a 5 mL FACS tube. Cells were washed once with 3 mLs of PBS+5%FBS and fixed in ice-cold 70% Ethanol. Cell suspension was stored at -20˚C overnight for fixation. Cells were then washed in PBS + 5% FBS and resuspended in 250 µL PBS solution containing RNAse A (10 µg/mL) to eliminate free RNA that would potentially confound results. 250 µL PBS with propidium iodide (100 µg/mL) was then added to the mixture to yield a final concentration of 5 µg/mL RNAse A and 50 µg/mL propidium iodide. Cells were incubated on ice for 1 hour prior to FACS analysis. Samples were analyzed on a FACS-CANTO II and data was processed analyzed using Flowjo Software Package (Version 9.03). Cell cycle distribution was determined using the Watson Pragmatic function within FlowJo. Total live cell number was counted and percentages were calculated with MS

Excel.

Luciferase reporter assays

Luciferase reporter assays were performed in HEK293T cells using the pmiR-Report system. pmiR-Report constructs possess a luciferase gene driven by a CMV promoter. A multiple cloning site downstream of the luciferase cassette allows cloning of a valid 3-UTR into the plasmid. Co-transfection with wither miRNA expressing plasmids, synthetic miRNAs, or miRNA inhibitors, provide a platform with which to test miRNA:mRNA relationships. HEK293T cells were plated at 6.0×10^5 cells/well in 24 well plates. After 24 hours, cells were co-transfected with a reporter construct containing either the 120 ng of *pmiR-Report* reporter construct (wild-type or mutant 3'UTR for *PKNOX1*, 10 ng of a control Renilla luciferase construct, and 600 ng of either *MSCV-PIG* or *MSCV-PIG-miR-17-19b*. Cells were cultured for 48 hrs and collected for luciferase analysis with the Promega Dual-Luciferase Reporter Assay System (Promega, Madison, #E1910) according to manufacturer's instructions. Due to the relatively loose attachment of HEK293T cells to a plate, chilled washing PBS was added directly to the well. Plates were swirled and PBS was used to rinse cells loose from plate. Cells were collected into 1.5 mL microcentrifuge tubes and centrifuged at 3000 rpm to pellet cells. PBS was removed by aspiration and cells were resuspended in 1X Passive Lysis buffer and kept at -20° C for future analysis. For experimental analysis, lysate was diluted 1:20 fold to bring luciferase concentration into the linear range of the luminometer immediately prior to luminometer measurements.

Luciferase activity was measured on a Femto manual luminometer using default

machine settings. 10 µL of each sample was added to the bottom of a 1.5 mL

microcentrifuge tube. 50 µL of LARII buffer was added to each tube and gently pipette

up and down to mix solution. Sample was immediately read in the machine to obtain

level of Firefly luciferase activity. 50 µL of freshly prepared Stop and Glo reagent was

added to each tube and briefly vortexed. Samples were immediately read to obtain

Renilla Luciferase activity level. To ensure fidelity of experimental reads, dilution levels

of samples was kept low enough to ensure that sample reading were below 10 million and

remained steady during the course of the integration time. Experiments were performed

in triplicate and measured in duplicates.

Protein isolation and western blotting

To collect proteins, cells were collected into a 1.5 mL microcentrifuge tube and

washed once in chilled PBS. Cell pellets were snap frozen on dry ice and stored at -80˚C

for future use. Cell pellets were handled in a manner determined by cell line. Pellets from

human leukemia cell lines were thawed on ice in 1X SDS loading buffer. Cells from

HEK293T cells were resuspended in IPH buffer (50 mM Tris-HCl, 150 mM NaCl, 5mM

EDTA, .5% NP-40) supplemented with 1:100 freshly added Protease inhibitor cocktail

(Sigma Aldrich, St. Louis, Cat# P8340). Cells were resuspended in IPH at a

concentration of $1x10^7$ cells/mL. If cells were not used for a co-IP experiment, they were

sonicated for 4 pulses at 20% power.

Cell pellets were thawed on ice in IPH buffer. Appropriate quantities were

mixed with 5X SDS loading buffer (250 mM Tris pH6.8, 500 mM DTT, 10% SDS, 0.5%

Bromophenol Blue, 50% Glycerol). Lysate solution was boiled for 5 minutes and

subsequently centrifuged at 13000 rpm for 5 mins at 4° C to clear lysate of any cellular debris.

Lysates were separated by Sodium Dodecyl Sulfate –Poly Acrylamide Gel Electrophooresis (SDS-PAGE). Gels were cast using the BioRad Mini-PROTEAN system. Gels were comprised of a 10% resolving gel (40% Acrylamide 2.5 mL, 1.5M Tris pH8.8 = 2.5 mL, 10% SDS = 100 ul, 10% APS = 50 ul, TEMED = 10 ul), and a 4% stacking gel (40% Bis-Acrylamide .5 mL, 1M Tris pH=6.8 = .625 mL, 10%SDS 50ul, 10% Ammonium Persulfate = 25 ul, TEMED = 5 ul, ddH2O 3.8 mL, TOTAL 5mL).

Samples were loaded into the gel and run in parallel with 5 µL of Kaleidescope ladder (BioRad, Hercules, Ca, Cat# 1610324). Gels were run in 1X Tris-Running buffer (15.1g Tris pH8.8, 94g Glycine, 5g SDS, H20 1L) at 50V for 15mins to condense protein into stacking gel, and 150V until dye front reached the bottom of the gel. Protein was transferred to Nitrocellulose membranes (BioRad, Hercules, Ca, Cat# 170-4158, 170-4159) using Trans BlotTurbo transfer system (BioRad, Hercules, Ca, Cat# 170-4155). BioRad, Hercules, Ca 1.5 mm gel program was used (2.5A, 25V, 10 mins). Transfer was verified by staining membrane briefly in .5% (w/v) Ponceau S solution (Sigma Aldrich, St. Louis, Cat # P7170), and subsequently washing in PBS-T until Ponceau stain was fully removed. Membranes were blocked overnight at 4˚C in blocking solution (PBS, .5% Tween, 5% dry milk).

Membranes were probed with anti-PKNOX1 (N15) (Santa Cruz Biotechnology, Santa Cruz, Cat# SC-6245) at 1:1000 in blocking buffer, anti-PBX1/2/3 (C-20) (Santa Cruz Biotechnology, Santa Cruz, Cat# SC-888) at 1:1000 in blocking buffer, anti-MEIS1

(Milipore, Billerica, MA, Cat# 05-779)) at 1:1000 in blocking buffer, anti-HOXA9

(Milipore, Billerica, MA, Cat#07-178) at 1:1000 in blocking buffer, or anti-Actin (Sigma

Aldrich, St. Louis, A5441) at 1:8000 in blocking buffer. Secondary antibody probing was

performed with TrueBlot anti-rabbit (eBioscience, San Diego, Cat# 18-8816-31) at

1:1000 in blocking buffer, anti-mouse-HRP (GE Life Sciences, Piscataway, NJ, Cat#

NA931VS) at 1:8000 in blocking buffer, or anti-Rabbit-HRP (GE Life Sciences,

Piscataway, NJ, Cat# NA934VS) at 1:8000 in blocking buffer. Western blots were

imaged using a Fuji LAS-3000 lightbox system. Images processed using MultiGauge

v3.0.

Co-immunoprecipitation assays

Cells for co-immunoprecipitation were collected and washed once in PBS. Cell

pellet was resuspended in IPH buffer (50 mM Tris-HCl, 150 mM NaCl, 5mM EDTA,

.5% NP-40) with 1:100 freshly added Protease inhibitor cocktail (Sigma Aldrich, St.

Louis, Cat# P8340). Co-Immunoprecipitation was performed in IPH buffer using

Agarose A beads (Santa Cruz Biotechnology, Santa Cruz, Cat# SC-2001) incubated

overnight at 4° C with $1.5X10^6$ cells. Equilibration and washes were performed with IPH

buffer with 1:1000 freshly added Protease inhibitor cocktail (Sigma Aldrich, St. Louis,

Cat# P8340).

20 µL of beads were used per reaction. Beads were equilibrated to IPH buffer by

washing beads IPH buffer with 1:1000 Protease inhibitor cocktail (Sigma Aldrich, St.

Louis, Cat# P8340) 3 times. For each wash, beads were pooled into a 1.5 mL

microcentrifuge tube and 500 µL of buffer was added. Mixture was vortexed briefly and

spun down at 6000 rpm for 30 seconds. Supernatant was removed, careful not to disrupt bead pellet. For the final round of equilibration, bead/buffer mixture was aliquoted to separate microcentrifuge tubes to the equivalent of 20 µL of beads per tube. After final round of equilibration, cell lysates from 150k cells was added to each tube in a volume of 150 ul. 5 µL of PBX1/2/3 antibody (Santa Cruz Biotechnology, Santa Cruz, Cat# SC-888) was added to each tube and gently mixed by flicking the tube several times. The lysate solution was incubated with beads and antibody at 4° C overnight on a rocker to allow complex-bead interactions to form. After incubation, beads were washed 3 times with 500 µL of IPH buffer (plus 1:1000 protease inhibitor cocktail), and resuspended in 30 µL of 2X SDS lysis buffer and boiled for 10 mins at 95° C. Lysate was cleared of Protein A beads by 10 mins of centrifugation at 13000 rpm at 4° C. 30 µL of each mixture was used for each well.

Colony assays for cells infected with Pknox1 expressing retrovirus

For the examination of *Pknox1* contribution to *MLL-AF9* transformed murine bone marrow subject to additional infections with either *MIGR1*, *MSCV-Meis1-pgk-EGFP*, or *MSCV-pKOF2-Prep1-GFP* were generated and checked for quality as described. After passing cells through methylcellulose for 4 weeks, cells were acclimated to liquid culture for 1 week and treated with additional spinoculations. I selected for successfully infected cells by FACS sorting for GFP positivity 48 hours after infection. Colony assays were performed over the course of 1 week, and were imaged.

FACS analysis of surface markers

Cell surface marker staining was performed on live cells to examine the

differentiation of cells after antagomir treatment. After 6 days of antagomir treatments,

cells from methylcellulose colony assays were isolated. 100k cells were suspended in a

chilled PBS + 2%PBS. Antibody panels were mixed into a master mix and added to

samples at a final dilution of antibodies. Cells were incubated in the dark, on ice for 20

minutes and washed with 500 µL of PBS+2%PBS. Cells were resuspended in 250 µL

PBS+2%FBS

Cell surface marker staining was performed as previously described [23] using

fluorophore conjugated antibodies against CD117-APC (eBioscience, San Diego, Cat#

17-1171-82), CD11B-PE (eBioscience, San Diego, Cat# 12-0112-85), GR-1-PE-Cy5

(eBioscience, San Diego, Cat# 15-5931-81). FACS analysis was performed with initial

gating on live cells. Secondary gating was for GFP + cells. Subsequent gates were

drawn by excluding cells in a negative control. Data was processed using FlowJo

Software Package.

CHAPTER 4

RESULTS

Antagomir uptake occurs in a dose dependent manner

Previous studies by our lab and others have utilized 'antagomirs' to examine the role of miRNA in MLL leukemia in a mouse model [11, 234, 235]. Characterization of the 'antagomir' pattern of modifications was initially performed *in vivo*, studying the knockdown of *miR-122* in the liver [232, 233]. To characterize uptake *in vitro*, cells were treated with a fluorescently labeled antagomir, and examined by FACS analysis, with antagomir uptake being detectable as an increase in fluorescence (Figure 9). As a negative control, cells were treated with *anti-Ce-miR-67*, while uptake was observed in treatments with *anti-Ce-miR-67-DY547*, an antagomir with a fluorescent label conjugated to the 5' end. Both *anti-Ce-miR-67* and *anti-Ce-miR-67-DY547* are designed to target a *C. elegans* miRNA that has no mammalian homolog. If antagomirs are taken up by the cells, then fluorescence would increase, indicated by a rightward shift in the FACS plot. Uptake was examined in THP1 cells (described in Methods) and *MLL-AF9* transduced murine bone marrow utilizing three different treatment regimens: 1) a superficial addition of antagomirs to the media at the final treatment concentration without any additional steps, 2) superficial addition with pre-incubation at 10X the final treatment concentration (as described in Materials and Methods), or 3) transfection by Lipofectamine 2000 (Figure 9). For THP1 cells, pre-incubation did not alter the uptake of fluorescently

labeled antagomir compared to superficial addition of antagomir to the media without

pre-incubation (Figure 9). For both superficial antagomir treatment and superficial

treatment with pre-incubation, *anti-Ce-miR-67-DY547*-treated THP1cells fluoresced at a

narrow peak centered to the right of the negative control, indicating that antagomir uptake

was both robust and very uniform. Lipofectamine treatment resulted in two populations

of cells with a very broad distribution of fluorescence indicating a lack of uniformity in

cellular uptake of antagomirs when introduced by Lipofectamine. The majority of cells

were positive for antagomir uptake, and the most brightly fluorescent cells were much

brighter than those treated with either the superficial addition or superficial addition with

pre-incubation. However, approximately 11% remained negative for fluorescence.

Antagomir uptake for *MLL-AF9*-transduced bone marrow was similar to that observed

for THP1 cells. However, antagomir uptake after treatment with the superficial addition

with pre-incubation protocol resulted in a slightly broader peak with an increase in the

most fluorescent cells, indicating an improved uptake for at least a small subset of cells.

As with THP1 cells, Lipofectamine treated *MLL-AF9* transformed bone marrow cells

were distributed into two populations with a very broad distribution of antagomir uptake.

Lipofectamine antagomir treatment resulted in a very high level of uptake compared to

either superficial addition or superficial with pre-incubation. However, approximately

45% of *MLL-AF9* cells remained negative.

To determine treatment concentrations for antagomirs, I treated multiple cell lines

with antagomir directed against either *anti-Ce-miR-67* or a fluorescent labeled *anti-Ce-miR-67-DY547* at concentrations of 20 nM, 200 nM, 500 nM, 1000 nM, and 2000 nM for

Figure 9. Antagomir uptake upon treatment with different methodologies
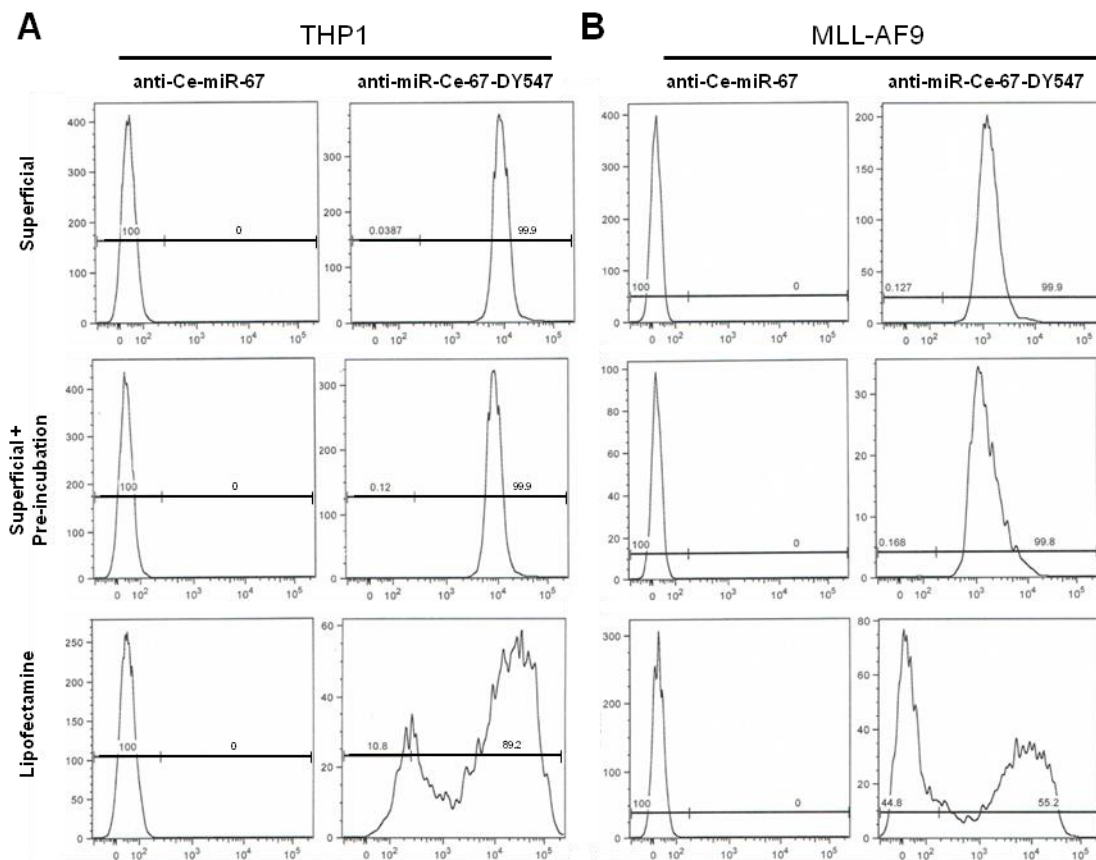
Antagomir treatments via different mechanisms of delivery. Antagomir uptake determined by FACS analysis for treatment with Grimes protocol (top), superficial addition (middle), and lipofectamine (bottom). Treatments were compared between a fluorescent labeled antagomir (*anti-Ce-miR-67-DY547*) and a non-fluorescent control (*anti-Ce-miR-67*). A) THP1 cells were examined with all three treatment regimens as a representative of human cell lines. B) *MLL-AF9* transformed bone marrow cells were examined with all three treatment regimens.

72 hrs and examined fluorescence by FACS analysis (Figure 10). As expected, treatment

with increasing concentrations of *anti-Ce-miR-67* without a fluorophore did not result in

fluorescence for any treatment. Treatment with *anti-Ce-miR-67-DY547* resulted in a

concomitant increase in fluorescence for MOLM-13, MV4-11, RS4;11, and *MLL-AF9*

transformed bone marrow. All treatments resulted in narrow peaks of fluorescence,

indicating uniform uptake at all treatment concentrations. The ratio of detected

fluorescence to treatment concentration remained linear even at the highest concentration,

indicating that 2 µM antagomirs treatment did not saturate the capacity for cells to take

up antagomirs. Antagomir uptake for each human leukemia cell line had roughly similar

patterns of uptake. *MLL-AF9* transduced bone marrow took up antagomir at a lower rate

than human leukemia cell lines. Further experiments for murine *MLL-AF9* utilized the

superficial with pre-incubation protocol, while treatment of human cell lines relied upon

superficial addition of antagomir to the media.

To determine the efficacy of antagomir treatment, I examined the capability of

antagomir treatment to reduce the levels of targeted miRNA.   Experiments examining

uptake do not indicate subcellular localization or function of the antagomirs, necessitating

further examination of antagomir function. To assess antagomir function, I treated

MOLM-13, RS4;11 and MV4-11 with antagomirs directed against *miR-17-5p*, *19a*, or

196b at concentrations of 1-2 µM (indicated in figure legend) and quantified target

miRNA levels relative to a control treatment (Figure 11). Both vehicle and *anti-Ce-miR-*

67 were used as controls to ensure that antagomir treatment did not result in a broad or

non-specific effect on untargeted antagomirs. *Anti-Ce-miR-67* is an antisense oligo

Figure 10. Antagomir uptake in human MLL leukemia cell lines
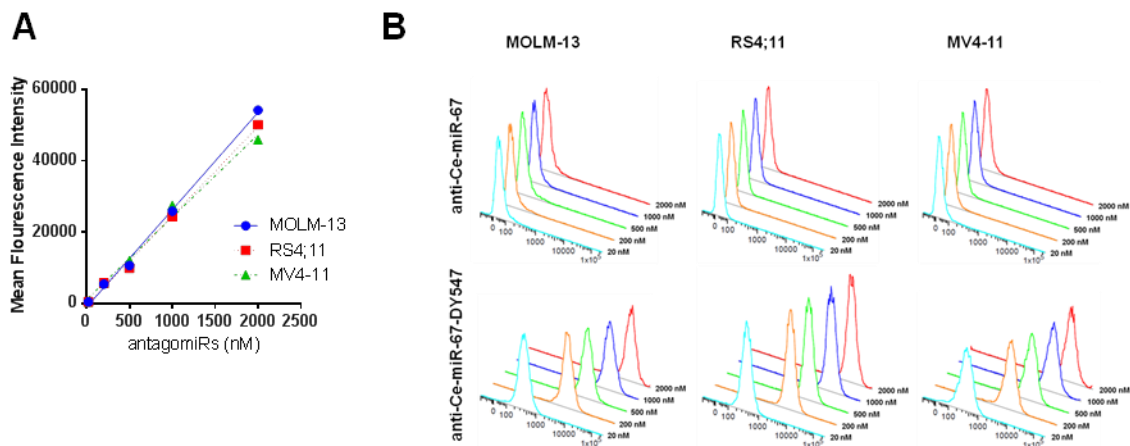
Antagomir uptake was determined by FACS analysis using a fluorescently labeled antagomir utilizing superficial antagomir treatment (20 nM – 2000 nM). A) Antagomir uptake quantified relative to treatment concentration. B) Treatments were compared between a fluorescent labeled antagomir (*anti-Ce-miR-67-DY547*) and a non-fluorescent control (*anti-Ce-miR-67*). Example plots of uptake for MOLM-13, RS4;11, and MV4-11 at 20 nM, 200 nM, 500 nM, 1000 nM, 2000 nM.

designed to hybridize with a miRNA from *C. elegans* with no homologous miRNA found in mammals. In antagomir treated cells, target miRNA levels decreased in response to antagomir treatments. *Anti-miR-17* treatment in MOLM-13, RS4;11, and MV4-11 resulted in a decrease to 16%, 5%, and 31%, respectively, when compared to *anti-Ce-miR-67*. When compared to vehicle, *anti-miR-17* treatment resulted in decreases to 2.5%, 7.8%, and 31% of *miR-17* miRNA levels of control treated cells. For MOLM-13, a non-specific decrease in *miR-17* and *miR-19a* levels was observed after treatment with *anti-Ce-miR-67* (data not shown). *MLL-AF9* transduced bone marrow cells were also tested for miRNA knockdown. Upon antagomir treatment with *anti-miR-196b*, relative levels of *miR-196b* decreased to 11% of levels observed in cells treated with *anti-Ce-miR-67*. Treatment concentration for all human cell line antagomir experiments was determined based on these standardization experiments.

Effect of individual antagomir treatment on colony forming ability of human leukemia cell lines

To examine MLL leukemia in a human model, I performed colony assays using human MLL leukemia cell lines (Figures 12-19). MOLM-13 was used to represent *MLL-AF9* gene fusion expressing leukemias, while MV4-11 and RS4;11 were used to represent *MLL-AF4* gene fusion expression leukemias. Colony assays were performed over the course of approximately 1 week and were not subjected to serial replating. While murine colony assays examined the role of miRNAs in the initiation of leukemia, human colony assays examine the role of miRNAs in cells that have previously been transformed. Similar to murine colony assays, I examined colony number, cell number,

Figure 11. Antagomir treatment results in a knockdown of target miRNAs.
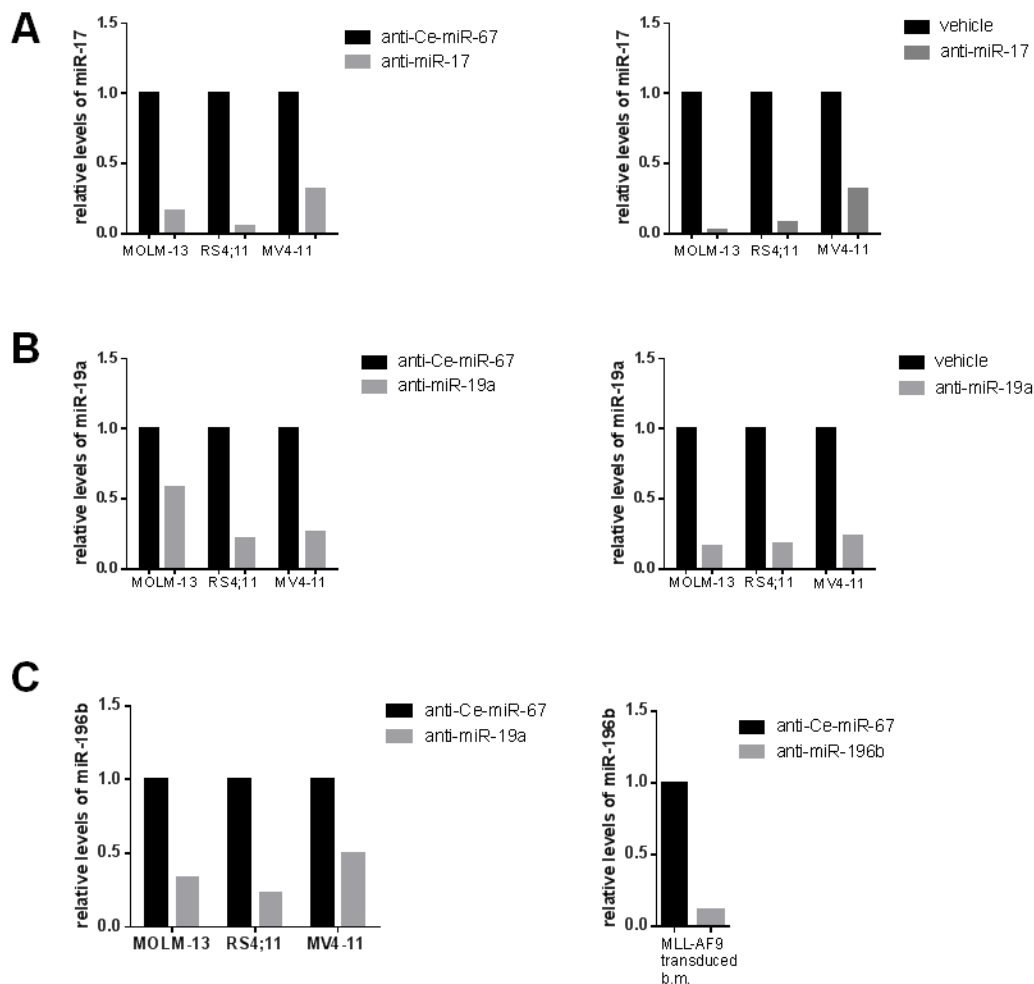
Antagomir mediated knockdown of target miRNAs was examined for *anti-miR-17*, *anti-miR-19a*, and *anti-miR-196b* in human. A) Antagomir treatment effects were examined for *anti-miR-17*. miRNA levels compared to cells treated with *anti-Ce-miR-67* (left) or vehicle (right). B) Antagomir treatment effects were examined for *anti-miR-19a*. miRNA levels compared to cells treated with *anti-Ce-miR-67* (left) or vehicle (right). C) Antagomir treatment effects were examined for *anti-miR-196b*. miRNA levels compared to cells treated with *anti-Ce-miR-67* in human cell lines (left) or in *MLL-AF9* transformed bone marrow (right).

colony morphology (Figures 12-19). I hypothesized that increased expression of individual miRNAs were essential for maintaining MLL leukemia cell proliferation and clonogenic capacity. MLL leukemia cell lines were treated with antagomirs directed against a subset of miRNAs overexpressed in MLL leukemia.

Colony assays were examined at 7-8 days after initial plating. Colony morphology was dramatically different from the standard murine colonies. While murine *MLL-AF9* transformed colonies are typically compact and consist of closer cell-cell contacts, human cell line colonies are widely diffuse and do not contain close cell-cell contacts. Number of cells plated per colony assay varied based on cell line as each cell line possesses a different baseline capability to form colonies. Colony assays were set up with a target of 70 colonies/plate. MOLM-13 cells were the most clonogenic with an approximate colony forming frequency of 1 colony per/2.04 cells (49.0%). RS4;11 formed colonies at a frequency of 1 colony per/3.34 cells (29.86%), and MV4-11 formed colonies at a frequency of 1 colony per/13.42 cells (7.45%).

Cells were treated with individual antagomirs using treatment methodology and concentrations determined in uptake and knockdown experiments (Figures 12-16). Antagomir treatments were directed against the individual miRNAs of the *miR-17-92* cluster (*anti-miR-17-5p*, *anti-miR-18a*, *anti-miR-19a*, *anti-miR-20a*, *anti-miR-19b*, and *anti-miR-92*). Additional, treatments were directed against additional miRNAs upregulated in MLL leukemia *miR-10a*, *miR-196b*, *miR-191* and *miR-93**. MOLM-13 and MV4-11 were treated at 2 μM concentrations, while RS4;11 was treated at 1 μM concentrations. Non-MLL cell lines were always treated at 2 μM concentrations to

control for both miRNA knockdown and potential non-specific toxic effects of antagomirs. Antagomir treatment at 2 µM concentrations resulted in the formation of a precipitate for several different treatments. Antagomir precipitation occurred upon 2 µM treatments of *anti-miR-67*, *anti-miR-18a*, *anti-miR-92*, *anti-miR-93**, and *anti-miR-191* in both liquid culture and methylcellulose. Notably, antagomir treatment with *anti-miR-18a* and *anti-miR-191* resulted in a very faint precipitate formation. This precipitation appears to be sequence specific and has been linked to the presence of the cholesterol tag at the 3'end of the oligo (technical support, Thermo). The mechanism of the effects of precipitate formation on cell growth and colony forming ability are currently unclear. Moreover, while aggregation was visible at 2 µM for the indicated antagomir, it is possible that sub-microscopic aggregations occur for other antagomirs and at lower concentrations. Though the exact mechanism by which *anti-Ce-miR-67* produced a toxic effect is unknown, it is likely that the toxicity is related to the precipitate which formed as a result of antagomir aggregation. Previous studies of antagomirs *in vivo* have indicated that antagomirs bind to lipoproteins as wells serum albumin, providing evidence for antagomir-protein interactions [224]. Thus, it is possible that the antagomir and its precipitates bind to the cell membrane and cellular proteins, impeding normal function.

Several antagomir treatments showed minimal effects upon treatment. *Anti-miR-10a*, *anti-miR-191*, and *anti-miR-93** all had minimal effect on colony forming ability (Figures 12, 13, 16). Treatment with *anti-miR-10a* or *anti-miR-191* showed lesser effects than treatment with the control antagomir *anti-Ce-miR-67* in several cell lines (Figures 12,16). The minor effects of these treatments (*anti-miR-10a* and *anti-miR-191*) suggests

that the miRNAs examined were either unnecessary to the function of MLL leukemia or

that their functions were redundant with other miRNAs in colony forming ability. As

these treatments did not decrease any outcomes in cell lines under consideration, and

either did not produce a precipitate in culture or produced a very faint precipitate, I have

utilized *anti-miR-10a* and *anti-miR-191* as a treatment controls in subsequent experiments

(indicated in figure legends). Antagomir treatment against members of the *miR-17*

family showed a decrease in colony number and total cell number in human MLL

leukemia cell lines. *Anti-miR-17* and *anti-miR-20a* both showed a decrease in colony

numbers relative to both the vehicle and the control antagomir-treatment (*anti-miR-10a*)

(Figure 14). The effect was most pronounced in MOLM-13 and MV4-11. Antagomir

treatment in MV4-11 resulted in a complete loss of colony forming ability (Figure 14).

Only *anti-miR-20a* treatment was significant in colony forming assays for RS4;11

(Figure 14). Cell numbers decreased similarly to colony numbers, but with a greater

decrease in percentage relative to vehicle. The decrease of cell number relative to colony

number is apparent in the changes in colony morphology. For both antagomir treatments,

colonies appeared smaller in radius and had an abnormal distribution of cells within the

colony.

Treatment against *miR-19a* or *miR-19b* resulted in a very limited decrease in

colony forming ability. Colony number decreased relative to vehicle, but was

insignificant in comparison to control antagomir. The only significant decrease observed

was the decrease of *anti-miR-19b* in MV4-11 (Figure 15). Cell number was decreased

slightly for *anti-miR-19b* in both MOLM-13 and MV4-11 (Figure 15). Colony

Figure 12. Antagomir treatment against *miR-10a* and *miR-196b* in human MLL leukemia cell lines
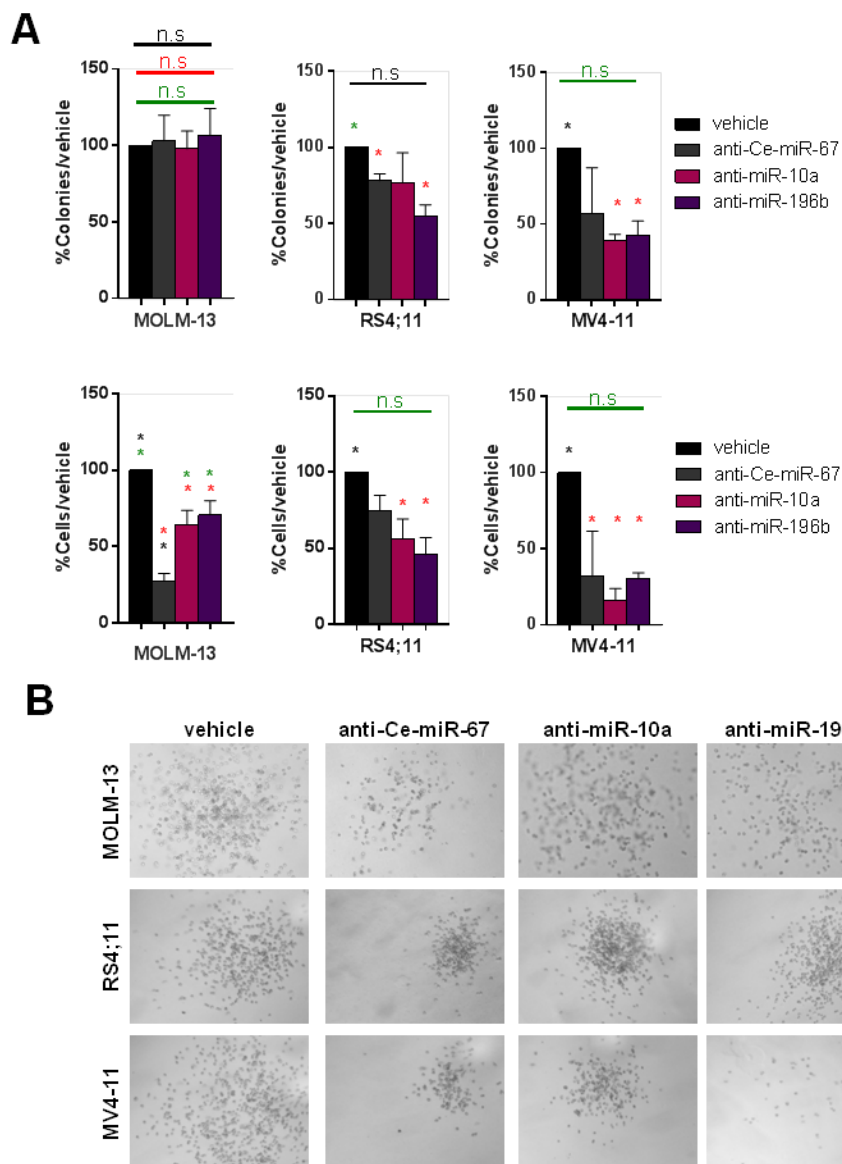
Individual antagomir treatments against *miR-10a* and *miR-196b*. A) Antagomir treatments were performed against individual miRNAs at a total concentration of 2 μM for MOLM-13 and MV4-11 and 1 μM for RS4;11. MOLM-13 and MV4-11 were tested in three independent experiments. MV4-11 was tested in two independent experiments. Significance was tested against a control antagomir using Student's t-test (α = .05). Significance against vehicle indicated in red. Significance against *anti-Ce-miR-67* indicated in green. Significance against *anti-miR-10a* indicated in black. B) Colony morphology from antagomir treated colony assays.

Figure 13. Antagomir treatment against *miR-18a* and *miR-92* in human MLL leukemia cell lines
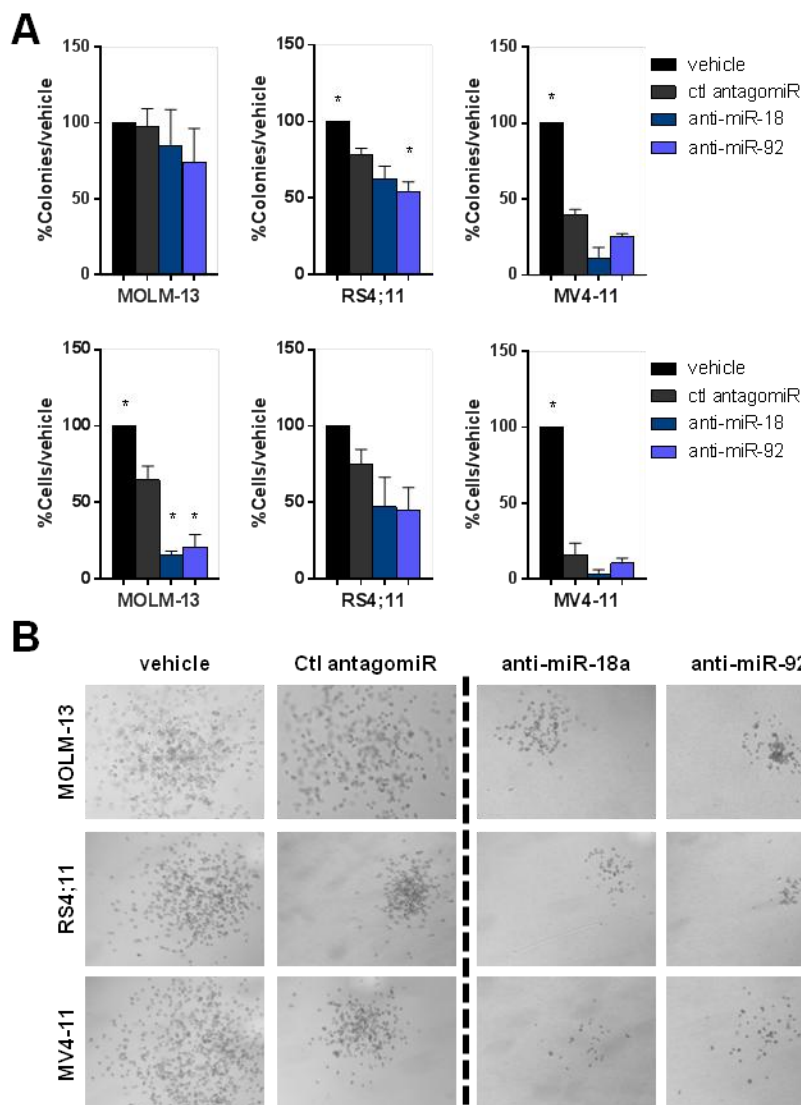
Individual antagomir treatments against *miR-18a* and *miR-92*. A) Antagomir treatments were performed against individual miRNAs at a total concentration of 2 μM for MOLM-13 and MV4-11 and 1 μM for RS4;11. MOLM-13 and MV4-11 were tested in three independent experiments. MV4-11 was tested in two independent experiments. Significance was tested against a control antagomir using Student's t-test (α = .05). *Anti-Ce-miR-67* was used as a control for RS4;11, and *anti-miR-10a* was used as a control for MOLM-13 and MV4-11. B) Colony morphology from antagomir treated colony assays.

Figure 14 . Antagomir treatment against *miR-17* and *miR-20a* in human MLL leukemia cell lines

Individual antagomir treatments against *miR-17-5p* and *miR-20a*. A) Antagomir treatments were performed against individual miRNAs at a total concentration of 2 μM for MOLM-13 and MV4-11 and 1 μM for RS4;11. MOLM-13 and MV4-11 were tested in three independent experiments. MV4-11 was tested in two independent experiments. Significance was tested against a control antagomir using Student's t-test (α = .05). *Anti-Ce-miR-67* was used as a control for RS4;11, and *anti-miR-10a* was used as a control for MOLM-13 and MV4-11. B) Colony morphology from antagomir treated colony assays.

Figure 15. Antagomir treatment against *miR-19a* and *miR-19b* in human MLL leukemia cell lines
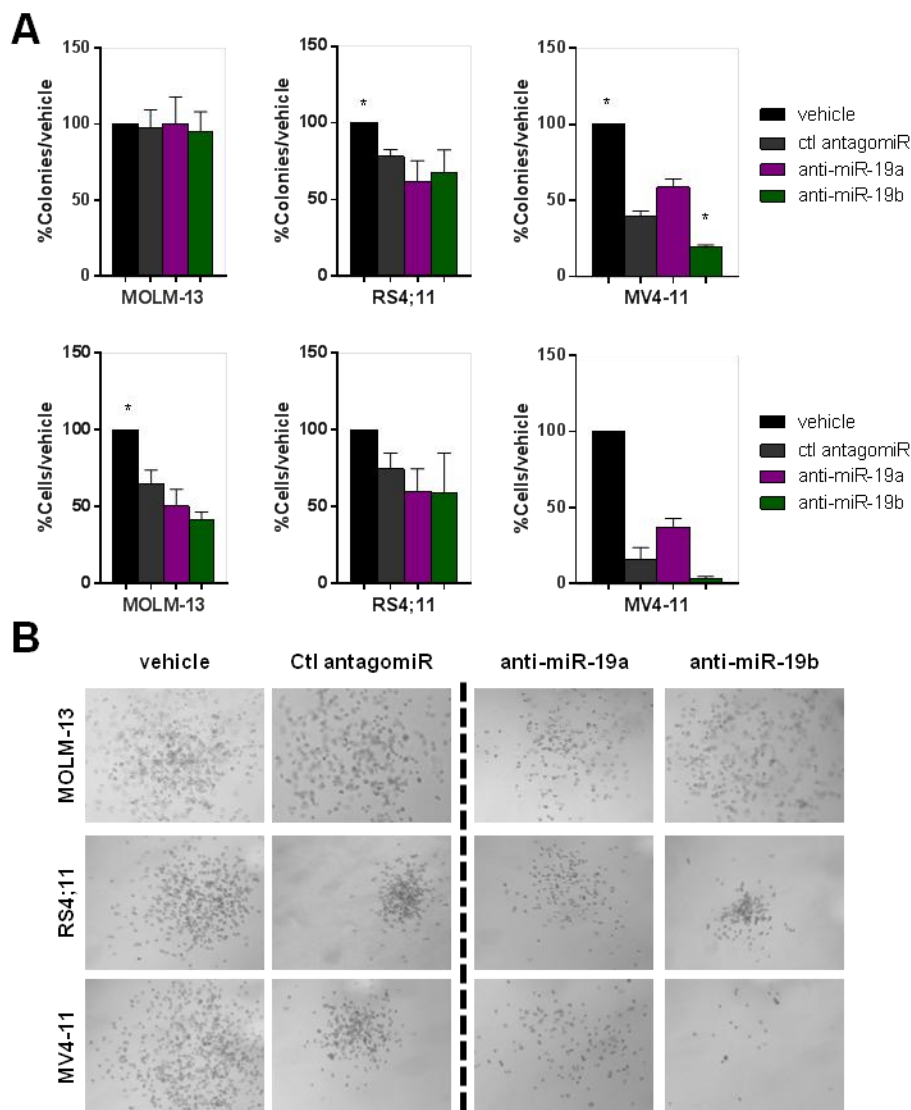
Individual antagomir treatments against *miR-19a* and *miR-19b*. A) Antagomir treatments were performed against individual miRNAs at a total concentration of 2 μM for MOLM-13 and MV4-11 and 1 μM for RS4;11. MOLM-13 and MV4-11 were tested in three independent experiments. MV4-11 was tested in two independent experiments. Significance was tested against a control antagomir using Student's t-test (α = .05). *Anti-Ce-miR-67* was used as a control for RS4;11, and *anti-miR-10a* was used as a control for MOLM-13 and MV4-11. B) Colony morphology from antagomir treated colony assays.

Figure 16. Antagomir treatment against *miR-93** and *miR-191* in human MLL leukemia cell lines
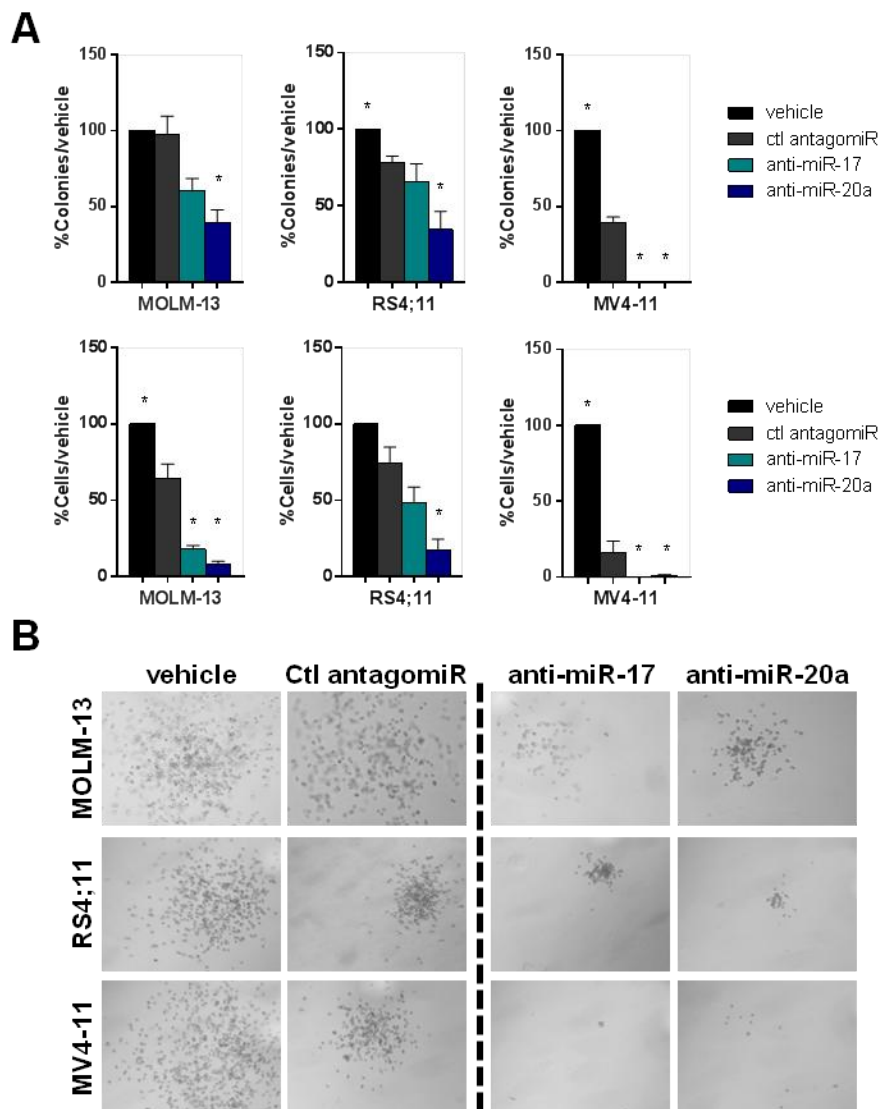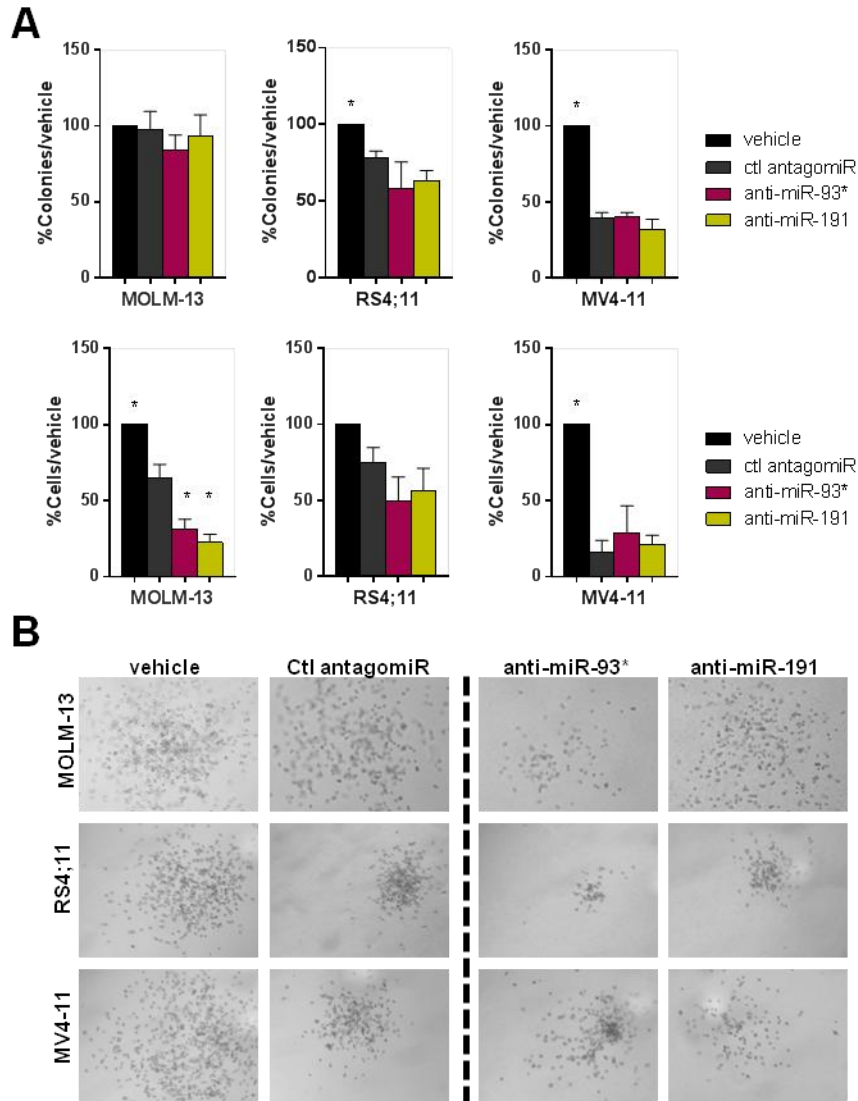

Individual antagomir treatments against *miR-93** and *miR-191*. A) Antagomir treatments were performed against individual miRNAs at a total concentration of 2 µM for MOLM-13 and MV4-11 and 1 µM for RS4;11. MOLM-13 and MV4-11 were tested in three independent experiments. MV4-11 was tested in two independent experiments. Significance was tested against a control antagomir using Student's t-test (α = .05). *Anti-Ce-miR-67* was used as a control for RS4;11, and *anti-miR-10a* was used as a control for MOLM-13 and MV4-11. B) Colony morphology from antagomir treated colony assays.

morphology did not change in response to antagomir treatment for *anti-miR-19a* or *anti-miR-19b* (Figure 15).

I additionally examined potential antagomir treatments against *miR-18a*, *miR-92*, and *miR-196b* (Figures 12, 13). For these antagomir treatments, no treatment effect were observed relative to control treatment for MOLM-13 or RS4;11. *Anti-miR-18a* and *anti-miR-92* resulted in a minor decrease in colony forming ability for MV4-11. Treatments against either *anti-miR-18a* or *anti-miR-92* showed minor, but significant decreases in cell number (Figure 13). Colony morphology reflected these treatment effects with minor decreases in colony size and sparseness.

Combined inhibition of *miR-17, 20a* or *miR-17, 19a* reduces colony formation and increases differentiation of MLL leukemia cells

Of the miRNAs overexpressed in MLL leukemia, several are classified into the same miRNA family based on miRNA seed sequence. I examined the effects of combinatorial antagomir treatments on human cell lines to determine whether simultaneously targeting multiple miRNAs with the same seed sequence or targeting multiple miRNAs with different seed sequences would potentiate the effects on colony forming capacity or proliferation. Combinatorial treatment resulted in a greater decrease in colony forming ability than treatment with either *anti-miR-17* or *anti-miR-20a* alone (Figure 17). Simultaneous inhibition of both *miR-19a* and *19b* resulted in decreased colony formation of RS4;11 and MV4-11 cell lines (Figure 17). Intriguingly, treatment with *anti-miR-17* and *anti-miR-19a* produced a dramatic effect beyond that observed for either antagomir individually. Further, this combination produced an effect beyond an

additive effect on colony and cell numbers. Morphologically, cells appear more differentiated with a greater cytoplasmic:nuclear ratio and increased vacuolarity (Figure 18). For all cell lines, combinatorial treatment with antagomirs directed against *miR-17*, and *miR-19a* resulted in a change in cell morphology (Figure 18).

miRNA contributions to MLL leukemia were further examined in combinatorial treatments against multiple miRNAs simultaneously. To avoid the potential for non-specific toxicity, combinatorial treatments were examined at a total concentration equal to that of individual treatments. I hypothesized that miRNA contributions were cooperative and that simultaneous inhibition of multiple miRNAs would produce a greater effect than individual treatments. In examining this hypothesis, I have tested against antagomirs directed against miRNAs of the same family and miRNAs of different families. While miRNAs from the same family possess the same seed region and would likely regulate similar targets, miRNAs of different families do not possess the sequence homology to target the same binding sites within the 3'UTR.

Combinatorial treatments against *miR-17* and *miR-20a* resulted in a dramatic decrease in colony forming ability and cell number (Figure 17). Effects for combinatorial treatment were more dramatic than for either single treatment suggesting that inhibition of miRNAs from the same family provides a superior model of therapeutic intervention. Treatment with *anti-miR-17* or *anti-miR-20a* produced the greatest decrease in colony forming ability in MOLM13, RS4;11, and MV4-11 cell lines(Figure 14, 17). *Anti-miR-20a* had more pronounced activity than *anti-miR-17* (Figures 14, 17)

Figure 17. Combinatorial antagomir treatment decreases colony forming ability and total cell number in colony assays.
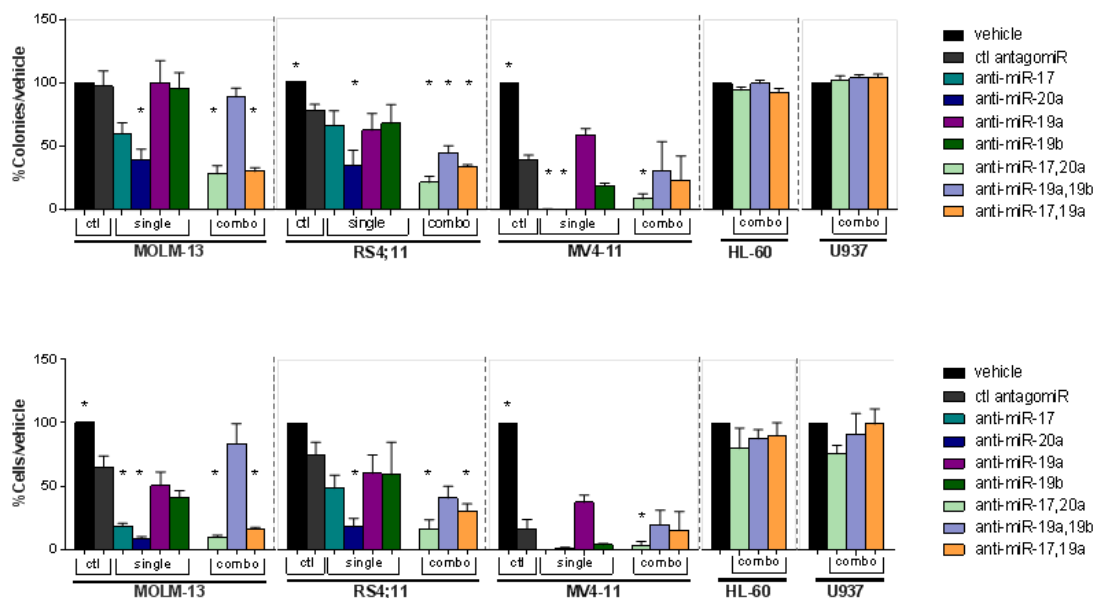
Combinatorial antagomir treatments result in a decrease in colony forming ability and total cell number. Antagomir treatments were performed against either individual miRNAs (*anti-miR-17, anti-miR-20a, anti-miR-19a,* or *anti-miR-19b*) or combinations of miRNAs (*anti-miR-17, 20a; anti-miR19ab;* or *anti-miR-17,19a*) at a total concentration of 2 μM for MOLM-13, MV4-11, HL-60, and U937 and 1 μM for RS4;11. MOLM-13, MV4-11, HL-60, and U937 were tested in three independent experiments. MV4-11 was tested in two independent experiments. Significance was tested against a control antagomir using Student's t-test (α = .05). *Anti-Ce-miR-67* was used as a control for RS4;11, and *anti-miR-10a* was used as a control for MOLM-13 and MV4-11.

Figure 18. Combinatorial antagomir treatment results in decreased colony density and a change in cell morphology.
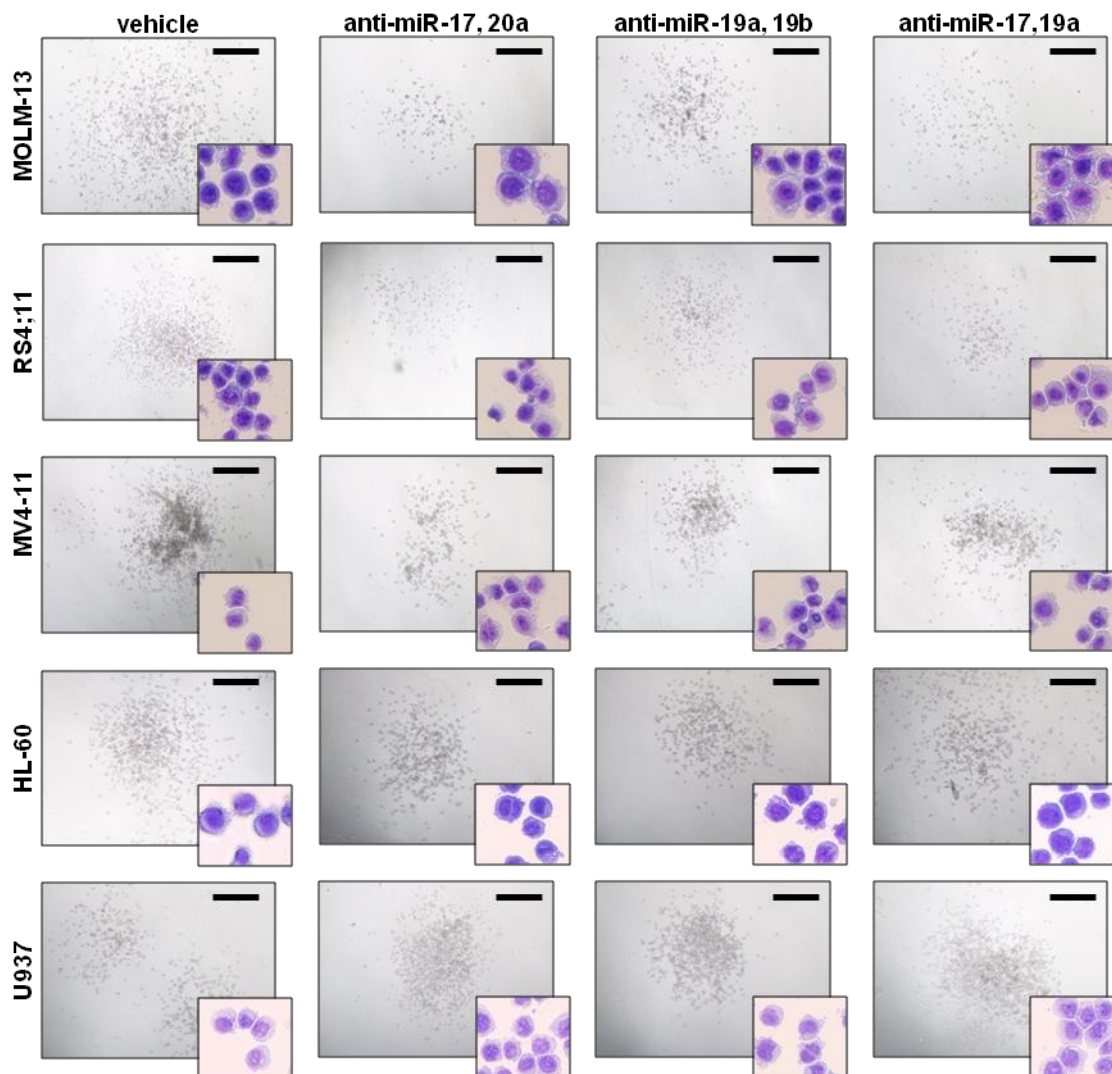
Colony and cell morphology from combinatorial antagomir treatments in colony assays at 1 week. Treatment with combinations of miRNAs (*anti-miR-17, 20a; anti-miR19ab;* or *anti-miR-17,19a*) relative to a vehicle control were examined. MOLM-13, MV4-11, HL-60, and U937 were treated at a total concentration of 2 µM. RS4;11 was treated at a total concentration of 1 µM. Scale bars represent 200 µm. Collected cells were stained with Wright-Giemsa (inset).

Therapeutic intervention against *miR-19a* and *miR-19b* resulted in a greater defect in colony forming ability than intervention against either miRNA alone. Single treatments did not result in significant changes for MOLM-13 or RS4;11. However, combinatorial treatments resulted in a 50% decrease in colony forming ability of RS4;11. Treatment against *miR-19a* caused no significant decrease relative to treatments with a control antagomir (Figure 15, 17). *Anti-miR-19b* treatment caused a decrease relative to both vehicle and control antagomir treatments in MV4-11 cells (Figures 15,17).

Colonies were smaller and contained fewer cells after treatment with either anti-*miR-17,20a*, *anti-miR-19a,19b*, or *anti-miR-17,19a* (Figure 17). Further, I observed a decrease in cell number that was greater than the decrease in colony number in our combinatorial treatments, suggesting that in addition to inhibition of colony forming ability, antagomir treatments either inhibited proliferation, or increased cell death and/or differentiation.

Both colony number and total cell number decreased in multiple antagomir treatment regimens. To determine whether any decrease in cell number was independent of decrease in colony number, I charted the relative decrease in cell number against the relative decrease in colony number (Figure 19). If a proliferative defect is present, independent of a colony defect, then cell number should decrease at a greater rate than colonies relatively to wild type control. For MV4-11 and RS4;11, cell and colony number decreased proportionately. MOLM-13 however had dramatic decreases in cell number without any accompanying decrease in colony number. This suggests that antagomir treatments affect proliferation in addition to colony forming ability.

Figure 19. Cell number varies similarly to colony number in antagomir treated colony assays.
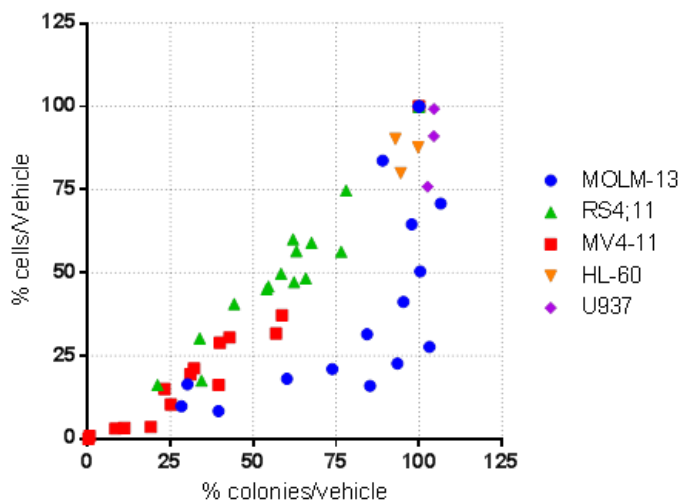
Values for cell number relative to vehicle compared to colony number relative to vehicle for human leukemia cell lines after antagomir treatment (2 µM). Plotted values indicate average of 3 independent experiments for MOLM-13, MV4-11, HL-60, and U937 and 2 independent experiments for MV4-11.

miRNA inhibition results in a modest decrease in cell number and accumulation of cells at G0/G1

To dissociate the possible proliferative effects of antagomir treatments from colony forming ability, antagomir treatments were performed in liquid culture (Figures 21-23). Decreased colony size suggests a potential deficiency in proliferation, decreases in cell number could potentially be attributed to a decrease in colony numbers. Further, colony assays require smaller initial cell numbers and effective treatment against specific miRNAs results in a final cell number insufficient to examine subtle changes in cell cycle. To examine the proliferation of cells upon antagomir treatment, cells were cultured according to standard culture conditions with antagomirs. After 4 days, cells were analyzed using Cell-Titer-Glo to determine the total cell number, and fixed for FACS analysis of cell cycle.

As with colony assay experiments, cells were subjected to both individual and combinatorial treatments. Individual antagomir treatments were performed at a concentration of 1 µM total concentration. Only *anti-miR-20a* and *anti-miR-92* resulted in significant decreases in cell number at 4 days (Figure 21). These effects were observed in RS4;11 and Molm13. No individual treatment resulted in significant decreases in MV4-11.

Combinatorial antagomir treatments were performed at both 1 µM total concentration (Figure 22) and 1 µM each antagomir (Figure 23). Treatments at higher concentrations included controls specific to each cell line to control for non-specific toxicity resulting from increased oligo concentrations. For each cell line, I selected

Figure 20. Linear relationship between cell number and CTG reading
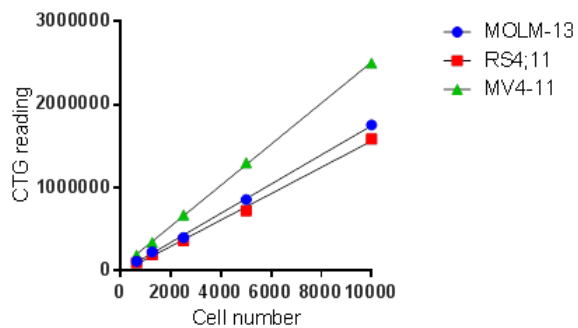
MOLM-13 $Y = 175.4*X - 7488$

RS4;11 $Y = 158.2*X - 19639$

MV4-11 $Y = 246.6*X + 45469$

Standard curve was a established for MOLM-13 (blue circles), RS4;11 (red square), and MV4-11 (green triangle) cell lines using Promega Cell Titer Glo. Best fit line and equations were determined using PRISM.

potential controls from the antagomir treatments which produced either no treatment effect in colony assays or very limited effects relative to vehicle (herein referred to as the least responding antagomir). For experiments with a total treatment concentration of 2 µM or 3 µM, I used the least responding antagomir at 2 µM or 3 µM, respectively, as a control. As an alternative, a combinatorial control treatment was performed using the least responding antagomir treatment in combination with the second least responding treatment at 1 µM each. For a 3 µM alternative control, the 3 least responsive antagomirs for each cell line were added at 1 µM each. Combinatorial treatments examined the treatment effect of antagomirs directed against miRNAs from the same family as well as treatments against miR-*17, 19a*, and *196b*. Cross family antagomir treatments were further divided into all 2 antagomir permutations of the *miR-17*, *19a*, *196b* combination.

Combinatorial antagomir treatment effects were observed for *anti-miR-17,20a* in Molm13 and RS4;11 at both concentrations (Figure 22-23). Cell cycle analysis indicated an accumulation of cells at G0/G1. No combinatorial antagomir treatments resulted in a significant decrease for MV4-11. All combinatorial treatments resulted in a significant decrease in RS4;11 at 1 µM. Due to a slight increase in toxicity, significance was less apparent at increased treatment concentrations RS4;11.

To examine the effects of antagomir treatment on proliferation, I treated human cell lines with antagomirs in liquid culture (Figure 21-23). Doing so allowed me to separate any proliferative defects from colony forming ability. I simultaneously tested both individual treatments and combinatorial treatments in human MLL cell lines. In

Figure 21. Single antagomir treated human MLL leukemia cell lines in liquid culture
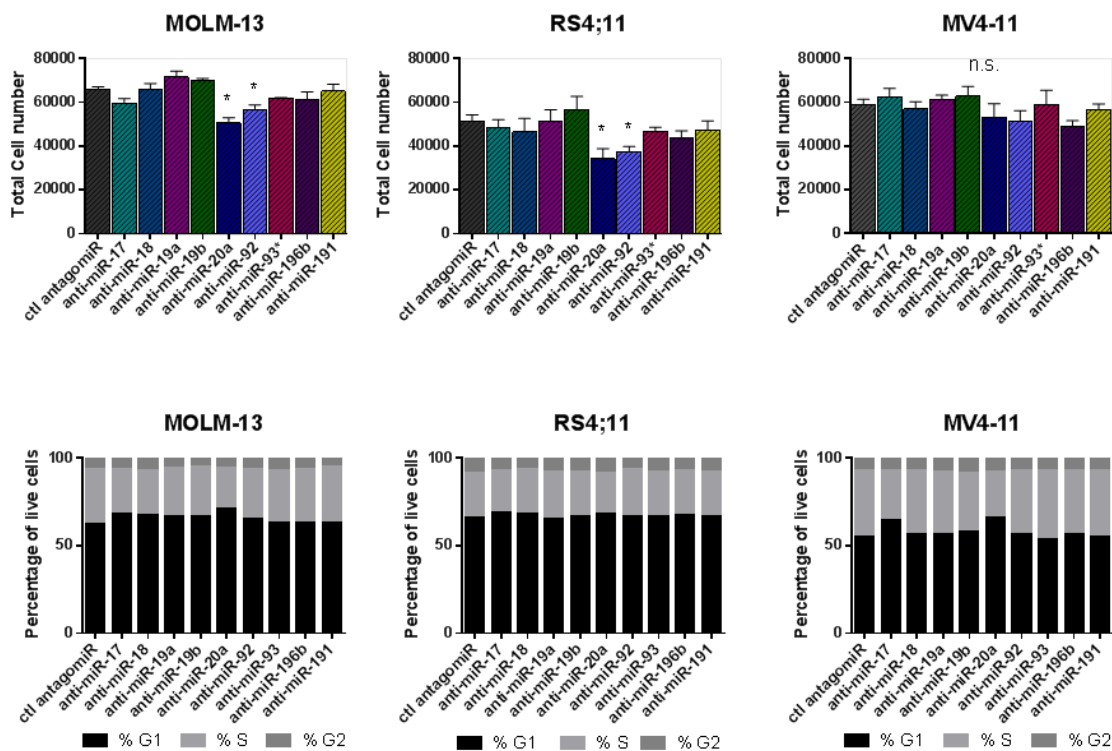
Individual antagomir treatments in liquid culture. A) Antagomir treatments were performed against individual miRNAs at a total concentration of 1 μM for MOLM-13, MV4-11, and RS4;11 for 4 days and cell number was determined using the Cell-Titer-Glo cell viability assay. All cell lines were tested in three independent experiments. Significance was tested against a control antagomir using Student's t-test (α = .05). *Anti-Ce-miR-67* was used as a control for RS4;11, and *anti-miR-10a* was used as a control for MOLM-13 and MV4-11. B) Cell Cycle distribution was analyzed in parallel with cell viability assays on day 4.

Figure 22. Combinatorial antagomir treated human MLL leukemia cell lines at 1 μM total concentration

Individual antagomir treatments in liquid culture. A) Antagomir treatments were performed against individual miRNAs at a total concentration of 1 μM for MOLM-13, MV4-11, and RS4;11 for 4 days and cell number was determined using the Cell-Titer-Glo cell viability assay. All cell lines were tested in three independent experiments. Significance was tested against a control antagomir using Student's t-test (α = .05). *Anti-Ce-miR-67* was used as a control for RS4;11, and *anti-miR-10a* was used as a control for MOLM-13 and MV4-11. B) Cell Cycle distribution was analyzed in parallel with cell viability assays on day 4.

Figure 23. Combinatorial antagomir treated human MLL leukemia cell lines at 1 µM each antagomir.
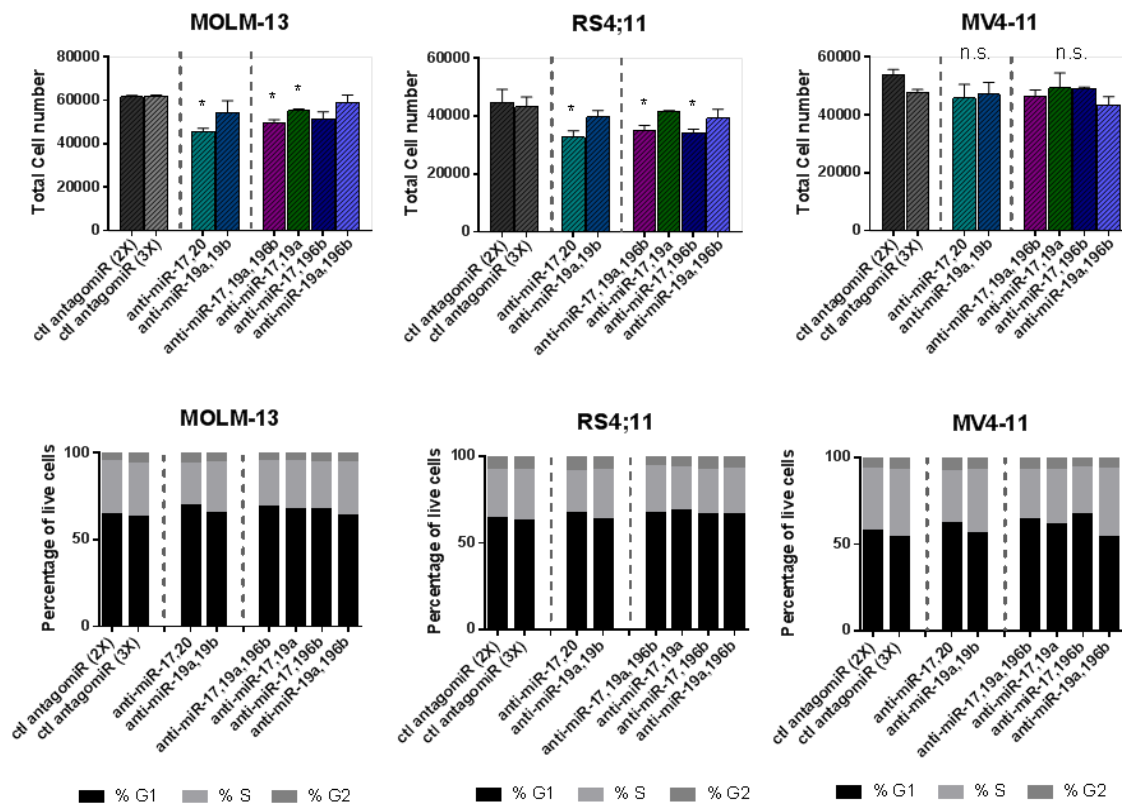
Combinatorial antagomir treatments in liquid culture. A) Antagomir treatments were performed against individual miRNAs at a total concentration of 1 µM for MOLM-13, MV4-11, and RS4;11 for 4 days and cell number was determined using the Cell-Titer-Glo cell viability assay. All cell lines were tested in three independent experiments. Significance was tested against a control antagomir using Student's t-test (α = .05). *Anti-miR-191* was used as a control for RS4;11, and *anti-miR-10a* was used as a control for MOLM-13. *Anti-miR-93** was used a control for MV4-11. B) Cell cycle distribution was analyzed in parallel with cell viability assays on day 4.

individual treatments, I observed decreases that largely mirrored our colony assay data.

Treatment with *anti-miR-17* or *anti-miR-20a* resulted in a decrease in total cell number at

4 days, while treatment with *anti-miR-19a* or *anti-miR-19b* were individually unaffected

(Figure 22, 23). Combinatorial treatment against *miR-17,20a* resulted in a decrease in

total cell number for RS4;11, while *anti-miR-17,20a* and *anti-miR-17,19a* were both

significant in MOLM-13 (Figure 22, 23). I did not detect any decrease relative to control

in MV4-11. Antagomir-treatment produced a less dramatic effect in liquid culture than in

colony assays.

To further examine proliferation, I examined cell cycle by propidium iodide

staining (Figures 21-23). Decreased cell numbers were accompanied by accumulation of

cells at G1/G0 for those antagomir. For example *anti-miR-17,20a* treatment in MOLM-

13 resulted in a modest decrease in cell number accompanied by an increase in cells at

G0/G1 (Figure 22). Collectively, these data indicate that decrease in colony forming

ability was accompanied by a mild proliferative defect.

Effect of antagomir treatment on colony forming ability of *MLL-AF9* transformed

murine bone marrow

To examine the contribution of miRNAs to MLL leukemia, I screened for

individual antaogmiR treatment effects in *MLL-AF9* transduced bone marrow (Figures

24, 25). Bone marrow was isolated, selected for c-Kit+ cells, spinoculated with *MLL-

AF9* expressing retrovirus, and treated with antagomirs with superficial addition and pre-

incubation.

Figure 24. Anatagomir treatment against *miR-19a* and *miR-196b* result in a decrease in colony formation of *MLL-AF9* transformed bone marrow
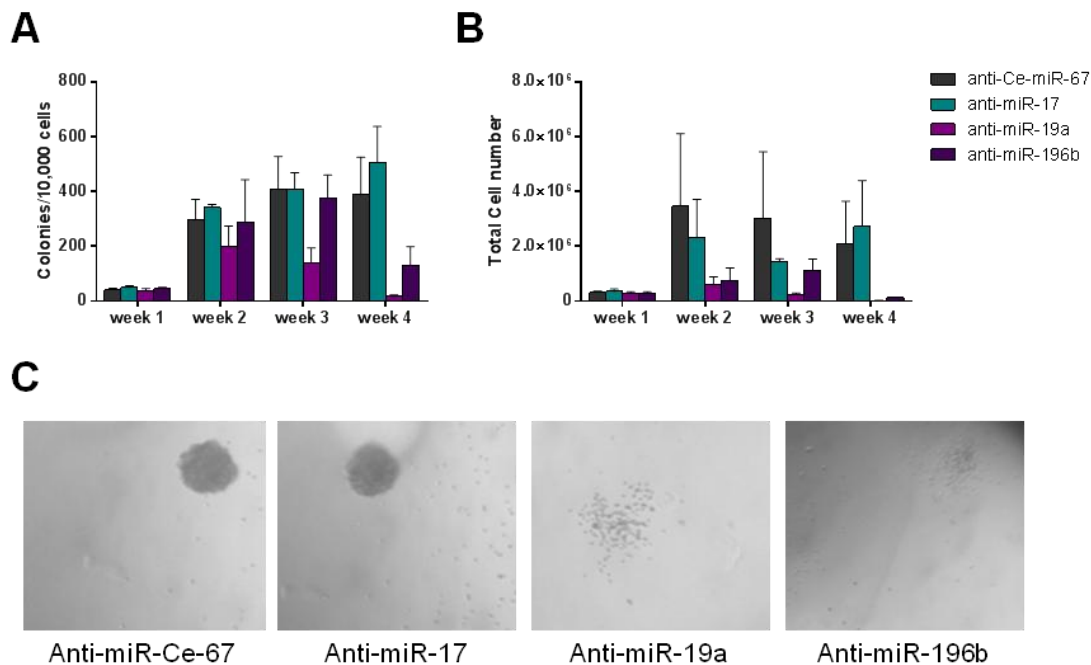
Antagomir treatments against *MLL-AF9* bone marrow cells that were serially treated with antagomir at 100 nM (n=3). A) Colony formation, B) Cell growth in colony forming assays, C) Example colonies observed in colony assays.

Previous studies by our lab, performed in collaboration with the Grimes lab, have shown that *miR-196b* is essential to the transformation process in *MLL-AF9* transformed bone marrow [11]. Treatment with *anti-miR-196b* resulted in a decrease in colony forming ability consistent with that observed these studies (Figure 24). Colony formation declined at 3 and 4 weeks of serial plating. Week 4 colonies assays indicated a complete collapse of colony forming ability. Cell number decreased along with colony number over the same time frame. Additionally, colony morphology was distinctly different between *anti-miR-196b* and control antagomir treatment. While *anti-Ce-miR-67* treated colonies were predominantly type 1 tight colonies, *anti-miR-196b* treated colonies were primarily type 3 by weeks 3 and 4. This change in colony morphology is indicative of more differentiated cell types and implies that the decrease in colony numbers is a result of differentiation over the course of 4 weeks.

Anti-miR-19a treatment resulted in a decrease in colony forming ability over the course of 4 weeks (Figure 24). Concurrently, cell number decreased with colony number. The decrease in colony number and cell number for *anti-miR-19a* was the most dramatic observed in these experiments and represented a complete loss of colony forming ability. In addition to the observed decrease in colony number, I observed a dramatic change in colony morphology. Similar to *anti-miR-196b* treatment, *anti-miR-19a* treatment results in a change in colony morphology from type I colonies to type III colonies (Figure 24).

Treatment of *MLL-AF9* transduced bone marrow with *anti-miR-17-5p* resulted in no significant difference in colony forming ability or colony morphology relative to control treated cells. However, total cell number was significantly decreased at 3 weeks.

Figure 25. Antagomir treatments in *MLL-AF9* transformed bone marrow
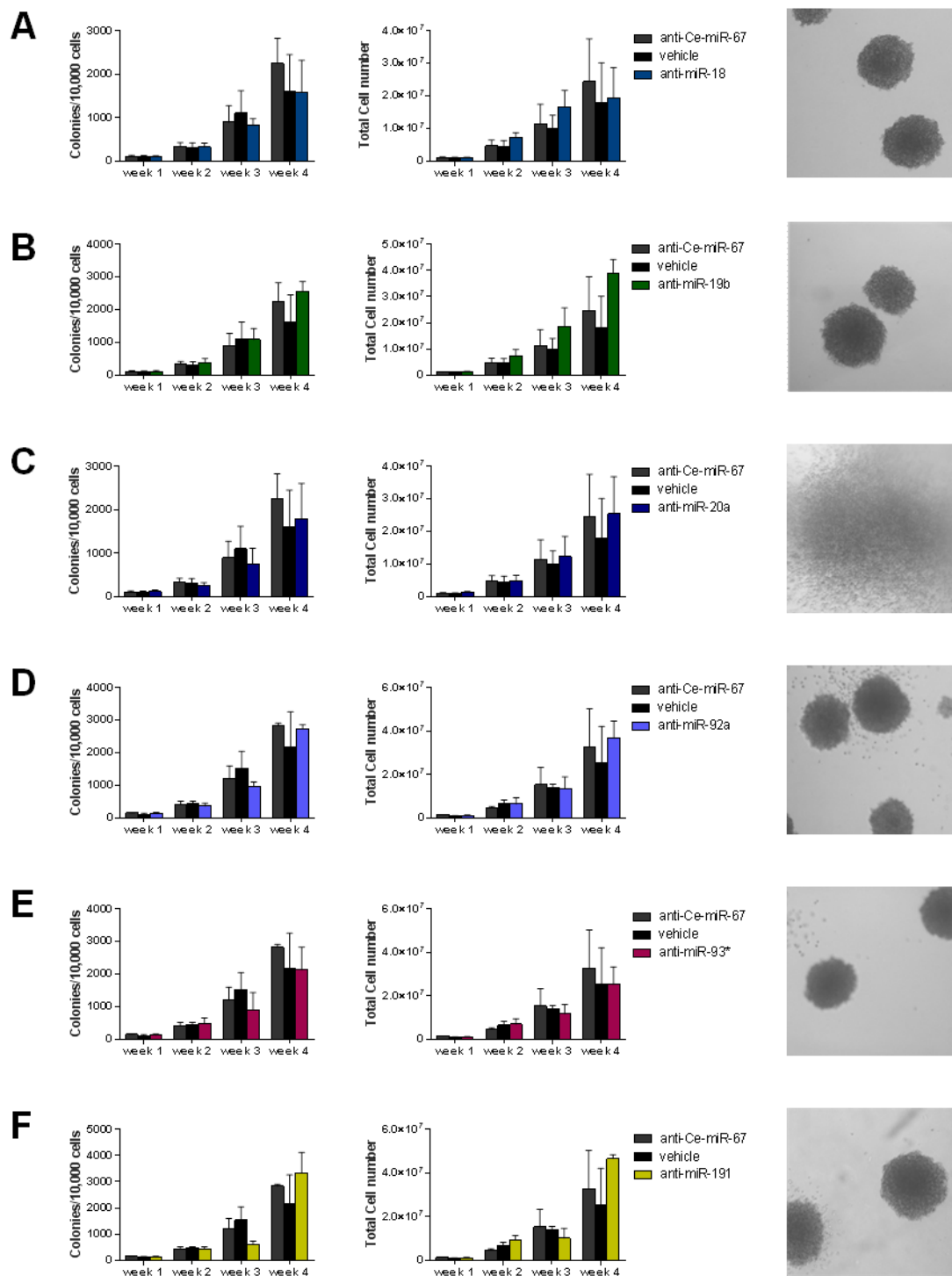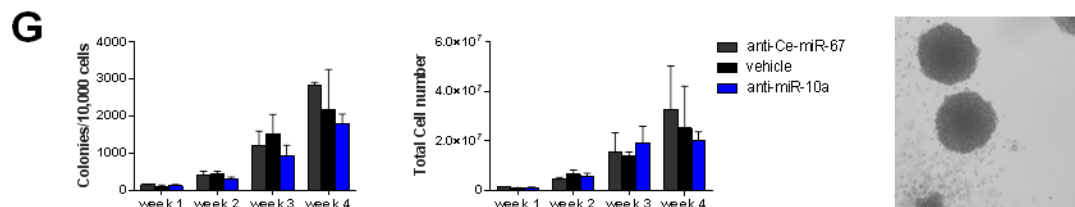
Antagomir treatments performed against *MLL-AF9* transformed bone marrow. Colony assays performed with 200 nM antagomiR treatments All antagomir treatments arranged similarly. Left panel indicates colony numbers, middle panel indicated cell number, and right panel indicates colony morphology. A) *anti-miR-18a*, B) *anti-miR-19b*, C) *anti-miR-20a*, D) *anti-miR-92*, E) *anti-miR-93**, F) *anti-miR-191*, G) *anti-miR-10a.*

The reason for the recovery of cell number at week 4 is not immediately clear, but could be due to selection for cells that have increased expression of compensatory factors that make miRNA involvement dispensable to leukemia development. Strikingly, the decrease in cell number did not correlate to any decrease in colony number or change in colony morphology, suggesting the decrease in cell number is not due to differentiation.

In addition to treatment against *miR-196b* and *miR-19a*, minor treatment effects were observed for *anti-miR-10a* treated cells (Figure 25). *Anti-miR-10a* treatment showed a minor but significant decrease in colony forming ability at 4 weeks. At weeks 1 and 2, a small proportion of colonies displayed an abnormal morphology of abnormally large and disperse colonies (Figure 25). No treatment effects were observed for additional colony assays performed with *anti-miR-18a*, *anti-miR-92*, *anti-miR-191*, *anti-miR-20a*, or *anti-miR-93** relative to either a control antagomir or vehicle (Figure 25). Similarly, neither colony morphology nor total cell number changed in response to treatment with these antagomirs (Figure 25).

PKNOX1 is a valid target of the *miR-17-92* cluster

I next sought to identify potential mRNA targets, focusing on mRNA transcripts predicted to be targeted by multiple miRNAs upregulated in MLL leukemia. Further, I focused on genes with functions potentially related to colony forming ability. Search results using multiple target prediction algorithms (miRanda, TargetScan, Diana-mT) identified the MEINOX family gene *PKNOX1* as an intriguing possibility. Previous studies in mouse models have indicated that complexes including *Hoxa9-Pknox1* functions distinctly from *Hoxa9-Meis1* [111-113].

Figure 26. The *PKNOX1* 3'UTR possesses multiple putative target sites for regulation by the *miR-17-92* cluster
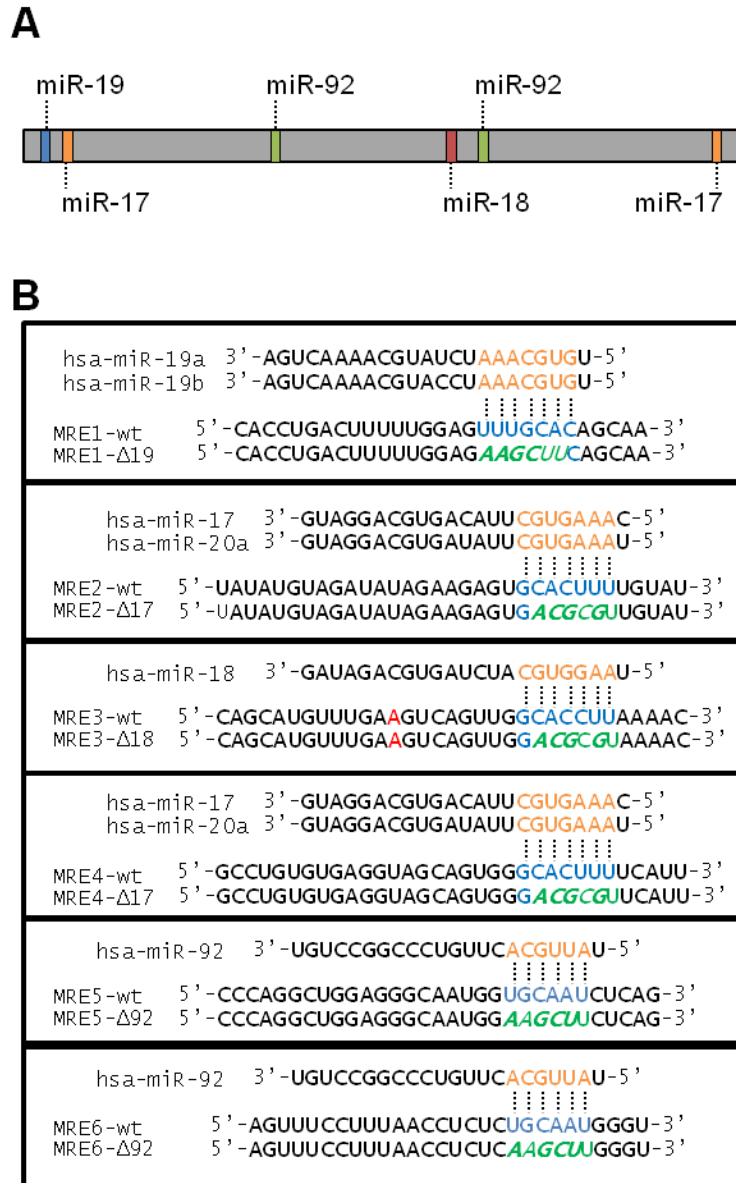
Positioning and sequences of putative microRNA response elements in the *PKNOX1* 3'UTR. A) Schematic of putative MRE location with identification of miRNA family predicted to target that site. B) Alignment of miRNAs with *PKNOX1* 3'UTR for wild type and mutated constructs. Seed region:mRNA interation indicated with dotted lines. MRE indicated in blue. Mutations indicated in green SNP observed in the putative MRE of *miR-18a* is indicated in red

Figure 27. *PKNOX1* **is a valid target of the** *miR-17-92* **cluster.**
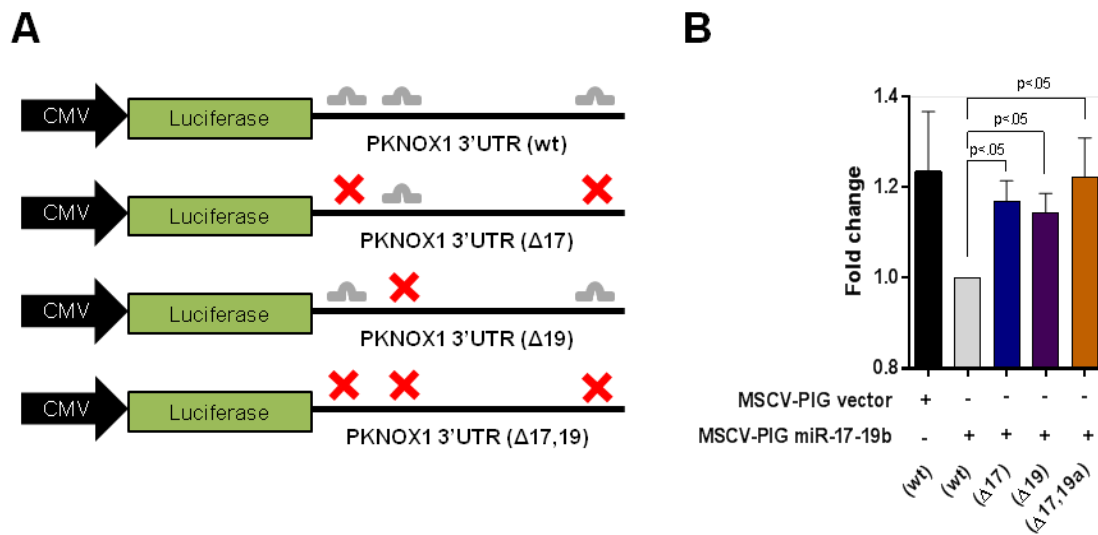
Luciferase assays were performed in HEK293T cells in 4 independent experiments. A) Schematic of luciferase construct with miRNA binding to *PKNOX1* 3'UTR. Putative miRNA binding sites are indicated with gray miRNAs above 3' UTR. Mutation of miRNA binding sites are indicated with red X's above 3'UTR. B) Readouts of Luciferase assays. Experiments were normalized to control (wild type *PKNOX1*3'UTR, treated with *MSCV-PIG-miR-17-19b*) in each experiment. Statistical significance was tested using student's t-test against wild-type *PKNOX1* 3'UTR treated with *MSCV-PIG-miR-17-19b*.

      PKNOX1 is predicted to be targeted by all miRNAs in the *miR-17-92* cluster. In total, the 3'UTR of *PKNOX1* possesses 7 putative binding sites for *miR-17-92* miRNAs (also known as miRNA Response Element or MREs) that are conserved between mouse and human (Figure 26). The *miR-17* family putatively targets the *PKNOX1* 3'UTR at 2 distinct sites, while *miR-19ab* putatively targets the *PKNOX1* 3' UTR at a single site. The *Pknox1* 3'UTR is putatively targeted by *miR-18a* at a single site and *miR-92* at 2 sites. Interestingly, I observed a single nucleotide polymorphism in the *miR-18a* binding site in the *PKNOX1* 3'UTR (Figure 26). The polymorphism consists of a G to C mutation outside of the seed region, and should not affect mRNA recognition.

      I hypothesized that *PKNOX1* was a valid target of regulation by the *miR-17-92* cluster. To examine the miRNA:mRNA relationship between the *miR-17-92* cluster and *PKNOX1*, I performed a luciferase reporter assay against the *PKNOX1* 3'UTR (Figure 27). I generated a construct fusing the *PKNOX1* 3'UTR to a luciferase reporter construct, as well as additional constructs with mutations in individual MREs as well as a compound mutant with mutations for all predicted MREs. If the relationship is valid, then mutations in the MREs will result in an increase in luciferase activity. Transfection with *MSCV-PIG-miR-17-19b* resulted in decreased levels of luminescence relative to control for the wild type plasmid (Figure 27). However, due to outliers, statistical significance was not apparent with 4 samples. Mutation of *miR-17, 20a* MREs in luciferase construct resulted in an increase in luminescence consistent with the hypothesis that *miR-17*, or *miR-20a* regulate *PKNOX1* at the mRNA level. Luminescence increased by 15% for the *miR-17* mutant, which encompassed mutations in 2 miRNA response elements (Figure

Figure 28. Steady-state levels of PKNOX1 in human cell lines
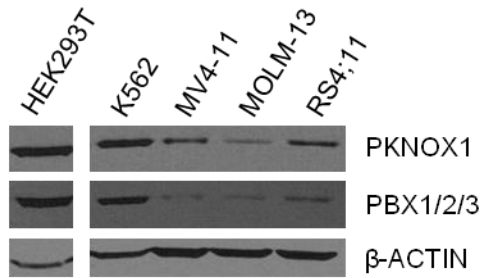
Steady state levels of PKNOX1were examined in several different human cell lines, including HEK293T (non-*MLL* adherent cell line), K562 (non-*MLL* AML cell line), MV4-11 (*MLL-AF4*), MOM-13 (*MLL-AF9*), and RS4;11 (*MLL-AF4*). Extraneous lanes cropped from blot.

27). Mutation of the single *miR-19ab* MRE resulted in an increase of approximately 15% (Figure 27). Compound mutation of all *miR-17-92* related MREs also resulted in a statistically significant increase (Figure 27). The compound mutant had an approximately 25% increase in luminescence. Though the increase is greater than that observed for individual miRNAs, no statistical significance was a reached when testing the compound mutation against either *miR-17* or *miR-19* mutants.

To further examine the relationship between the *miR-17-92* cluster, I examined the changes in Pknox1 at the protein level in HEK293T cells transfected with increasing concentrations of *MSCV-miR-17-19b* (Figure 29). HEK293T cells express relatively high endogenous levels of PKNOX1 (Figure 28,29). If *PKNOX1* is a valid target of the miRNAs, protein level should decrease with increased concentrations of transfected *MSCV-PIG-miR-17-19b* in a dose dependent manner. Consistent with the hypothesis, PKNOX1 levels decreased in response to increased concentrations of *miR-17-92* transfection (Figure 29).

I examined the endogenous levels of PKNOX1 and PBX1/2/3 at the protein level between adherent cell lines and MLL fusion containing leukemia cell lines (Figure 28). It was important to determine the basal levels of PKNOX1 in MLL leukemia cell lines in order to ensure the potential validity of my model. If PKNOX1 is highly expressed in *MLL-AF9* leukemia cell lines, then PKNOX1 modulation by miRNA is not likely to be physiologically important to leukemia. Simultaneously, PBX levels are an important potential limiting factor for the integrity of the model. I hypothesized that PKNOX1 and PBX levels were lower in MLL fusion containing cell lines. As expected, I observed low

Figure 29. PKNOX1 decreases in response to exogenous *miR-17-19b* expression
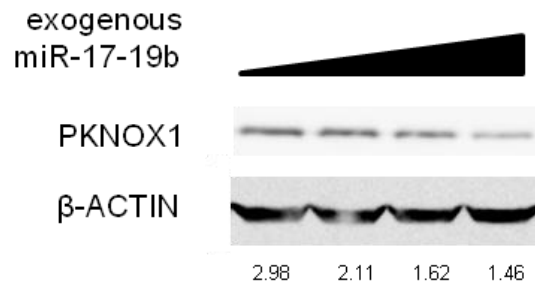
HEK293T cells expressing with increasing concentrations of exogenous *miR-17-19b*. Blot representative of 3 independent experiments. Numbers represent PKNOX1/ACTIN ratios for the depicted blot.

levels of PKNOX1 in all three cell lines (Figure 28) relative to HEK293T and K562 cells

(representing an adherent cell line and non-MLL leukemia cell line). MOLM-13 cells

expressed the least amount of PKNOX1 followed by MV4-11 and RS4;11. Further, I

observed low levels of PBX1/2/3 in all three MLL leukemia cell lines relative to

HEK293T and K562 cell lines (Figure 28). Use of a an anti-PBX1/2/3 antibody made it

impossible to discern the relative levels of each PBX homolog, but allows to determine

the overall combined levels of PBX1/2/3 containing complexes.

While experiments testing the miRNA:mRNA relationship utilized HEK293T

cells as a model system, these experiments do not establish that the miRNA:mRNA

relationship is relevant in MLL leukemia cells or that the protein levels change in

response to miRNA disregulation. To examine antagomir-mediated regulation of

PKNOX1, I examined the change in PKNOX1 protein levels in response to combinatorial

antagomir treatments (Figure 30). If PKNOX1 is regulated by the *miR-17-92* cluster in

MLL leukemia cell lines, inhibition of miRNAs that target the *PKNOX1* mRNA will

result in a de-repression of the mRNA transcript and subsequent increase in protein level.

I hypothesized that PKNOX1 level would increase upon antagomir treatment relative to

levels observed for cells treated with a control antagomir. Cells were cultured in liquid

culture for 3 days at 2 μM treatment concentration for MOLM-13 and 1 μM total

concentration for RS4;11. Consistent with my hypothesis, PKNOX1 protein levels

increased in response to the treatment with antagomir combinations, indicating that

antagomir treatment results in increased PKNOX1 (Figure 30).

Figure 30. PKNOX1 levels increase in response to combinatorial antagomir treatments
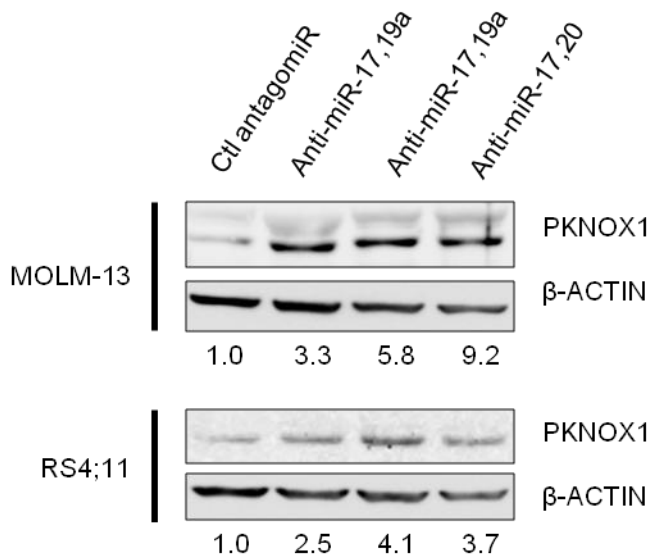
Antagomir treatment results in increased PKNOX1 protein levels relative to treatment with a control antagomir (*anti-miR-10a*). Human leukemia cell lines were treated with antagomirs (2 μM for 72 hrs) and analyzed for PKNOX1 levels by western blot. Numbers below bots indicate relative values of PKNOX1 after normalization to Actin for blot depicted.

PKNOX1 and MEIS1 compete for participation in PBX-containing complexes

Physiologically, *PKNOX1* upregulation has several potential outcomes. PKNOX1 and MEIS1 share high homology in their PBX interacting domains and homeodomains and have both been documented to form ternary complexes with PBX and HOX proteins, suggesting that these proteins compete for inclusion into ternary complexes. However, ChIP-seq analysis of co-occupancies indicate that Meis1-Hox and Pknox1-Pbx complexes are abundant during murine embryonic development [111]. Thus disregulation of MEIS1 or PKNOX1 in leukemia could alternatively drive the formation of binary complexes without affecting the balance of MEIS1 or PKNOX1 inclusion in ternary complexes. I hypothesized that increased PKNOX1 expression would result in a decrease in MEIS1 inclusion into these complexes.

To test for MEINOX competition within ternary PBX-containing complexes, I examined the composition of PBX-containing complexes for the relative levels of MEIS1/2/3 and PKNOX1 upon transfection with increasing concentrations of Meis1 (0 ug, .5 ug, 1 ug, 2 ug, 4 ug) and co-immunoprecipitation of PBX-containing complexes using an anti-PBX1/2/3 antibody (Figure 31). Immunoprecipitation was performed with an antibody targeting PBX1/2/3 to pull down all PBX containing complexes in a non-biased fashion. HEK293T cells express reasonably high levels of PKNOX1 and PBX1/2/3 proteins and barely detectable levels of MEIS1/2/3 (Figure 31). If a competitive mechanism is not present, then total complex participation would not change in response to modulation of either MEINOX component. However, if PKNOX1 competes for utilization of the same partner components, then exogenous expression of

Figure 31. PKNOX1 is a direct competitor of MEIS1 in PBX-containing complexes
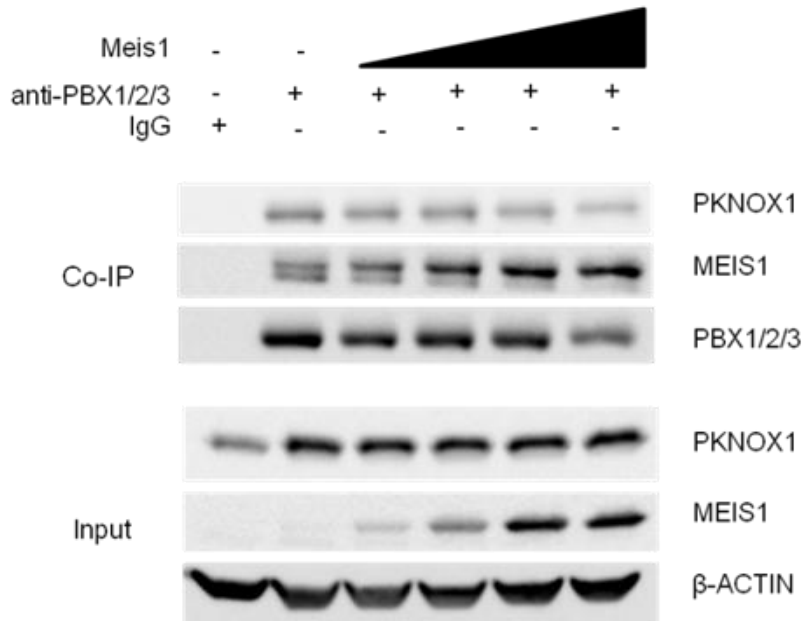
HEK293T cells were transfected with *Meis1* expressing plasmid and subjected to co-immunoprecipitation for PBX1/2/3. 20% input (left) was subject to western blotting for PKNOX1 and MEIS1. Co-immunoprecipitation was performed using antibody against PBX1/2/3

MEIS1 should result in a decrease of PKNOX1 when immunoprecipitating PBX-containing complexes. Upon treatment with increasing levels of Meis1, I observed a decrease in PKNOX1 participation in these complexes, indicating that MEIS1 and PKNOX1 compete for inclusion into the same complexes (Figure 31). Intriguingly, at very high concentrations of Meis1, I observed a decrease in the total levels of immunoprecipitated complex as indicated by blotting for PBX1/2/3 (Figure 31).

Pknox1 overexpression decreases the colony formation, promotes differentiation, and results in a decrease in cell number in _MLL-AF9_ transformed bone marrow

Pknox1 has previously been examined in the cooperation with *Hoxa9* for transformation in mouse models [94]. These studies indicate that *Pknox1* lacks the oncogenic capability of *Meis1* in a *Hoxa9*-dependent transformation model. Further, developmental studies indicate that Pknox1-containing complexes and Meis1-containing complexes often operate in opposition to each other [111]. Previous studies have relied upon co-infection of *HoxA9* and *Pbx1* with *Meis1* or *Pknox1*. In these studies, *Pknox1-Meis1* complex partners are highly expressed under viral promoters and do not need to compete for inclusion into potentially limited complexes.

The role of *Pknox1* within an *MLL-AF9* context remains to be tested. I hypothesized that over-expression of *Pknox1* would have an inhibitory role in an *MLL-AF9* leukemia models. To examine this question, I infected *MLL-AF9* transformed bone marrow with *MIGR1*, *MSCV-Meis1-PGK-GFP*, or *MSCV-pKOF2-Prep1-PGK-GFP* (Figure 32). These viruses serve as an empty vector control (*MIGR1*), a *Meis1*-expressing virus (*MSCV-Meis1-PGK-GFP*), and a *Pknox1* expressing virus (*MSCV-*

Figure 32. *Pknox1* overexpression reduces colony forming ability in *MLL-AF9* transformed bone marrow
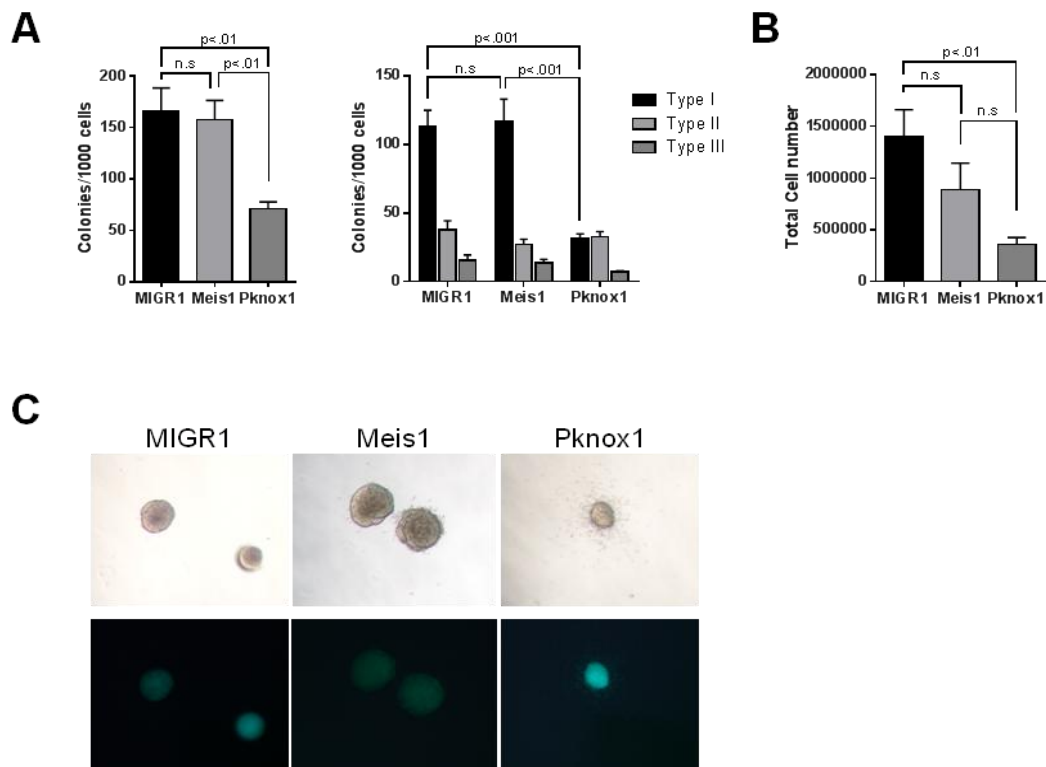
MLL-AF9 transformed bone marrow was infected with *MIGR1*, *Meis1* expressing virus, or *Pknox1* expressing virus. Colony assays were performed in 4 independent experiments. Statistical analysis was performed using Student's t-test. A) Total colony count/10000 cells plated (left) and Colony type (right). B) Total cell number. C) Representative colony pictures displayed for each treatment. Top panels in bright field microscopy, with lower panels utilizing fluorescent microscopy. GFP fluorescence indicates successful infection with retrovirus.

Figure 33. *Pknox1* **overexpression in** *MLL-AF9* **transformed bone marrow results in an increase in differentiation-associated surface markers**
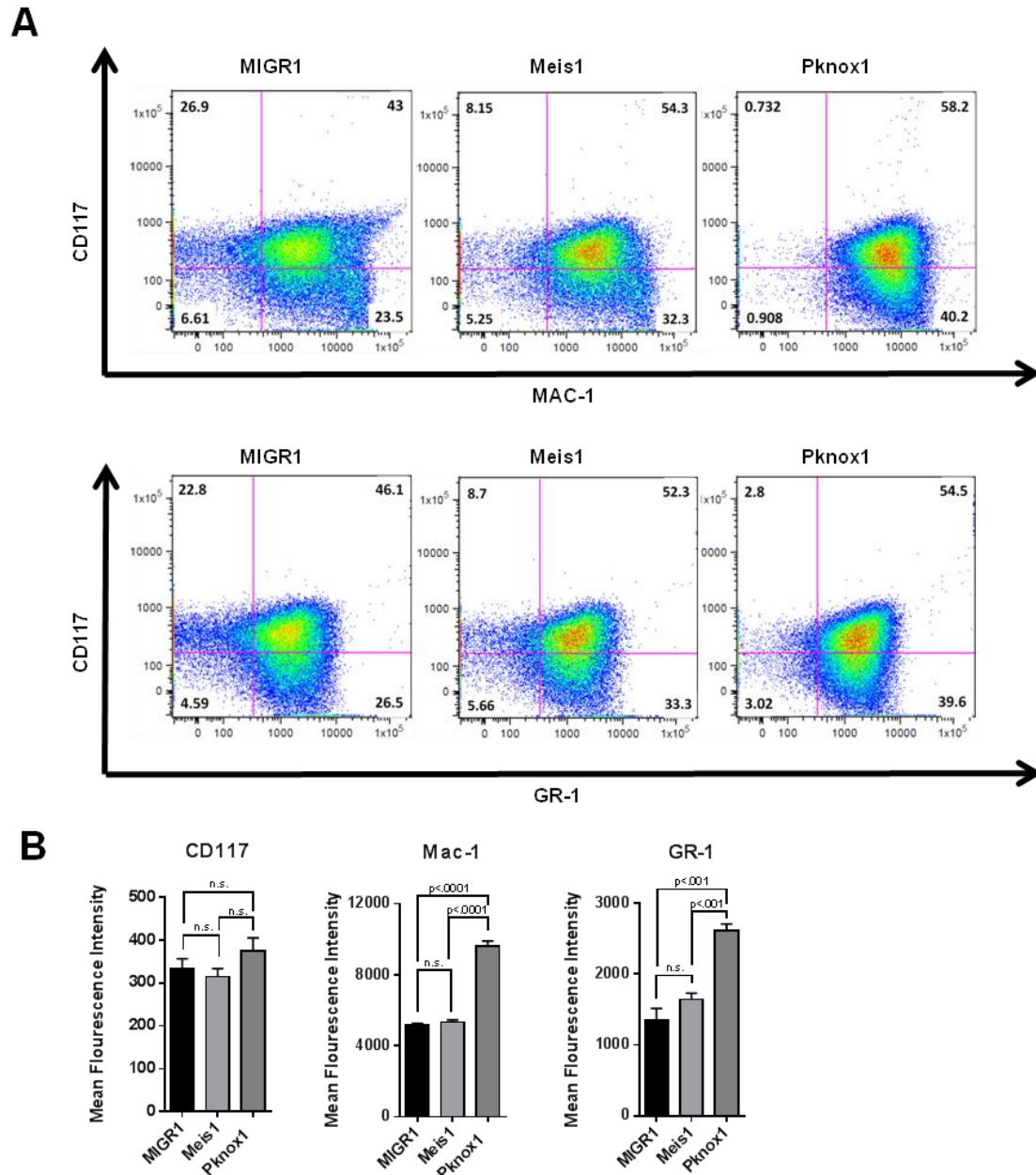
Cells from colony assays were analyzed for surface markers was performed for 3 independent experiments. A) Representative plots showing CD117, MAC-1 and GR-1 staining. B) Mean fluorescence intensity shown from 4 independent experiments. Statistical significance was tested using Student's t-test. *Pknox1* infected cells showed statistically significant increases in mean fluorescence intensity for both Mac-1 ($p < .0001$) and GR-1 ($p < .001$), relative to levels in either *MIGR1*, or *Meis1* infected cells.

pKOF2-Prep1-PGK-GFP). *MLL-AF9* transformed bone marrow readily forms colonies at a high rate. If *Pknox1* has an inhibitory role in MLL leukemia, then enforced overexpression of *Pknox1* will result in a decrease in colony forming ability. To prevent unsuccessfully infected cells from confounding experimental readouts, all infections were sorted for GFP positivity 48 hrs post infection, prior to plating in methylcellulose (not shown). Additionally, colonies were verified for GFP expression at counting. Intriguingly, *Pknox1* infection resulted in a larger GFP negative population at 48 hrs, suggesting a selective pressure against *Pknox1* expressing cells (data not shown).

Infection with *Pknox1* expressing virus resulted in a decrease in colony number relative to both control *MIGR1* treated cells and *Meis1* infected cells (Figure 32). When I examined the composition of colonies by subtype, I observed that the decrease in colony number came primarily from a decrease in Type I colonies. No significant differences were observed in type 2 colonies or type 3 colonies. Total cell number isolated from each colony assay also decreased upon *Pknox1* overexpression. *Meis1* overexpression resulted in a modest but statistically insignificant decrease in cell number.

As type I colonies represent the least differentiated cells, I hypothesized that *Pknox1* overexpression caused a loss of stemness (Figure 33). To examine this possibility, I isolated cells from colony assays at one week and stained with fluorophore conjugated antibodies against CD117, Sca-1, CD11B, and GR-1 for FACS analysis (Figure 33). CD117 (a.k.a. C-kit) and Sca-1 are markers for stemness within hematopoiesis. Conversely, MAC-1 and GR-1 are markers for differentiation.

Figure 34. *Pknox1* **overexpression reduces total cell number in** *MLL-AF9* **transformed bone marrow**
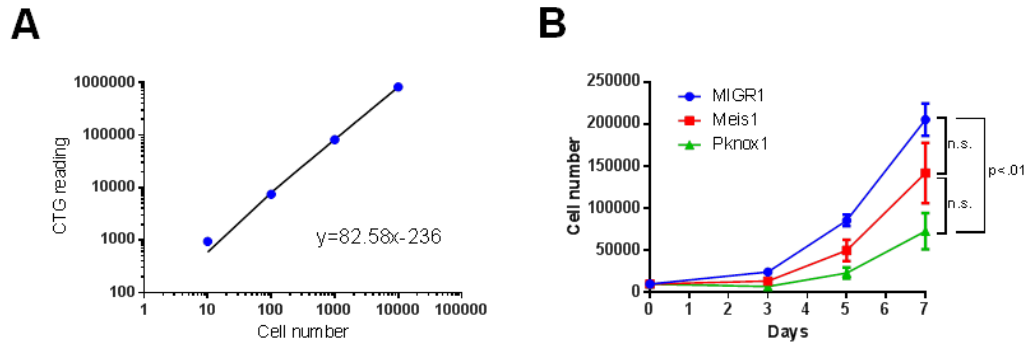
A) Standard curve for calculating cell number of *MLL-AF9* transformed bone marrow B) Proliferation curve for *MLL-AF9* bone marrow infected with *MIGR1*, *Meis1*, or *Pknox1* expressing virus in 3 independent experiments.

Figure 35. *Pknox1* **overexpression results in an accumulation of cells at G0/G1 in** *MLL-AF9* **transformed bone marrow**
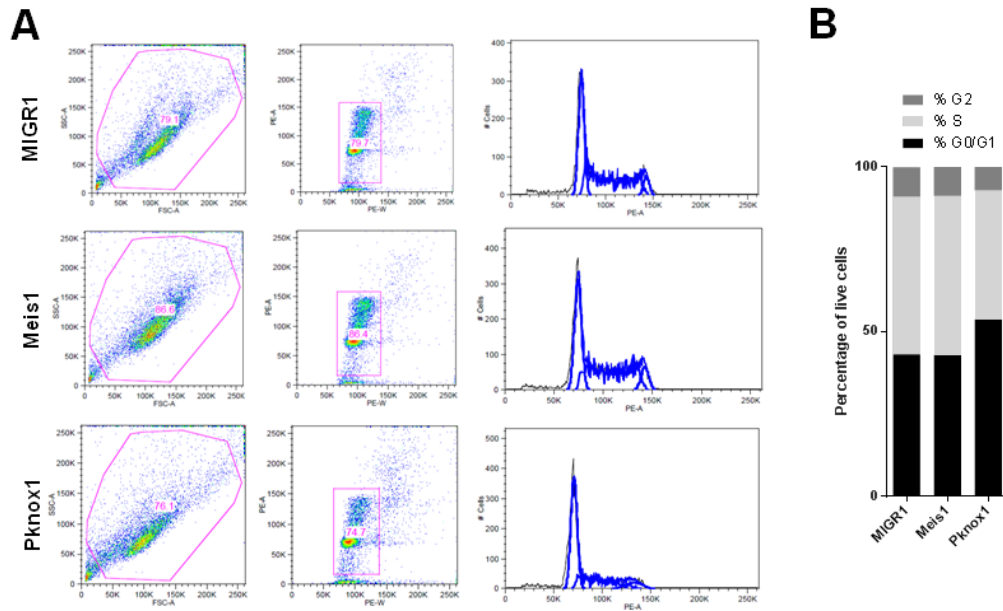
Cell cycle distribution was documented after 7 days in liquid culture by FACS analysis for 4 independent experiments. A) Representative FACS plots with gating. B) distribution of live cells measured for *MLL-AF9* transformed bone marrow infected with *MIGR1*, *Meis1*, or *Pknox1*.

Exogenous overexpression of *Pknox1* resulted in both a decrease in c-kit expression and in increase in differentiation markers GR-1 and Mac-1 (Figure 32).

As with human colony assays, examination of the proliferation and cell cycle in colony assays remains confounded by the decrease in colony forming ability and the limited number of cells. To distinguish the effects of *Pknox1* on proliferation from the decrease in total cell number in colony assays, I infected *MLL-AF9* transformed bone marrow cells and plated cells in liquid culture. I examined the proliferation curve of cells over the course of several days, measuring the cell number at days 3, 5, and 7 (Figure 34). As with human cell lines, total cell number was calculated based on comparing Cell-Titer-Glo assay readouts to a previously established standard curve. Enforced expression of *Pknox1* resulted in a decrease in proliferation over the course of 7 days (Figure 34). Surprisingly, enforced overexpression of *Meis1* also resulted in a small, though insignificant, decrease relative to *MIGR1* infected cells (Figure 34).

The remaining cells were analyzed by FACS for cell cycle (Figure 35). As with my human cell line experiments, I observed a modest accumulation of cells at G0/G1 (Figure 35). This observation is consistent with our model of differentiation and proliferative arrest observed in human cell lines. Collectively, this data suggests that decrease in *Pknox1* infected *MLL-AF9* transformed cells is the result of either a cell cycle arrest at G1, senescence, or differentiation. The lack of a significant increase in a <G0/G1 populations suggests that apoptosis in not likely the cause of *Pknox1* mediated decrease in cell number.

CHAPTER 5

DISCUSSION

This dissertation examines the contribution of miRNAs to MLL leukemia through knockdown of miRNAs that have increased expression in MLL AMLs relative to non-MLL AMLs. I have identified miRNAs critical to colony forming ability in *MLL* translocated human cell lines, through individual and combinatorial knockdown of miRNAs. Additionally, I have validated *PKNOX1* as a target of the *miR-17* and *miR-19* families of the *miR-17-92* cluster through luciferase reporter studies and examination of protein levels upon miRNA level manipulation. Finally, this dissertation demonstrates the competitive relationship between PKNOX1 and MEIS1 in PBX complex formation and the inhibitory role of *PKNOX1* in an *MLL* specific context (Figure 36).

I have determined the requirement of specific miRNAs in the *miR-17-92* cluster to maintain the transformed phenotype of MLL leukemia by antagonizing miRNAs over-expressed in this subtype of leukemia. Treatment with antagomirs against *miR-17* or *miR-20a* individually caused a decrease in MLL leukemia colony forming ability (Figure 14). For antagomir treatments against either *miR-17* or *miR-20a* alone, colony forming ability decreased by >40% in MOLM-13, >30% in RS4;11, and >99% in MV4-11. These treatment effects underscore the importance of the *miR-17* family in MLL leukemia and suggest that inhibiting even a single family member is sufficient to disrupt the delicate regulatory balance they enforce. Combinations of multiple antagomirs for treatment

132

caused a further decrease in colony forming ability (Figure 15). In particular,

antagonizing both *miR-17* and *miR-20a*, or both *miR-17* and *miR-19a* resulted in a

dramatic decreases in colony forming ability in methylcellulose colony assays (Figure

15). In this study, I approached combinatorial antagomir treatments by targeting either

related miRNAs of the same miRNA family (e.g. *miR-17, 20a*) or targeting unrelated

miRNAs (e.g. *miR-17,19a*). Antagonizing related miRNAs of the same family would

potentially block redundant functions caused by multiple miRNA family members'

ability to target the same mRNA transcript. Antagonizing unrelated miRNAs would

potentially expose areas of miRNA coordination in regulating a phenotype. Strikingly,

antagonism of non-family miRNAs, *miR-17* and *miR-19a* showed a more dramatic effect

beyond that observed for targeting only the constituent individual miRNA family

members, indicating that the miRNAs from different families function are coordinated

(Figure 17). This could be due to regulation of different target gene mRNAs or because

multiple miRNAs simultaneously and more efficiently target the same critical mRNA.

I observed that several single antagomir treatments have no effects relative to the

control antagomir treatment (Figures 12, 16). *miR-10a* is located in the *HOX* clusters and

has been documented as being upregulated in MLL leukemias relative to non-MLL

AMLs [148]. *miR-191* is a negative prognostic indicator for AML, suggesting the

possibility of a functional role in disease development [155]. However, neither inhibition

of *miR-10a* nor of *miR-191* resulted in a decrease in colony forming ability. It is possible

that these miRNAs share redundant functions with other miRNAs, and inhibition of a

single miRNA is unable to relieve the repression of a target mRNA. Alternatively, these

miRNAs may be upregulated but have no functional importance in leukemia.

The antagomir treatment effects varied in scale between the different cell lines examined (Figure 12-17). These studies utilized human cell lines with either t(4;11) or t(9;11) translocations, resulting in *MLL-AF4* or *MLL-AF9* fusions, respectively. Despite their genetic similarities, the human cell lines examined in my experiments had somewhat different results in colony assays. MV4-11 showed the most dramatic effects upon antagomir treatment with massive decreases in colony forming ability and total cell number, while MOLM-13 and RS4;11 showed smaller, but still significant effects. For example, *anti-miR-20a* treatment results in a significant decrease in colony forming ability of MOLM-13 and RS4;11 with decreases of 62% and 42% relative to the control antagomir treatment. However, in MV4-11, colony forming ability was completely lost (Figure 14). It is possible that the differences in colony forming potential are caused by differences in genetic factors not related to the MLL fusion protein, including: cooperating mutations incurred throughout several decades of cell culture, or differences in gene expression for critical factors in colony formation. For example, the cell lines I examined showed differential basal levels of PBX1/2/3 (Figure 28). It is also possible that there is variance in the basal levels of miRNAs necessary for MLL leukemia. In this case, a decrease in colony forming ability may be more easily obtainable upon antagomir treatment, as decreasing the miRNA levels below the minimal required amount for colony formation may be more easily achieved. Alternatively, another potential cause could be the different clonogenic potentials of the cell lines utilized. Loss of colony forming ability was most severe in MV4-11, which possesses the lowest baseline

clonogenicity. The decreased clonogenicity could result in a greater sensitivity to antagomir treatments. It is not immediately clear what factors govern the differences in clonogenicity between cell lines.

After observing decreased colony size and a decrease in cell number in methylcellulose, I hypothesized that loss of colony forming ability was accompanied by a decrease in proliferation. I only observed a modest difference in the number of antagomir treated cells in liquid culture relative to control treatments that corresponded to the colony assays (Figure 22-23). Nor did I observe a sizable change in cell cycle distribution (Figure 22-23). This could indicate that the decrease in cell number observed in colony assays is dependent on the colony forming ability. However, because colony assays reflect the capabilities of only a small subset of cells, it is possible that the proliferative defect is only apparent in these cells, and any subsequent decrease on cell number is the result of an absence of colonies. Alternatively, expression of target gene mRNAs may vary based on the difference in culture conditions between methylcellulose and liquid culture. However, the molecular aspects of cells in methylcellulose are of greater interest because methylcellulose colony forming ability has been utilized as a surrogate for Leukemia Stem Cell (LSC) activity in MLL and the ability to block colony forming ability in methylcellulose may be used to identify factors essential to MLL leukemia.

In addition to examining miRNA inhibition in human cell lines, I have additionally utilized antagomirs for miRNA inhibition of *MLL-AF9* transformed murine bone marrow progenitor cells in colony formation assays (Figures 24-25). Antagomir

treatments have previously been utilized by our lab in this type of murine system. The decrease in colony forming ability in *anti-miR-196b* treated cells was expected as it confirmed the role established for *miR-196b* by a previous member of our lab Dr. Relja Popovic [11]. Relja's work, in collaboration with the Grimes lab (Cincinnati Children's Hospital), show that inhibition of *miR-196b* results in a loss of colony forming ability [11]. Decrease in colony number and change in colony morphology was observed and suggest a loss of stemness. However, no treatment effect is observed for *MLL-AF9* transformed bone marrow treated with *anti-miR-19b*, despite the high homology between *miR-19a* and *miR-19b* (Figure 24-25). It is possible that the non-seed region nucleotides involved in stabilization of the miRNA:mRNA interaction provide the critical balance in whether or not a functionally important target mRNA is successfully targeted.

Numerous potential causes could explain the differences in results between the human and murine systems. Primarily, the human cell lines used contain a myriad of additional mutations accumulated over decades in culture. To address this possibility, further work may utilize primary patient derived samples. Additionally, there may be a difference in gene regulation, as each system may present different target mRNAs or may express common target mRNAs at different levels. Finally, the human and mouse model systems utilize cells at different disease stages.

In addition to the miRNAs examined in this work, recent advancements have identified several miRNAs possessing critical functions in MLL leukemia. *miR-9* has been shown to be upregulated in MLL leukemia relative to both non-MLL AML and normal cells [246]. Inhibition of *miR-9* through a miRNA-binding sponge results in a

decrease of *MLL-AF9* transformation ability *in vitro* and *in vivo*, while over expression of

miR-9 in conjunction with *MLL-AF9* transformation increases the transformation ability

of *MLL-AF9* in colony forming assays and *in vivo* experiments [246]   Studies performed

by our collaborator, Dr. Grimes (Cincinnati Children's Hospital), identify *miR-21* and

miR-196b as a having synergistic roles in AML development [234, 247]. Both *miR-196b*

and *miR-21* are negatively regulated by the transcriptional repressor GFI1, which

functions in opposition to HOXA9 mediated transcriptional activation [247]. In *HOX*-

dependant transcriptional programs, including *MLL-AF9* mediated transformation,

antagomir inhibition of *miR-196b*, *miR-21*, or both, reduced colony forming ability and *in*

vivo leukemogenesis through targeting leukemia initiating cells (LIC) activity [234].

Collectively, these studies implicate an additional miRNA, *miR-21*, in the development of

MLL leukemia, and further illustrate the importance of *miR-196b* in MLL leukemia.

While this study focused on several miRNAs upregulated in MLL leukemia, it does not

address the roles of miRNAs that are downregulated or lost in MLL leukemia, which

contribute to transformation. Several miRNAs, including *miR-495*, the *miR-181* family

(*miR-181a/b/c/d*), and *miR-150* have been identified as tumor suppressors and have been

shown to be down regulated in MLL leukemias [86, 148, 248, 249]. Several

downregulated miRNAs function through regulation of the Hox complex components

essential to MLL leukemogenesis. MLL leukemias show downregulation of, the *miR-181*

family (*miR-181a/b/c/d*), relative to non-MLL AMLs [152]. Examination of *miR-181*

among cytogenetically abnormal AMLs, identify loss of *miR-181* as a negative

prognostic indicator [86]. Further, a signature of 4 *miR-181* targets, *HOXA7*, *HOXA9*,

HOXA11, and *PBX3* are upregulated, and have been functionally evaluated *in vitro* and *in vivo* [86]. Overexpression of *miR-495* is downregulated in MLL leukemias relative to non-MLL AMLs. Overexpression of *miR-495* has been shown to reduce colony forming ability *in vitro* and leukemogenesis *in vivo* by targeting both *PBX3* and *MEIS1* [248]. *MiR-150* has been implicated as a tumor suppressor miRNA down regulated in most AMLs relative to normal controls [249]. The MLL-fusion/Myc/LIN28 axis represses *miR-150* maturation [249]. *MiR-150* regulates Myb and Flt3 resulting in a decrease in the Myb regulatory targets *Hoxa9* and *Meis1* [249]. Ectopic overexpression of *miR-150* in *MLL-AF9* transformed bone marrow reduced colony formation *in vitro* and in leukemogenesis *in vivo* [249, 250]. Critically, these miRNAs and their contributions to MLL leukemia are linked to regulation of components of the HOX-PBX-MEINOX complexes required for MLL leukemia. However, my work differs from these critical studies, in that I examine the contribution of miRNAs in MLL leukemia through regulation of a MEIS1 competitor.

My data demonstrates that *PKNOX1* is a valid downstream target of the *miR-17-92* cluster (Figure 27). Multiple different miRNAs from this cluster simultaneously regulate *PKNOX1* mRNA through binding to 3 separate miRNA response elements (Figure 27). Four of the 6 miRNAs of the *miR-17-92* cluster (*miR-17*, *20a*, *19a*, and *19b*) regulate *PKNOX1*. This redundancy of miRNAs targeting the same mRNA suggest that the relationship of *miR-17-92* and *PKNOX1* functions as an important regulatory switch which may respond to various cellular signals. To determine the interactions between miRNAs and the *PKNOX1* 3' UTR, I performed a luciferase reporter experiment with a

luciferase construct modified to encode the *PKNOX1* 3'UTR downstream of the

luciferase coding sequence. Mutation of *PKNOX1* 3'UTR at the miRNA response

elements to which the miRNAs bind for either the *miR-17* family or the *miR-19* family

show an increase in luciferase activity relative to a wild type *PKNOX1* 3' UTR (Figure

27). Simultaneous targeting of a single 3'UTR by multiple miRNAs has been reported to

regulate mRNA levels in a cooperative manner utilizing AGO1, AGO3, and AGO4-

containing RISC complexes [251]. Efficient miRNA cooperativity requires relatively

close proximity of MREs within the target 3'UTR, approximately 13-35 nts between the

start of the seed region binding [252]. A transcriptome-wide examination of miRNA

binding sites (utilizing HITS-CLIP and PAR-CLIP) found an enrichment of miRNA-

binding sites located 15-26 nts apart [253]. Within the *PKNOX1* mRNA, the initial *miR-

17* family binding site (MRE1) and the sole *miR-19* family binding site are located at

nucleotide positions 20 and 52 of the 3'UTR, respectively. This 32 nt difference in

position, is close enough to suggest that *miR-17* and *miR-19* family miRNAs negatively

regulate *PKNOX1* through cooperative targeting of the same mRNA. It is possible that

combinatorial miRNA effects may additionally occur through non-cooperative targeting

on separate mRNA transcripts where the overall ratio of miRNAs to mRNAs controls the

final level of mRNA available for translation, through productive single miRNA

mediated silencing of mRNA transcripts.

I observed a polymorphism within the predicted *miR-18* binding site of the

PKNOX1 3'UTR (Figure 26). This polymorphism, encoding a G to A mutation at

position 2811 of the *PKNOX1* 3' UTR, is located outside of the sequence targeted by the

seed region and should not affect the core targeting of the *PKNOX1* 3' UTR by *miR-18*, but may affect the binding stability of the *miR-18* miRNA:RISC complex to the *PKNOX1* 3'UTR. Previous studies have identified MRE single nucleotide polymorphisms as having functional roles in miRNA:mRNA interactions and as serving as prognostic indicators for cancers [254-256]. This polymorphism I observed is predicted to be involved in stabilization of binding with the *miR-18* containing miRNA:RISC complex through interaction with the uracil located at position 15 of *miR-18a*. In the previously documented mRNA transcript, the guanine base interacts with the uracil through a wobble base pairing. The polymorphism, encoding an adenine in place of the guanine, would result in an improved binding stability between the *PKNOX1* 3'UTR and the *miR-18* containing RISC complex.

The *miR-17-92* cluster is one of the best studied miRNA clusters to date, with targets involved in processes including cell death, cell cycle, development, and a number of different cancers, including lymphoma, and breast cancer (reviewed in [173-175]). In addition to *PKNOX1*, *miR-17* and *miR-19a* also target other mRNA transcripts that are important to MLL leukemia. *PTEN* has been validated as a target for both *miR-17* and *miR-19a* [190, 257] *PTEN* mRNA levels have been reported to inversely vary with miRNA overexpression for both *miR-17* and *miR-19b* in transformed bone marrow [12]. *MiR-17* has additionally been shown to be important in regulating the G1 checkpoint by regulating both *CDKN1A (p21)* and *E2F1* [177, 183]. While shRNA knockdown of *CDKN1A (p21)* in an MLL leukemia model phenocopies overexpression of the *miR-17-19b* [183], it is not currently known to be targeted by *miR-19a*. My data indicate only a

minor G0/G1 arrest, suggesting that the *miR-17-92* cluster functions through other

mechanisms (Figure 22-23). A lack of visible G0/G1 arrest in cell cycle assays may be

attributable to a decrease in cell cycle progression through both G1 and G2 checkpoints.

Previous work performed by our lab has identified the G2/M checkpoint regulator *WEE1*

as a *bona fide* target of the *miR-17-92* cluster [258]. My antagomir treatment data

indicate a more severe phenotype upon combinatorial treatment with *anti-miR-17* and

anti-miR-19a (Figure 17). As a result, I focused on a target that is regulated by both *miR-*

17 and *miR-19a*. While binding affinity to *PKNOX1* transcript is predicted to be

thermodynamically stable, it is likely that other mRNAs are targeted simultaneously

dependent on availability of targets.

The nature of miRNA function suggests that a great deal of binding promiscuity is

possible. MiRNAs bind to target mRNAs based on Watson-Crick base pairing between

the seed region and a target mRNA. While this study has characterized a single transcript

that is regulated by miRNAs in MLL leukemia, *PKNOX1* is not the sole target of the

miR-17-92 cluster. A previous study by our collaborator, Dr. Jianjun Chen, observed that

overexpression of the *miR-17-92* cluster in murine bone marrow results in

downregulation of 363 potential target genes predicted to be regulated by the *miR-17-92*

cluster by at least one miRNA target prediction algorithm, suggesting that disregulation

of the *miR-17-92* cluster has broad implications in target mRNA regulation [12].

Currently, miRNA target prediction algorithms focus on predicting the actions of

individual miRNAs. MiRNA target prediction algorithms have predicted a number of

target mRNAs that are shared between numerous miRNAs. 2 PBX family members,

PBX1 and *PBX3*, are predicted to be common targets of *miR-196b* and the *miR-17-92* cluster. *PBX1* is predicted to be targeted by the *miR-19* family and *miR-196b*, while *PBX3* is predicted to be targeted by the *miR-17* family and *miR-196b*. While *PBX3* is a known oncogene with a critical role in the formation of MLL leukemia, the role of *PBX1* is less clearly defined, and may lack the ability to promote oncogenesis. If *PBX1* lacks the oncogenic capabilities of *PBX3*, miRNA regulation of the *PBX1* transcript could potentially contribute to MLL leukemia through elimination of PBX1 competition with PBX3 for inclusion in HOXA9-MEIS1 complexes, similar to the effect I observed for miRNA regulation of *PKNOX1*.

Studies to determine the role of the *miR-17-92* cluster in MLL leukemia are complicated by presence of its 2 homologous clusters, *miR-106a-363* and *miR-106b-25*. While direct regulation of the *miR-17-92* cluster by MLL fusion proteins has been verified, the regulation of *miR-106a-363* and *miR-106b-25* in MLL leukemia has not yet been explored.

The potential implications of upregulation of the *miR-106* clusters is further complicated by the composition of each cluster. The *miR-17-92* cluster is composed of 2 members of the *miR-17* family, 2 members of the *miR-19* family, a member of the *miR-18* family, and member of the *miR-92* family (see Figure 7). However, *miR106a-363* and *miR-106b-25* clusters are composed of different proportions of constituent miRNAs (Figure 7). If these miRNA clusters are simultaneously upregulated in MLL leukemia, then we must further consider the potential cooperative pathways between the *miR-92* and *miR-18* families, as their representation among miRNA:RISC complexes would be

increased.

In addition to the regulation by the *miR-17-92 cluster*, additional miRNAs have been documented as regulators of *PKNOX1*. A study performed by Zhuang, *et al* examined the mRNA targets of *miR-223* in macrophages in adipose tissue inflammation [259]. They identified *PKNOX1* as a valid targeted of *miR-223* and determined that it regulates macrophage polarization, driving macrophage activation towards a classical M1 pro-inflammatory Macrophage activation [259]. Additional studies have identified *miR-223* as a critical factor in granulopoiesis, with *miR-223* deficient mice showing defects in differentiation [260, 261]. One study has identified *miR-223* as being regulated by CEBPA binding and downregulated in AML [262]. However, no studies have identified *miR-223* as being upregulated in leukemia.

Future studies to expand on miRNA function may reveal additional mechanisms of action, and subsequently expand our understanding of miRNA contribution to diseases. Though miRNA were originally identified through complementary binding to the 3' UTR of target mRNAs, there is evidence that miRNAs can also target the 5'UTRs to downregulate target genes [143]. Further, miRNAs such as *miR-10a* possess novel regulatory mechanisms [144]. For example, *miR-10a* has been shown to bind to the TOP motifs within 5' UTR of target genes and results in an increase in transcription [144]. Further, recent experiments utilizing HITS-CLIP sequencing, an unbiased immunoprecipitation for RISC bound mRNAs, have indicated that miRNAs bind to a more diverse collection of mRNA targets than had previously been thought [146]. As future studies continue to unveil new miRNA functions, our understanding of the role

miRNAs in diseases will evolve to include new classes of targets.

Western blotting indicated an additional band present in PKNOX1 western blots running slightly above the expected molecular weight (Figure 30). This data suggests PKNOX1 may be regulated through post-transcriptional modifications (e.g. phosphorylation). While there have been no documented post-translational modification to PKNOX1 in the literature, such a mechanism could potentially add to the complexity of control of PKNOX1 levels.

I have examined the effects of exogenous overexpression of *Pknox1* in *MLL-AF9* transformed murine bone marrow to determine the role of *Pknox1* in MLL leukemia. (Figures 32, 33, 35). PKNOX1 and MEIS1 are homologous in their PBX-interacting domains and homeodomains [72, 73]. However, Meis1 oncogenic activity is dependent on its C-terminal domain, which is not shared with Pknox1 [94]. The C-terminal domain of Meis1 is known to have multiple protein-protein interactions. It is currently unclear whether the Pknox1 C-terminal domain has any protein-protein interactions of its own. Functional examination of the Pknox1 C-terminal domain is required to determine the mechanism of Pknox1 regulation of target genes. Previous studies found that infection with *Pknox1*-expressing virus fails to accelerate leukemia similarly to *Meis1* when co-expressed with *Hoxa9* [94]. This dissertation demonstrates that altering the balance of PKNOX1 to MEIS1 levels affects MLL leukemia cell proliferation and colony-forming ability. *Pknox1* overexpression in a murine MLL leukemia model decreased colony forming ability, primarily from a loss of less differentiated colonies. Antagomir treatment of human MLL leukemia cells had a similar outcome on colony forming ability, which

could possibly be due to increasing the PKNOX1:MEIS1 ratio within these cells. Colony forming capability has been used as a measure of leukemia stem cell activity in the MLL leukemia model system. Thus, loss of colony forming ability in response to antagomir treatments suggests that MLL leukemia stem cell activity may be predominantly targeted by these miRNAs. Future work could determine whether specific cell contact-mediated pathways are particularly influenced by *miR-17-92* cluster miRNAs in MLL leukemia.

I observed a greater decrease in proliferation upon *Pknox1* overexpression than upon antagomir treatment. This difference may be attributed to multiple factors, such as dosage of *Pknox1,* effectiveness of antagomir delivery, or inherent differences between mouse and human cell lines. Exogenous overexpression of *Pknox1* from a viral promoter would result in a much higher amount of Pknox1 relative to Meis1. While removing the inhibition of the miRNAs through use of antagomirs allows Pknox1 levels to increase, exogenous overexpression drives Pknox1 levels very high. Cell cycle analysis of *Meis1* transduced cells indicates no significant change in the cell cycle distribution relative to control vector-transduced cells. The minor decrease in *Meis1* transduced cells is thus not likely to be of similar origin as the decrease observed with *Pknox1*.

Pknox1 has additionally been characterized as a tumor suppressor in an *Eµ-Myc* lymphoma model with *Pknox1* hypomorph mutants and *Pknox1* heterozygotes resulting in increased tumor size and accelerated onset of lymphoma [109]. The *Eµ-Myc* lymphoma model is driven by the constituent activity of the *c-Myc* proto-oncogene behind an immunoglobulin promoter, designed to simulate a B-cell lymphoma [263]. Loss of *Pknox1* expression within this context leads to a shift in the B-cell population;

with *Eµ-Myc*; *Pknox1(+/-)* mice having more immature phenotypes, consisting of Pro-
and Pre-B-cells, and *Eµ-Myc; Pknox (+/+)* mice having more mature phenotypes [264].

It is possible that *Pknox1* competition with *Meis1* may regulate the development of B-
Cells, such that loss of *Pknox1* may result in decreased B-Cell differentiation.

These findings indicate that the canonical HOXA9-MEIS1 pathway is regulated
through the coordinated action of multiple miRNAs. miRNAs including *miR-495*, *miR-
181a/b*, and *miR-150*, which would negatively regulate the expression of the HOXA9-
PBX3-MEIS1 complexes, are down regulated, relieving the repression of HOXA9-
MEIS1 transcriptional regulation. Opposing these effects, previous work has indicated
that *miR-196b* down regulates both *Hoxa9* and *Meis1*, resulting in an initial delay in
leukemia onset in a murine leukemia model, but ultimately with development of a more
aggressive leukemia [163]. *miR-196b* functions as both a tumor suppressor and oncogene
through repression of *HOXA* and *MEIS1* and *FAS*, respectively [163]. Because *HOXA9*
and *MEIS1* are essential for MLL leukemia, and *miR-196b* is upregulated in MLL
leukemias, this relationship presents a unique puzzle. If *HOXA9* and *MEIS1* are
downregulated, additional factors must either restore HOXA9 and MEIS1 levels or
otherwise ameliorate the effect. Both *miR-196b* and *miR-17-92* are directly regulated by
MLL, and are upregulated in MLL leukemias [12, 64, 152]. I propose that the *miR-17-92*
cluster acts as a counterbalance to the tumor suppressor properties of *miR-196b*. As
miRNA regulation of *HOXA9* and *MEIS1* is held in a delicate balance, regulation of the
MEIS1 competitor *PKNOX1* provides a critical mechanism for regulation of HOXA9-
MEIS1 activity. During leukemogenesis, *miR-17-92* expression results in a decrease in

PKNOX1 expression, alleviating competition with MEIS1 for PBX-HOX complex inclusion. Additional work has indicated that 5' Hox transcription factors, acting in conjunction with a Cdx2 partner, positively regulate the expression of *miR-196b* in neural tube development [265]. As a result, a negative feedback loop would be present, limiting the overall expression of *Meis1*.

Meis1 overexpression in *MLL-AF9* transformed bone marrow resulted in an intermediate phenotype with cell surface markers and *Meis1* overexpression resulted in a decrease in cellular proliferation (Figure 33, 35). Exogenous overexpression of *Meis1*, in addition to *MLL-AF9* transformation mediated overexpression of *Meis1*, appears to have its own toxicity. Exogenous *Meis1* overexpression is potentially toxic to the cells and may result in a decrease in exogenous Meis1 expression. The mechanism of toxicity is not yet apparent, but may be caused by a variety of factors, including mitotic catastrophe or apoptosis, among other possibilities. Overall levels of Meis1 may need to be maintained below a certain level. Though *Meis1* overexpression was originally utilized as a negative control for *Pknox1* overexpression, Meis1 activity may present its own complications attributable to the regulation of target genes.

Complex regulatory circuits involving miRNAs are starting to be defined in MLL leukemia. This includes those regulating the HOX-PBX-MEIS trimeric protein complex. Both *HOXA9* and *MEIS1* are directly regulated by MLL and are necessary for MLL leukemia development [6, 24, 91, 113]. *HOXA9* and *MEIS1* are negatively regulated by *miR-196b*, one of the miRNAs overexpressed in MLL leukemia, thus limiting the amounts of these proteins available for incorporation into HOX-PBX-MEIS complexes.

Although this causes an initial delay in the onset of leukemia, increased *miR-196b* expression ultimately contributes to a more aggressive leukemia [163]. HOX-PBX3 protein-protein interaction is also essential for MLL leukemia development and inhibition of this interaction with a small peptide selectively kills cells dependent on *HOXA* and *PBX3* overexpression [87]. MiRNAs in the *miR-17-92* cluster are also overexpressed in MLL leukemia. I show here that m*iR-17-92* cluster miRNAs, including *miR-17* and *miR-19a*, target *PKNOX1* and that antagonizing these miRNAs causes increased PKNOX1 expression. I also show that MEIS1 and PKNOX1 can compete for binding in HOX-PBX-containing complexes and that manipulation of relative MEIS1/PKNOX1 levels has a dramatic effect on MLL leukemia. More HOX-PBX-MEIS1 complexes as compared to HOX-PBX-PKNOX1 complexes potentiate MLL leukemia colony forming activity. Together, this suggests that HOX-MEIS-PBX complexes may be a limiting factor in MLL leukemia which may be amenable to functional disruption via antagonizing critical regulatory miRNAs.

Recently, the Blasi group published data which support and complement my findings [112, 113]. They found that Prep1 (Pknox1) competes with Meis1 for binding to Pbx1, and *Prep1* depletion enabled *Meis1* to transform MEFs [112]. The authors transfected *Prep1* hypomorphic MEFs with *Meis1* and *Prep1*, and observed that *Meis1* transfected MEFs form colonies in soft agar colony assays. Co-transfection with *Prep1* results in a decrease in Meis1 stability and colony capability. Further, *Meis1* colony formation in MEFs as well as Pknox1 mediated inhibition of Meis1 requires Pbx1. The authors further examined the complex formation, and identified the Ddx3 and Ddx5 as

critical complex components which are required for colony formation. These findings support my hypothesis that PKNOX1 competes with MEIS1 for inclusion into PBX-containing complexes. My studies utilize HEK293T cell with increasing expression of exogenously introduced MEIS1 to examine the competitive role between MEIS1 and PKNOX1, which my data supports. It is unclear whether Ddx3, and Ddx5 are functionally important for Meis1 activity in MLL leukemia. A subsequent study by the same group identified that deficiency of *Pknox1* accelerated the onset of *Meis1-Hoxa9*-mediated leukemogenesis in a murine model of serial transplantation [113]. Critically, the Blasi group examined the effects of a lack of *Pknox1* as a factor involved in the acceleration of leukemogenesis. I am interested in the opposite effects - in potentially increasing Pknox1 levels as a mechanism to block *Meis1-Hoxa9* mediated transformation in hematopoietic cells. Further, while the Blasi group utilized exogenous overexpression of *Meis1* and *Hoxa9*, my studies assessed the relationship between MEIS1 and PKNOX1 within an *MLL-AF9* context. They hypothesized that increasing PKNOX1 levels may be an important area for future therapeutic development [112]. My work agrees with this suggestion.

To examine the target genes regulated by *Meis1* and *Pknox1*, the Sauvegeau lab examined the gene expression profiles of cells infected bone marrow progenitor cells with viruses expressing either: *Hoxa9 + Pknox1*, *Hoxa9 + Meis*, or *Hoxa9 + Pknox1-MC* (a chimeric Pknox1 possessing the oncogenic Meis1 CTD appended to the C-terminus). Critically, cells with exogenously overexpressed *Hoxa9 + Pknox1* or *Hoxa9 + Meis1*, resulted in very different gene expression profiles [94]. *Hoxa9 + Meis1* infection results

in the upregulation of 1202 genes with a significant upregulation of genes related to chromosomal organization, cell cycle, DNA damage response. However, *Hoxa9 + Pknox1* infection resulted in upregulation of 885 genes, with no significant enrichment in genes related to any cellular process. Numerous target genes were of particular interest to the development and function of leukemia. For example, mRNA levels of the *Meis1* target *Flt3* was differentially regulated between *Meis1+ Hoxa9* and *Pknox1+ Hoxa9* [94]. Moreover, transformation with either *Hoxa9 + Meis1*or *Hoxa9 + Pknox1-MC* results in the upregulation of *Meis1*, suggesting the possibility of a positive feedback mechanism whereby *Hoxa9* and *Meis1* contribute to the elevation of *Meis1* levels [94].

My studies examine PKNOX1 as a competitor with MEIS1 for inclusion into HOX-PBX-MEINOX complexes. However, changes in the binary complex composition may also vary in response to Pknox1 upregulation. Examination of Pknox1, Meis1, Hox and Pbx during murine embryonic development by Penkov and colleagues identify commonly occurring binary complexes that form in addition to Meinox-Pbx-Hox ternary complexes [111]. Pknox1 forms binary complexes with Pbx that bind throughout the coding sequences and have an inhibitory role in gene regulation [111]. Meis1, meanwhile, was observed in binary complexes with Hox associated with promoter regions and contributing to gene expression [111]. The interaction of Meis-Hox binary complexes occurs through the binding between Hox proteins and the Meis1 C-terminal domain [84]. PBX participation within a ternary complex is essential to HOXA9-MEIS1 activity as disruption of the HOX-PBX interaction through a peptide, HRX9, blocks leukemia formation [87]. The peptide used was designed to mimic the conserved motif

found within HOX proteins which interacts with PBX binding partners [266]. Though

initially utilized to block HOX-PBX dimers in melanoma [266], multiple myeloma [267],

and ovarian cancer [266]; within MLL leukemia, this peptide implicates the ternary

complexes as the active HOXA9-MEIS1 effectors in leukemia because disruption of the

HOX-PBX interaction would only alter levels of HOXA9-PBX-MEIS1 ternary

complexes and not HOXA9-MEIS1 complexes. However, if the MEIS1-HOXA9 binary

complexes are similarly capable of upregulating target genes, this may provide an avenue

of escape for leukemia cells treated with antagomirs. Further, HOX protein availability

would still be limited due to HOX incorporation into HOX-PBX-PKNOX1 complexes.

The possibility of PKNOX1-PBX1 binary complex formation could potentially raise

issues with this explanation. However, the extent of binary PKNOX1-PBX complex

formation is unclear.

It is additionally possible that complex formation varies between the different

PBX components. My Co-IP experiments utilize an anti-PBX1/2/3 antibody, and thus do

not distinguish between any of the PBX homologs. This was a deliberate choice in

experimental design to avoid any bias towards any PBX homolog and to account for

MEINOX inclusion into any PBX containing complexes. However, additional

experiments may be required to discern which PBX family members are bound by

PKNOX1 in MLL leukemia. Inclusion of different PBX components may alter binding

specificity to DNA sequences. Many of the initial studies to characterize the binding and

function of PBX proteins were performed using overexpressed PBX1 – the founding

member of the PBX family. However, the biochemical differences between the different

PBX family members is an area of potential further study.

Further studies may strengthen these finding by examining antagomir treatment effects in conjunction with *PKNOX1* knockdown. My studies have shown that antagomir treatment results in a decrease in colony formation and a change in colony and cellular morphology (Figure 12-18), and PKNOX1 protein levels (Figure 30). To ensure that the antagomir treatment effect is attributable to changes in PKNOX1 protein levels, further studies may seek to rescue colony formation ability by knocking down *PKNOX1* via siRNA or shRNA in conjunction with antagomir treatments. If antagomir mediated decreases in colony forming ability is mediated by an increase in PKNOX1, then *PKNOX1* knockdown will result in an increase in colony numbers.

It would be of further interest to examine the effects of antagomir treatment *in vivo*. This dissertation focuses on antagomir mediated treatment effects *in vitro*, utilizing colony forming ability as a surrogate for leukemogenesis. Further studies utilizing *in vivo* antagomir treatments against *MLL-AF9* transformed bone marrow would provide a more complete picture of the potential of antagomirs as a therapeutic option. However, *in vivo* studies are potentially complicated by the delivery of antagomirs to a therapeutic level in leukemic cells. Though antagomirs were originally developed for *in vivo* use, their delivery may be enhanced through the use of various nanoparticles currently under development, including dendrimers. It is not clear whether *in vivo* therapeutic targeting of a limited number of miRNAs would have significant toxicity issues; however, it would be worthwhile to explore as an additional therapeutic approach for MLL leukemia. My data indicates that the antagomir treatments were particularly effective in human cell

lines and that exogenously added *Pknox1* effectively reduced colony forming ability in a mouse model. To bridge the gap between the two sets of data, future rescue experiments should be performed using both model systems.

Additional studies are needed to further clarify the functional difference associated with PKNOX1 and MEIS1. Publicly available datasets from the Gene Expression commons [268] indicate that *Pknox1* RNA levels increase throuhout hematopoiesis differentiation while *Meis1* RNA levels decrease (Figure 4). This inverse level of expression suggests that *Pknox1* may be an important factor in guiding differentiation. As such, indirect upregulation of *Pknox1* mediated by downregulation of *Pknox1*-regulating miRNAs could guide cells along a particular differentiation pathway. This is consistent with my results in the human cell antagomir treatments, where combinatorial antagomir treatment resulted in changes to cellular morphology that include increased vacuolarity and a decrease in nuclear to cytoplasmic ratio, possibly indicating monocytic differentiation (Figure 18). Further, transfection of *MLL-AF9* transformed bone marrow with a *Pknox1* expressing retrovirus resulted in a change in surface markers consistent with differentiation relative to cells infected with a *MIGR1* control virus (Figure 33). To understand the mechanism of PKNOX1 in MLL leukemia, ChIP experiments could be performed in human leukemia cell lines upon antagomir treatment. I would predict that PKNOX1 would associate with HOXA9 and PBX1 at selected target genes. Treatment with antagomirs would result in an increase of PKNOX1 association at target genes known to be regulated by MEIS1-HOXA9 complexes and a decrease of MEIS1 association, as MEIS1 would be excluded from PBX containing

complexes and degraded. To date, many MLL leukemia studies have operated on a sense

of equivalency of different components of the same protein families. Functional studies

are needed to determine the different roles of PBX components and how these relate to

pairing with either MEIS1 of PKNOX1.

My findings contribute to an increasing body of evidence illustrating the potential

for miRNA inhibition by anti-miRNA oligo nucleotides (AMOs) as a therapeutic tool. At

the dosages utilized in these studies, I observed some cellular toxicity upon antagomir

treatment (Figures 12-17), including a modest decrease in colony forming ability.

However, these modest treatment effects may be overcome by altering the dosages

slightly, or by employing a modified delivery system that would improve efficacy at a

lower dosage.

Collectively, this dissertation implicates the *miR-17-92* cluster as an essential

component of MLL leukemia through the role of *miR-17* and *miR-19a* in their repression

of the MEIS1 competitor, *PKNOX1* (Figure 36). MLL fusion proteins aberrantly maintain

the expression of a variety of target genes including *HOX* genes, *MEIS1*, and several

miRNAs, including *miR-196b*, *miR-10a*, and the *miR-17-92* cluster. Previous studies

have shown *HOXA9* and *MEIS1* genes are essential for MLL leukemia. HOXA9 and

MEIS1 form ternary complexes with a PBX family member to regulate numerous

downstream targets. This study examined the necessity of specific miRNAs to MLL

leukemia through the inhibition of miRNAs using highly specific anti-miRNA

oligonucleotides. Here, I establish that *miR-17* and *miR-19a* are essential to MLL

leukemia and cooperate in their contribution to MLL leukemia. This effect is mediated

through *miR-17* and *miR-19a* regulation of *PKNOX1*, which competes for inclusion into PBX containing complexes. Blocking of *miR-17* and *miR-19a* results in upregulation of PKNOX1 and an altered balance of HOX/PBX gene regulatory complexes, resulting in a skewing away from MEIS1-containing HOX/PBX complexes and a loss of leukemogenic ability. In summary, I conclude that expression of several miRNAs of the *miR-17-92* cluster are critical for the continued survival of MLL leukemia . Further examination of the role of miRNAs and PKNOX1 would serve to both deepen our understanding of complex regulatory mechanisms that guide the development of leukemia, and also to aid in the development of targeted therapeutics which may someday provide a valuable clinical tool in leukemia treatment.

Figure 36. Model for miRNA involvement in MLL leukemia.
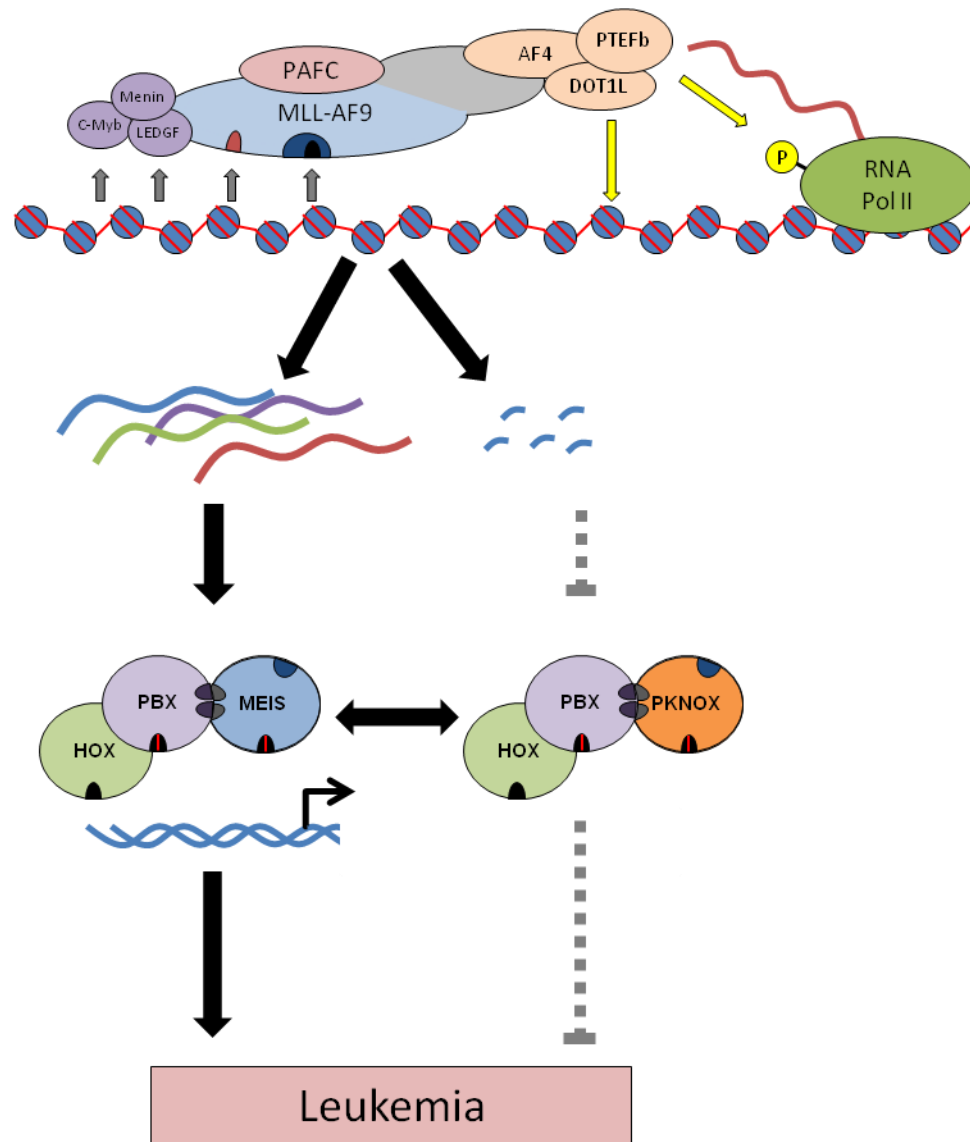
Model of miRNA involvement in MLL leukemia. MLL fusion containing complexes maintain the expression of the components of oncogenic HOX-PBX-MEIS complexes as well as miRNAs including the *miR-17-92* cluster. MiRNAs regulate the complex composition through downregulation of the non-oncogenic component PKNOX1, which serves as a competitor to MEIS1 for complex inclusion and whose overexpression has an inhibitory effect on MLL leukemia function.

REFERENCES

1. Meyer, C., J. Hofmann, T. Burmeister, D. Groger, T.S. Park, M. Emerenciano, M. Pombo de Oliveira, A. Renneville, P. Villarese, E. Macintyre, H. Cave, E. Clappier, K. Mass-Malo, J. Zuna, J. Trka, E. De Braekeleer, M. De Braekeleer, S.H. Oh, G. Tsaur, L. Fechina, V.H. van der Velden, J.J. van Dongen, E. Delabesse, R. Binato, M.L. Silva, A. Kustanovich, O. Aleinikova, M.H. Harris, T. Lund-Aho, V. Juvonen, O. Heidenreich, J. Vormoor, W.W. Choi, M. Jarosova, A. Kolenova, C. Bueno, P. Menendez, S. Wehner, C. Eckert, P. Talmant, S. Tondeur, E. Lippert, E. Launay, C. Henry, P. Ballerini, H. Lapillone, M.B. Callanan, J.M. Cayuela, C. Herbaux, G. Cazzaniga, P.M. Kakadiya, S. Bohlander, M. Ahlmann, J.R. Choi, P. Gameiro, D.S. Lee, J. Krauter, P. Cornillet-Lefebvre, G. Te Kronnie, B.W. Schafer, S. Kubetzko, C.N. Alonso, U. zur Stadt, R. Sutton, N.C. Venn, S. Izraeli, L. Trakhtenbrot, H.O. Madsen, P. Archer, J. Hancock, N. Cerveira, M.R. Teixeira, L. Lo Nigro, A. Moricke, M. Stanulla, M. Schrappe, L. Sedek, T. Szczepanski, C.M. Zwaan, E.A. Coenen, M.M. van den Heuvel-Eibrink, S. Strehl, M. Dworzak, R. Panzer-Grumayer, T. Dingermann, T. Klingebiel, and R. Marschalek, *The MLL recombinome of acute leukemias in 2013.* Leukemia, 2013. **27**(11): p. 2165-76.

2. Chen, J., O. Odenike, and J.D. Rowley, *Leukaemogenesis: more than mutant genes.* Nat Rev Cancer, 2010. **10**(1): p. 23-36.

3. Slany, R.K., *The molecular biology of mixed lineage leukemia.* Haematologica, 2009. **94**(7): p. 984-93.

4. Milne, T.A., S.D. Briggs, H.W. Brock, M.E. Martin, D. Gibbs, C.D. Allis, and J.L. Hess, *MLL targets SET domain methyltransferase activity to Hox gene promoters.* Mol Cell, 2002. **10**(5): p. 1107-17.

5. Zeisig, B.B., T. Milne, M.P. Garcia-Cuellar, S. Schreiner, M.E. Martin, U. Fuchs, A. Borkhardt, S.K. Chanda, J. Walker, R. Soden, J.L. Hess, and R.K. Slany, *Hoxa9 and Meis1 are key targets for MLL-ENL-mediated cellular immortalization.* Mol Cell Biol, 2004. **24**(2): p. 617-28.

6. Ayton, P.M. and M.L. Cleary, *Transformation of myeloid progenitors by MLL oncoproteins is dependent on Hoxa7 and Hoxa9.* Genes Dev, 2003. **17**(18): p. 2298-307.

7.   Faber, J., A.V. Krivtsov, M.C. Stubbs, R. Wright, T.N. Davis, M. van den Heuvel-Eibrink, C.M. Zwaan, A.L. Kung, and S.A. Armstrong, *HOXA9 is required for survival in human MLL-rearranged acute leukemias.* Blood, 2009. **113**(11): p. 2375-85.

8.   Mian, Y.A. and N.J. Zeleznik-Le, *MicroRNAs in leukemias: emerging diagnostic tools and therapeutic targets.* Curr Drug Targets, 2010. **11**(7): p. 801-11.

9.   Bartel, D.P., *MicroRNAs: genomics, biogenesis, mechanism, and function.* Cell, 2004. **116**(2): p. 281-97.

10.   Kozomara, A. and S. Griffiths-Jones, *miRBase: annotating high confidence microRNAs using deep sequencing data.* Nucleic Acids Res, 2014. **42**(Database issue): p. D68-73.

11.   Popovic, R., L.E. Riesbeck, C.S. Velu, A. Chaubey, J. Zhang, N.J. Achille, F.E. Erfurth, K. Eaton, J. Lu, H.L. Grimes, J. Chen, J.D. Rowley, and N.J. Zeleznik-Le, *Regulation of mir-196b by MLL and its overexpression by MLL fusions contributes to immortalization.* Blood, 2009. **113**(14): p. 3314-22.

12.   Mi, S., Z. Li, P. Chen, C. He, D. Cao, A. Elkahloun, J. Lu, L.A. Pelloso, M. Wunderlich, H. Huang, R.T. Luo, M. Sun, M. He, M.B. Neilly, N.J. Zeleznik-Le, M.J. Thirman, J.C. Mulloy, P.P. Liu, J.D. Rowley, and J. Chen, *Aberrant overexpression and function of the miR-17-92 cluster in MLL-rearranged acute leukemia.* Proc Natl Acad Sci U S A, 2010. **107**(8): p. 3710-5.

13.   Lennox, K.A. and M.A. Behlke, *Chemical modification and design of anti-miRNA oligonucleotides.* Gene Ther, 2011. **18**(12): p. 1111-20.

14.   Dias, N. and C.A. Stein, *Antisense oligonucleotides: basic concepts and mechanisms.* Mol Cancer Ther, 2002. **1**(5): p. 347-55.

15.   Thirman, M.J., H.J. Gill, R.C. Burnett, D. Mbangkollo, N.R. McCabe, H. Kobayashi, S. Ziemin-van der Poel, Y. Kaneko, R. Morgan, A.A. Sandberg, and et al., *Rearrangement of the MLL gene in acute lymphoblastic and acute myeloid leukemias with 11q23 chromosomal translocations.* N Engl J Med, 1993. **329**(13): p. 909-14.

16.   Mrozek, K., D.P. Harper, and P.D. Aplan, *Cytogenetics and molecular genetics of acute lymphoblastic leukemia.* Hematol Oncol Clin North Am, 2009. **23**(5): p. 991-1010, v.

17.   Mrozek, K. and C.D. Bloomfield, *Clinical significance of the most common chromosome translocations in adult acute myeloid leukemia.* J Natl Cancer Inst Monogr, 2008(39): p. 52-7.

18.   Schoch, C., S. Schnittger, M. Klaus, W. Kern, W. Hiddemann, and T. Haferlach, *AML with 11q23/MLL abnormalities as defined by the WHO classification: incidence, partner chromosomes, FAB subtype, age distribution, and prognostic impact in an unselected series of 1897 cytogenetically analyzed AML cases.* Blood, 2003. **102**(7): p. 2395-402.

19.   Ferrando, A.A., S.A. Armstrong, D.S. Neuberg, S.E. Sallan, L.B. Silverman, S.J. Korsmeyer, and A.T. Look, *Gene expression signatures in MLL-rearranged T-lineage and B-precursor acute leukemias: dominance of HOX dysregulation.* Blood, 2003. **102**(1): p. 262-8.

20.   Popovic, R. and N.J. Zeleznik-Le, *MLL: how complex does it get?* J Cell Biochem, 2005. **95**(2): p. 234-42.

21.   Zeleznik-Le, N.J., A.M. Harden, and J.D. Rowley, *11q23 translocations split the "AT-hook" cruciform DNA-binding region and the transcriptional repression domain from the activation domain of the mixed-lineage leukemia (MLL) gene.* Proc Natl Acad Sci U S A, 1994. **91**(22): p. 10610-4.

22.   Xia, Z.B., M. Anderson, M.O. Diaz, and N.J. Zeleznik-Le, *MLL repression domain interacts with histone deacetylases, the polycomb group proteins HPC2 and BMI-1, and the corepressor C-terminal-binding protein.* Proc Natl Acad Sci U S A, 2003. **100**(14): p. 8342-7.

23.   Cierpicki, T., L.E. Risner, J. Grembecka, S.M. Lukasik, R. Popovic, M. Omonkowska, D.D. Shultis, N.J. Zeleznik-Le, and J.H. Bushweller, *Structure of the MLL CXXC domain-DNA complex and its functional role in MLL-AF9 leukemia.* Nat Struct Mol Biol, 2010. **17**(1): p. 62-8.

24.   Erfurth, F.E., R. Popovic, J. Grembecka, T. Cierpicki, C. Theisler, Z.B. Xia, T. Stuart, M.O. Diaz, J.H. Bushweller, and N.J. Zeleznik-Le, *MLL protects CpG clusters from methylation within the Hoxa9 gene, maintaining transcript expression.* Proc Natl Acad Sci U S A, 2008. **105**(21): p. 7517-22.

25.   Wang, Z., J. Song, T.A. Milne, G.G. Wang, H. Li, C.D. Allis, and D.J. Patel, *Pro isomerization in MLL1 PHD3-bromo cassette connects H3K4me readout to CyP33 and HDAC-mediated repression.* Cell, 2010. **141**(7): p. 1183-94.

26. Fair, K., M. Anderson, E. Bulanova, H. Mi, M. Tropschug, and M.O. Diaz, *Protein interactions of the MLL PHD fingers modulate MLL target gene regulation in human cells.* Mol Cell Biol, 2001. **21**(10): p. 3589-97.

27. Park, S., U. Osmers, G. Raman, R.H. Schwantes, M.O. Diaz, and J.H. Bushweller, *The PHD3 domain of MLL acts as a CYP33-regulated switch between MLL-mediated activation and repression.* Biochemistry, 2010. **49**(31): p. 6576-86.

28. Nakamura, T., T. Mori, S. Tada, W. Krajewski, T. Rozovskaia, R. Wassell, G. Dubois, A. Mazo, C.M. Croce, and E. Canaani, *ALL-1 is a histone methyltransferase that assembles a supercomplex of proteins involved in transcriptional regulation.* Mol Cell, 2002. **10**(5): p. 1119-28.

29. Eissenberg, J.C. and A. Shilatifard, *Histone H3 lysine 4 (H3K4) methylation in development and differentiation.* Dev Biol, 2010. **339**(2): p. 240-9.

30. Hsieh, J.J., E.H. Cheng, and S.J. Korsmeyer, *Taspase1: a threonine aspartase required for cleavage of MLL and proper HOX gene expression.* Cell, 2003. **115**(3): p. 293-303.

31. Hsieh, J.J., P. Ernst, H. Erdjument-Bromage, P. Tempst, and S.J. Korsmeyer, *Proteolytic cleavage of MLL generates a complex of N- and C-terminal fragments that confers protein stability and subnuclear localization.* Mol Cell Biol, 2003. **23**(1): p. 186-94.

32. La, P., A.C. Silva, Z. Hou, H. Wang, R.W. Schnepp, N. Yan, Y. Shi, and X. Hua, *Direct binding of DNA by tumor suppressor menin.* J Biol Chem, 2004. **279**(47): p. 49045-54.

33. Yokoyama, A., Z. Wang, J. Wysocka, M. Sanyal, D.J. Aufiero, I. Kitabayashi, W. Herr, and M.L. Cleary, *Leukemia proto-oncoprotein MLL forms a SET1-like histone methyltransferase complex with menin to regulate Hox gene expression.* Mol Cell Biol, 2004. **24**(13): p. 5639-49.

34. Caslini, C., Z. Yang, M. El-Osta, T.A. Milne, R.K. Slany, and J.L. Hess, *Interaction of MLL amino terminal sequences with menin is required for transformation.* Cancer Res, 2007. **67**(15): p. 7275-83.

35. Yokoyama, A. and M.L. Cleary, *Menin critically links MLL proteins with LEDGF on cancer-associated target genes.* Cancer Cell, 2008. **14**(1): p. 36-46.

36. Jin, S., H. Zhao, Y. Yi, Y. Nakata, A. Kalota, and A.M. Gewirtz, *c-Myb binds MLL through menin in human leukemia cells and is an important driver of MLL-associated leukemogenesis.* J Clin Invest, 2010. **120**(2): p. 593-606.

37. Couture, J.F., E. Collazo, and R.C. Trievel, *Molecular recognition of histone H3 by the WD40 protein WDR5.* Nat Struct Mol Biol, 2006. **13**(8): p. 698-703.

38. Steward, M.M., J.S. Lee, A. O'Donovan, M. Wyatt, B.E. Bernstein, and A. Shilatifard, *Molecular regulation of H3K4 trimethylation by ASH2L, a shared subunit of MLL complexes.* Nat Struct Mol Biol, 2006. **13**(9): p. 852-4.

39. Cao, F., Y. Chen, T. Cierpicki, Y. Liu, V. Basrur, M. Lei, and Y. Dou, *An Ash2L/RbBP5 heterodimer stimulates the MLL1 methyltransferase activity through coordinated substrate interactions with the MLL1 SET domain.* PLoS One, 2010. **5**(11): p. e14102.

40. Ernst, P., J. Wang, M. Huang, R.H. Goodman, and S.J. Korsmeyer, *MLL and CREB bind cooperatively to the nuclear coactivator CREB-binding protein.* Mol Cell Biol, 2001. **21**(7): p. 2249-58.

41. Ogryzko, V.V., R.L. Schiltz, V. Russanova, B.H. Howard, and Y. Nakatani, *The transcriptional coactivators p300 and CBP are histone acetyltransferases.* Cell, 1996. **87**(5): p. 953-9.

42. Ruthenburg, A.J., W. Wang, D.M. Graybosch, H. Li, C.D. Allis, D.J. Patel, and G.L. Verdine, *Histone H3 recognition and presentation by the WDR5 module of the MLL1 complex.* Nat Struct Mol Biol, 2006. **13**(8): p. 704-12.

43. Wang, K.C., Y.W. Yang, B. Liu, A. Sanyal, R. Corces-Zimmerman, Y. Chen, B.R. Lajoie, A. Protacio, R.A. Flynn, R.A. Gupta, J. Wysocka, M. Lei, J. Dekker, J.A. Helms, and H.Y. Chang, *A long noncoding RNA maintains active chromatin to coordinate homeotic gene expression.* Nature, 2011. **472**(7341): p. 120-4.

44. Yu, B.D., R.D. Hanson, J.L. Hess, S.E. Horning, and S.J. Korsmeyer, *MLL, a mammalian trithorax-group gene, functions as a transcriptional maintenance factor in morphogenesis.* Proc Natl Acad Sci U S A, 1998. **95**(18): p. 10632-6.

45. Yu, B.D., J.L. Hess, S.E. Horning, G.A. Brown, and S.J. Korsmeyer, *Altered Hox expression and segmental identity in Mll-mutant mice.* Nature, 1995. **378**(6556): p. 505-8.

46. Hess, J.L., B.D. Yu, B. Li, R. Hanson, and S.J. Korsmeyer, *Defects in yolk sac hematopoiesis in Mll-null embryos.* Blood, 1997. **90**(5): p. 1799-806.

47. Betti, C.J., M.J. Villalobos, M.O. Diaz, and A.T. Vaughan, *Apoptotic triggers initiate translocations within the MLL gene involving the nonhomologous end joining repair system.* Cancer Res, 2001. **61**(11): p. 4550-5.

48. McLean, C.M., I.D. Karemaker, and F. van Leeuwen, *The emerging roles of DOT1L in leukemia and normal development.* Leukemia, 2014. **28**(11): p. 2131-8.

49. Steger, D.J., M.I. Lefterova, L. Ying, A.J. Stonestrom, M. Schupp, D. Zhuo, A.L. Vakoc, J.E. Kim, J. Chen, M.A. Lazar, G.A. Blobel, and C.R. Vakoc, *DOT1L/KMT4 recruitment and H3K79 methylation are ubiquitously coupled with gene transcription in mammalian cells.* Mol Cell Biol, 2008. **28**(8): p. 2825-39.

50. Bernt, K.M., N. Zhu, A.U. Sinha, S. Vempati, J. Faber, A.V. Krivtsov, Z. Feng, N. Punt, A. Daigle, L. Bullinger, R.M. Pollock, V.M. Richon, A.L. Kung, and S.A. Armstrong, *MLL-rearranged leukemia is dependent on aberrant H3K79 methylation by DOT1L.* Cancer Cell, 2011. **20**(1): p. 66-78.

51. Krivtsov, A.V., Z. Feng, M.E. Lemieux, J. Faber, S. Vempati, A.U. Sinha, X. Xia, J. Jesneck, A.P. Bracken, L.B. Silverman, J.L. Kutok, A.L. Kung, and S.A. Armstrong, *H3K79 methylation profiles define murine and human MLL-AF4 leukemias.* Cancer Cell, 2008. **14**(5): p. 355-68.

52. Chang, M.J., H. Wu, N.J. Achille, M.R. Reisenauer, C.W. Chou, N.J. Zeleznik-Le, C.S. Hemenway, and W. Zhang, *Histone H3 lysine 79 methyltransferase Dot1 is required for immortalization by MLL oncogenes.* Cancer Res, 2010. **70**(24): p. 10234-42.

53. Daigle, S.R., E.J. Olhava, C.A. Therkelsen, C.R. Majer, C.J. Sneeringer, J. Song, L.D. Johnston, M.P. Scott, J.J. Smith, Y. Xiao, L. Jin, K.W. Kuntz, R. Chesworth, M.P. Moyer, K.M. Bernt, J.C. Tseng, A.L. Kung, S.A. Armstrong, R.A. Copeland, V.M. Richon, and R.M. Pollock, *Selective killing of mixed lineage leukemia cells by a potent small-molecule DOT1L inhibitor.* Cancer Cell, 2011. **20**(1): p. 53-65.

54. Muntean, A.G., J. Tan, K. Sitwala, Y. Huang, J. Bronstein, J.A. Connelly, V. Basrur, K.S. Elenitoba-Johnson, and J.L. Hess, *The PAF complex synergizes with MLL fusion proteins at HOX loci to promote leukemogenesis.* Cancer Cell, 2010. **17**(6): p. 609-21.

55. Luo, Z., C. Lin, and A. Shilatifard, *The super elongation complex (SEC) family in transcriptional control.* Nat Rev Mol Cell Biol, 2012. **13**(9): p. 543-7.

56. Mohan, M., C. Lin, E. Guest, and A. Shilatifard, *Licensed to elongate: a molecular mechanism for MLL-based leukaemogenesis.* Nat Rev Cancer, 2010. **10**(10): p. 721-8.

57. Smith, E., C. Lin, and A. Shilatifard, *The super elongation complex (SEC) and MLL in development and disease.* Genes Dev, 2011. **25**(7): p. 661-72.

58.   Krivtsov, A.V. and S.A. Armstrong, *MLL translocations, histone modifications and leukaemia stem-cell development.* Nat Rev Cancer, 2007. **7**(11): p. 823-33.

59.   So, C.W., M. Lin, P.M. Ayton, E.H. Chen, and M.L. Cleary, *Dimerization contributes to oncogenic activation of MLL chimeras in acute leukemias.* Cancer Cell, 2003. **4**(2): p. 99-110.

60.   Martin, M.E., T.A. Milne, S. Bloyer, K. Galoian, W. Shen, D. Gibbs, H.W. Brock, R. Slany, and J.L. Hess, *Dimerization of MLL fusion proteins immortalizes hematopoietic cells.* Cancer Cell, 2003. **4**(3): p. 197-207.

61.   Milne, T.A., Y. Dou, M.E. Martin, H.W. Brock, R.G. Roeder, and J.L. Hess, *MLL associates specifically with a subset of transcriptionally active target genes.* Proc Natl Acad Sci U S A, 2005. **102**(41): p. 14765-70.

62.   Armstrong, S.A., J.E. Staunton, L.B. Silverman, R. Pieters, M.L. den Boer, M.D. Minden, S.E. Sallan, E.S. Lander, T.R. Golub, and S.J. Korsmeyer, *MLL translocations specify a distinct gene expression profile that distinguishes a unique leukemia.* Nat Genet, 2002. **30**(1): p. 41-7.

63.   Wang, Q.F., G. Wu, S. Mi, F. He, J. Wu, J. Dong, R.T. Luo, R. Mattison, J.J. Kaberlein, S. Prabhakar, H. Ji, and M.J. Thirman, *MLL fusion proteins preferentially regulate a subset of wild-type MLL target genes in the leukemic genome.* Blood, 2011. **117**(25): p. 6895-905.

64.   Li, Z., R.T. Luo, S. Mi, M. Sun, P. Chen, J. Bao, M.B. Neilly, N. Jayathilaka, D.S. Johnson, L. Wang, C. Lavau, Y. Zhang, C. Tseng, X. Zhang, J. Wang, J. Yu, H. Yang, S.M. Wang, J.D. Rowley, J. Chen, and M.J. Thirman, *Consistent deregulation of gene expression between human and murine MLL rearrangement leukemias.* Cancer Res, 2009. **69**(3): p. 1109-16.

65.   Stam, R.W., P. Schneider, J.A. Hagelstein, M.H. van der Linden, D.J. Stumpel, R.X. de Menezes, P. de Lorenzo, M.G. Valsecchi, and R. Pieters, *Gene expression profiling-based dissection of MLL translocated and MLL germline acute lymphoblastic leukemia in infants.* Blood, 2010. **115**(14): p. 2835-44.

66.   Argiropoulos, B. and R.K. Humphries, *Hox genes in hematopoiesis and leukemogenesis.* Oncogene, 2007. **26**(47): p. 6766-76.

67.   Lappin, T.R., D.G. Grier, A. Thompson, and H.L. Halliday, *HOX genes: seductive science, mysterious mechanisms.* Ulster Med J, 2006. **75**(1): p. 23-31.

68.   Mallo, M. and C.R. Alonso, *The regulation of Hox gene expression during animal development.* Development, 2013. **140**(19): p. 3951-63.

69. Nakamura, T., D.A. Largaespada, M.P. Lee, L.A. Johnson, K. Ohyashiki, K. Toyama, S.J. Chen, C.L. Willman, I.M. Chen, A.P. Feinberg, N.A. Jenkins, N.G. Copeland, and J.D. Shaughnessy, Jr., *Fusion of the nucleoporin gene NUP98 to HOXA9 by the chromosome translocation t(7;11)(p15;p15) in human myeloid leukaemia.* Nat Genet, 1996. **12**(2): p. 154-8.

70. Golub, T.R., D.K. Slonim, P. Tamayo, C. Huard, M. Gaasenbeek, J.P. Mesirov, H. Coller, M.L. Loh, J.R. Downing, M.A. Caligiuri, C.D. Bloomfield, and E.S. Lander, *Molecular classification of cancer: class discovery and class prediction by gene expression monitoring.* Science, 1999. **286**(5439): p. 531-7.

71. Ladam, F. and C.G. Sagerstrom, *Hox regulation of transcription: more complex(es).* Dev Dyn, 2014. **243**(1): p. 4-15.

72. Burglin, T.R., *Analysis of TALE superclass homeobox genes (MEIS, PBC, KNOX, Iroquois, TGIF) reveals a novel domain conserved between plants and animals.* Nucleic Acids Res, 1997. **25**(21): p. 4173-80.

73. Mukherjee, K. and T.R. Burglin, *Comprehensive analysis of animal TALE homeobox genes: new conserved motifs and cases of accelerated evolution.* J Mol Evol, 2007. **65**(2): p. 137-53.

74. Longobardi, E., D. Penkov, D. Mateos, G. De Florian, M. Torres, and F. Blasi, *Biochemistry of the tale transcription factors PREP, MEIS, and PBX in vertebrates.* Dev Dyn, 2013.

75. Chang, C.P., Y. Jacobs, T. Nakamura, N.A. Jenkins, N.G. Copeland, and M.L. Cleary, *Meis proteins are major in vivo DNA binding partners for wild-type but not chimeric Pbx proteins.* Mol Cell Biol, 1997. **17**(10): p. 5679-87.

76. Knoepfler, P.S., K.R. Calvo, H. Chen, S.E. Antonarakis, and M.P. Kamps, *Meis1 and pKnox1 bind DNA cooperatively with Pbx1 utilizing an interaction surface disrupted in oncoprotein E2a-Pbx1.* Proc Natl Acad Sci U S A, 1997. **94**(26): p. 14553-8.

77. Shen, W.F., S. Rozenfeld, A. Kwong, L.G. Kom ves, H.J. Lawrence, and C. Largman, *HOXA9 forms triple complexes with PBX2 and MEIS1 in myeloid cells.* Mol Cell Biol, 1999. **19**(4): p. 3051-61.

78. Schnabel, C.A., Y. Jacobs, and M.L. Cleary, *HoxA9-mediated immortalization of myeloid progenitors requires functional interactions with TALE cofactors Pbx and Meis.* Oncogene, 2000. **19**(5): p. 608-16.

79. Shanmugam, K., N.C. Green, I. Rambaldi, H.U. Saragovi, and M.S. Featherstone, *PBX and MEIS as non-DNA-binding partners in trimeric complexes with HOX proteins.* Mol Cell Biol, 1999. **19**(11): p. 7577-88.

80. Jacobs, Y., C.A. Schnabel, and M.L. Cleary, *Trimeric association of Hox and TALE homeodomain proteins mediates Hoxb2 hindbrain enhancer activity.* Mol Cell Biol, 1999. **19**(7): p. 5134-42.

81. Sarno, J.L., H.J. Kliman, and H.S. Taylor, *HOXA10, Pbx2, and Meis1 protein expression in the human endometrium: formation of multimeric complexes on HOXA10 target genes.* J Clin Endocrinol Metab, 2005. **90**(1): p. 522-8.

82. Longobardi, E., D. Penkov, D. Mateos, G. De Florian, M. Torres, and F. Blasi, *Biochemistry of the tale transcription factors PREP, MEIS, and PBX in vertebrates.* Dev Dyn, 2014. **243**(1): p. 59-75.

83. Milech, N., N.G. Gottardo, J. Ford, D. D'Souza, W.K. Greene, U.R. Kees, and P.M. Watt, *MEIS proteins as partners of the TLX1/HOX11 oncoprotein.* Leuk Res, 2010. **34**(3): p. 358-63.

84. Williams, T.M., M.E. Williams, and J.W. Innis, *Range of HOX/TALE superclass associations and protein domain requirements for HOXA13:MEIS interaction.* Dev Biol, 2005. **277**(2): p. 457-71.

85. Shen, W.F., J.C. Montgomery, S. Rozenfeld, J.J. Moskow, H.J. Lawrence, A.M. Buchberg, and C. Largman, *AbdB-like Hox proteins stabilize DNA binding by the Meis1 homeodomain proteins.* Mol Cell Biol, 1997. **17**(11): p. 6448-58.

86. Li, Z., H. Huang, Y. Li, X. Jiang, P. Chen, S. Arnovitz, M.D. Radmacher, K. Maharry, A. Elkahloun, X. Yang, C. He, M. He, Z. Zhang, K. Dohner, M.B. Neilly, C. Price, Y.A. Lussier, Y. Zhang, R.A. Larson, M.M. Le Beau, M.A. Caligiuri, L. Bullinger, P.J. Valk, R. Delwel, B. Lowenberg, P.P. Liu, G. Marcucci, C.D. Bloomfield, J.D. Rowley, and J. Chen, *Up-regulation of a HOXA-PBX3 homeobox-gene signature following down-regulation of miR-181 is associated with adverse prognosis in patients with cytogenetically abnormal AML.* Blood, 2012. **119**(10): p. 2314-24.

87. Li, Z., Z. Zhang, Y. Li, S. Arnovitz, P. Chen, H. Huang, X. Jiang, G.M. Hong, R.B. Kunjamma, H. Ren, C. He, C.Z. Wang, A.G. Elkahloun, P.J. Valk, K. Dohner, M.B. Neilly, L. Bullinger, R. Delwel, B. Lowenberg, P.P. Liu, R. Morgan, J.D. Rowley, C.S. Yuan, and J. Chen, *PBX3 is an important cofactor of HOXA9 in leukemogenesis.* Blood, 2013. **121**(8): p. 1422-31.

88. Moskow, J.J., F. Bullrich, K. Huebner, I.O. Daar, and A.M. Buchberg, *Meis1, a PBX1-related homeobox gene involved in myeloid leukemia in BXH-2 mice.* Mol Cell Biol, 1995. **15**(10): p. 5434-43.

89. Smith, J.E., Jr., J.A. Bollekens, G. Inghirami, and K. Takeshita, *Cloning and mapping of the MEIS1 gene, the human homolog of a murine leukemogenic gene.* Genomics, 1997. **43**(1): p. 99-103.

90. Nakamura, T., D.A. Largaespada, J.D. Shaughnessy, Jr., N.A. Jenkins, and N.G. Copeland, *Cooperative activation of Hoxa and Pbx1-related genes in murine myeloid leukaemias.* Nat Genet, 1996. **12**(2): p. 149-53.

91. Wong, P., M. Iwasaki, T.C. Somervaille, C.W. So, and M.L. Cleary, *Meis1 is an essential and rate-limiting regulator of MLL leukemia stem cell potential.* Genes Dev, 2007. **21**(21): p. 2762-74.

92. Kumar, A.R., Q. Li, W.A. Hudson, W. Chen, T. Sam, Q. Yao, E.A. Lund, B. Wu, B.J. Kowal, and J.H. Kersey, *A role for MEIS1 in MLL-fusion gene leukemia.* Blood, 2009. **113**(8): p. 1756-8.

93. Wang, G.G., M.P. Pasillas, and M.P. Kamps, *Meis1 programs transcription of FLT3 and cancer stem cell character, using a mechanism that requires interaction with Pbx and a novel function of the Meis1 C-terminus.* Blood, 2005. **106**(1): p. 254-64.

94. Bisaillon, R., B.T. Wilhelm, J. Krosl, and G. Sauvageau, *C-terminal domain of MEIS1 converts PKNOX1 (PREP1) into a HOXA9-collaborating oncoprotein.* Blood, 2011. **118**(17): p. 4682-9.

95. Mamo, A., J. Krosl, E. Kroon, J. Bijl, A. Thompson, N. Mayotte, S. Girard, R. Bisaillon, N. Beslu, M. Featherstone, and G. Sauvageau, *Molecular dissection of Meis1 reveals 2 domains required for leukemia induction and a key role for Hoxa gene activation.* Blood, 2006. **108**(2): p. 622-9.

96. Annesley, C.E. and P. Brown, *The Biology and Targeting of FLT3 in Pediatric Leukemia.* Front Oncol, 2014. **4**: p. 263.

97. Morgado, E., S. Albouhair, and C. Lavau, *Flt3 is dispensable to the Hoxa9/Meis1 leukemogenic cooperation.* Blood, 2007. **109**(9): p. 4020-2.

98. Hess, J.L., C.B. Bittner, D.T. Zeisig, C. Bach, U. Fuchs, A. Borkhardt, J. Frampton, and R.K. Slany, *c-Myb is an essential downstream target for homeobox-mediated transformation of hematopoietic cells.* Blood, 2006. **108**(1): p. 297-304.

99. Pillay, L.M., A.M. Forrester, T. Erickson, J.N. Berman, and A.J. Waskiewicz, *The Hox cofactors Meis1 and Pbx act upstream of gata1 to regulate primitive hematopoiesis.* Dev Biol, 2010. **340**(2): p. 306-17.

100. Argiropoulos, B., L. Palmqvist, E. Yung, F. Kuchenbauer, M. Heuser, L.M. Sly, A. Wan, G. Krystal, and R.K. Humphries, *Linkage of Meis1 leukemogenic activity to multiple downstream effectors including Trib2 and Ccl3.* Exp Hematol, 2008. **36**(7): p. 845-59.

101. Argiropoulos, B., E. Yung, P. Xiang, C.Y. Lo, F. Kuchenbauer, L. Palmqvist, C. Reindl, M. Heuser, S. Sekulovic, P. Rosten, A. Muranyi, S.L. Goh, M. Featherstone, and R.K. Humphries, *Linkage of the potent leukemogenic activity of Meis1 to cell-cycle entry and transcriptional regulation of cyclin D3.* Blood, 2010. **115**(20): p. 4071-82.

102. Huang, Y., K. Sitwala, J. Bronstein, D. Sanders, M. Dandekar, C. Collins, G. Robertson, J. MacDonald, T. Cezard, M. Bilenky, N. Thiessen, Y. Zhao, T. Zeng, M. Hirst, A. Hero, S. Jones, and J.L. Hess, *Identification and characterization of Hoxa9 binding sites in hematopoietic cells.* Blood, 2012. **119**(2): p. 388-98.

103. Chen, H., C. Rossier, Y. Nakamura, A. Lynn, A. Chakravarti, and S.E. Antonarakis, *Cloning of a novel homeobox-containing gene, PKNOX1, and mapping to human chromosome 21q22.3.* Genomics, 1997. **41**(2): p. 193-200.

104. Berthelsen, J., L. Viggiano, H. Schulz, E. Ferretti, G.G. Consalez, M. Rocchi, and F. Blasi, *PKNOX1, a gene encoding PREP1, a new regulator of Pbx activity, maps on human chromosome 21q22.3 and murine chromosome 17B/C.* Genomics, 1998. **47**(2): p. 323-4.

105. Ferretti, E., H. Schulz, D. Talarico, F. Blasi, and J. Berthelsen, *The PBX-regulating protein PREP1 is present in different PBX-complexed forms in mouse.* Mech Dev, 1999. **83**(1-2): p. 53-64.

106. Berthelsen, J., V. Zappavigna, E. Ferretti, F. Mavilio, and F. Blasi, *The novel homeoprotein Prep1 modulates Pbx-Hox protein cooperativity.* EMBO J, 1998. **17**(5): p. 1434-45.

107. Berthelsen, J., V. Zappavigna, F. Mavilio, and F. Blasi, *Prep1, a novel functional partner of Pbx proteins.* EMBO J, 1998. **17**(5): p. 1423-33.

108. Ferretti, E., J.C. Villaescusa, P. Di Rosa, L.C. Fernandez-Diaz, E. Longobardi, R. Mazzieri, A. Miccio, N. Micali, L. Selleri, G. Ferrari, and F. Blasi, *Hypomorphic mutation of the TALE gene Prep1 (pKnox1) causes a major reduction of Pbx and*

Meis proteins and a pleiotropic embryonic phenotype. Mol Cell Biol, 2006. **26**(15): p. 5650-62.

109. Longobardi, E., G. Iotti, P. Di Rosa, S. Mejetta, F. Bianchi, L.C. Fernandez-Diaz, N. Micali, P. Nuciforo, E. Lenti, M. Ponzoni, C. Doglioni, M. Caniatti, P.P. Di Fiore, and F. Blasi, *Prep1 (pKnox1)-deficiency leads to spontaneous tumor development in mice and accelerates EmuMyc lymphomagenesis: a tumor suppressor role for Prep1.* Mol Oncol, 2010. **4**(2): p. 126-34.

110. Berthelsen, J., C. Kilstrup-Nielsen, F. Blasi, F. Mavilio, and V. Zappavigna, *The subcellular localization of PBX1 and EXD proteins depends on nuclear import and export signals and is modulated by association with PREP1 and HTH.* Genes Dev, 1999. **13**(8): p. 946-53.

111. Penkov, D., D. Mateos San Martin, L.C. Fernandez-Diaz, C.A. Rossello, C. Torroja, F. Sanchez-Cabo, H.J. Warnatz, M. Sultan, M.L. Yaspo, A. Gabrieli, V. Tkachuk, A. Brendolan, F. Blasi, and M. Torres, *Analysis of the DNA-binding profile and function of TALE homeoproteins reveals their specialization and specific interactions with Hox genes/proteins.* Cell Rep, 2013. **3**(4): p. 1321-33.

112. Dardaei, L., E. Longobardi, and F. Blasi, *Prep1 and Meis1 competition for Pbx1 binding regulates protein stability and tumorigenesis.* Proc Natl Acad Sci U S A, 2014. **111**(10): p. E896-905.

113. Dardaei, L., L. Modica, G. Iotti, and F. Blasi, *The deficiency of tumor suppressor prep1 accelerates the onset of meis1- hoxa9 leukemogenesis.* PLoS One, 2014. **9**(5): p. e96711.

114. Lee, R.C., R.L. Feinbaum, and V. Ambros, *The C. elegans heterochronic gene lin-4 encodes small RNAs with antisense complementarity to lin-14.* Cell, 1993. **75**(5): p. 843-54.

115. Reinhart, B.J., F.J. Slack, M. Basson, A.E. Pasquinelli, J.C. Bettinger, A.E. Rougvie, H.R. Horvitz, and G. Ruvkun, *The 21-nucleotide let-7 RNA regulates developmental timing in Caenorhabditis elegans.* Nature, 2000. **403**(6772): p. 901-6.

116. Pasquinelli, A.E., B.J. Reinhart, F. Slack, M.Q. Martindale, M.I. Kuroda, B. Maller, D.C. Hayward, E.E. Ball, B. Degnan, P. Muller, J. Spring, A. Srinivasan, M. Fishman, J. Finnerty, J. Corbo, M. Levine, P. Leahy, E. Davidson, and G. Ruvkun, *Conservation of the sequence and temporal expression of let-7 heterochronic regulatory RNA.* Nature, 2000. **408**(6808): p. 86-9.

117. Calin, G.A., C. Sevignani, C.D. Dumitru, T. Hyslop, E. Noch, S. Yendamuri, M. Shimizu, S. Rattan, F. Bullrich, M. Negrini, and C.M. Croce, *Human microRNA genes are frequently located at fragile sites and genomic regions involved in cancers.* Proc Natl Acad Sci U S A, 2004. **101**(9): p. 2999-3004.

118. Lee, Y., M. Kim, J. Han, K.H. Yeom, S. Lee, S.H. Baek, and V.N. Kim, *MicroRNA genes are transcribed by RNA polymerase II.* EMBO J, 2004. **23**(20): p. 4051-60.

119. Borchert, G.M., W. Lanier, and B.L. Davidson, *RNA polymerase III transcribes human microRNAs.* Nat Struct Mol Biol, 2006. **13**(12): p. 1097-101.

120. Cullen, B.R., *Transcription and processing of human microRNA precursors.* Mol Cell, 2004. **16**(6): p. 861-5.

121. Kim, V.N., J. Han, and M.C. Siomi, *Biogenesis of small RNAs in animals.* Nat Rev Mol Cell Biol, 2009. **10**(2): p. 126-39.

122. Lee, Y., C. Ahn, J. Han, H. Choi, J. Kim, J. Yim, J. Lee, P. Provost, O. Radmark, S. Kim, and V.N. Kim, *The nuclear RNase III Drosha initiates microRNA processing.* Nature, 2003. **425**(6956): p. 415-9.

123. Han, J., Y. Lee, K.H. Yeom, Y.K. Kim, H. Jin, and V.N. Kim, *The Drosha-DGCR8 complex in primary microRNA processing.* Genes Dev, 2004. **18**(24): p. 3016-27.

124. Denli, A.M., B.B. Tops, R.H. Plasterk, R.F. Ketting, and G.J. Hannon, *Processing of primary microRNAs by the Microprocessor complex.* Nature, 2004. **432**(7014): p. 231-5.

125. Bohnsack, M.T., K. Czaplinski, and D. Gorlich, *Exportin 5 is a RanGTP-dependent dsRNA-binding protein that mediates nuclear export of pre-miRNAs.* RNA, 2004. **10**(2): p. 185-91.

126. Hutvagner, G., J. McLachlan, A.E. Pasquinelli, E. Balint, T. Tuschl, and P.D. Zamore, *A cellular function for the RNA-interference enzyme Dicer in the maturation of the let-7 small temporal RNA.* Science, 2001. **293**(5531): p. 834-8.

127. Gregory, R.I., T.P. Chendrimada, N. Cooch, and R. Shiekhattar, *Human RISC couples microRNA biogenesis and posttranscriptional gene silencing.* Cell, 2005. **123**(4): p. 631-40.

128. Park, J.H. and C. Shin, *MicroRNA-directed cleavage of targets: mechanism and experimental approaches.* BMB Rep, 2014. **47**(8): p. 417-23.

129. Schwarz, D.S., G. Hutvagner, T. Du, Z. Xu, N. Aronin, and P.D. Zamore, *Asymmetry in the assembly of the RNAi enzyme complex.* Cell, 2003. **115**(2): p. 199-208.

130. Kuchen, S., W. Resch, A. Yamane, N. Kuo, Z. Li, T. Chakraborty, L. Wei, A. Laurence, T. Yasuda, S. Peng, J. Hu-Li, K. Lu, W. Dubois, Y. Kitamura, N. Charles, H.W. Sun, S. Muljo, P.L. Schwartzberg, W.E. Paul, J. O'Shea, K. Rajewsky, and R. Casellas, *Regulation of microRNA expression and abundance during lymphopoiesis.* Immunity, 2010. **32**(6): p. 828-39.

131. Lewis, B.P., C.B. Burge, and D.P. Bartel, *Conserved seed pairing, often flanked by adenosines, indicates that thousands of human genes are microRNA targets.* Cell, 2005. **120**(1): p. 15-20.

132. Ritchie, W. and J.E. Rasko, *Refining microRNA target predictions: sorting the wheat from the chaff.* Biochem Biophys Res Commun, 2014. **445**(4): p. 780-4.

133. Peterson, S.M., J.A. Thompson, M.L. Ufkin, P. Sathyanarayana, L. Liaw, and C.B. Congdon, *Common features of microRNA target prediction tools.* Front Genet, 2014. **5**: p. 23.

134. Pratt, A.J. and I.J. MacRae, *The RNA-induced silencing complex: a versatile gene-silencing machine.* J Biol Chem, 2009. **284**(27): p. 17897-901.

135. Liu, J., M.A. Carmell, F.V. Rivas, C.G. Marsden, J.M. Thomson, J.J. Song, S.M. Hammond, L. Joshua-Tor, and G.J. Hannon, *Argonaute2 is the catalytic engine of mammalian RNAi.* Science, 2004. **305**(5689): p. 1437-41.

136. Valencia-Sanchez, M.A., J. Liu, G.J. Hannon, and R. Parker, *Control of translation and mRNA degradation by miRNAs and siRNAs.* Genes Dev, 2006. **20**(5): p. 515-24.

137. Paroo, Z., Q. Liu, and X. Wang, *Biochemical mechanisms of the RNA-induced silencing complex.* Cell Res, 2007. **17**(3): p. 187-94.

138. Dweep, H., C. Sticht, and N. Gretz, *In-Silico Algorithms for the Screening of Possible microRNA Binding Sites and Their Interactions.* Curr Genomics, 2013. **14**(2): p. 127-36.

139. John, B., A.J. Enright, A. Aravin, T. Tuschl, C. Sander, and D.S. Marks, *Human MicroRNA targets.* PLoS Biol, 2004. **2**(11): p. e363.

140. Maragkakis, M., P. Alexiou, G.L. Papadopoulos, M. Reczko, T. Dalamagas, G. Giannopoulos, G. Goumas, E. Koukis, K. Kourtis, V.A. Simossis, P. Sethupathy,

T. Vergoulis, N. Koziris, T. Sellis, P. Tsanakas, and A.G. Hatzigeorgiou, *Accurate microRNA target prediction correlates with protein repression levels.* BMC Bioinformatics, 2009. **10**: p. 295.

141. Miranda, K.C., T. Huynh, Y. Tay, Y.S. Ang, W.L. Tam, A.M. Thomson, B. Lim, and I. Rigoutsos, *A pattern-based method for the identification of MicroRNA binding sites and their corresponding heteroduplexes.* Cell, 2006. **126**(6): p. 1203-17.

142. Dweep, H., C. Sticht, P. Pandey, and N. Gretz, *miRWalk--database: prediction of possible miRNA binding sites by "walking" the genes of three genomes.* J Biomed Inform, 2011. **44**(5): p. 839-47.

143. Lytle, J.R., T.A. Yario, and J.A. Steitz, *Target mRNAs are repressed as efficiently by microRNA-binding sites in the 5' UTR as in the 3' UTR.* Proc Natl Acad Sci U S A, 2007. **104**(23): p. 9667-72.

144. Orom, U.A., F.C. Nielsen, and A.H. Lund, *MicroRNA-10a binds the 5'UTR of ribosomal protein mRNAs and enhances their translation.* Mol Cell, 2008. **30**(4): p. 460-71.

145. Lee, I., S.S. Ajay, J.I. Yook, H.S. Kim, S.H. Hong, N.H. Kim, S.M. Dhanasekaran, A.M. Chinnaiyan, and B.D. Athey, *New class of microRNA targets containing simultaneous 5'-UTR and 3'-UTR interaction sites.* Genome Res, 2009. **19**(7): p. 1175-83.

146. Chi, S.W., J.B. Zang, A. Mele, and R.B. Darnell, *Argonaute HITS-CLIP decodes microRNA-mRNA interaction maps.* Nature, 2009. **460**(7254): p. 479-86.

147. Schmittgen, T.D., *Regulation of microRNA processing in development, differentiation and cancer.* J Cell Mol Med, 2008. **12**(5B): p. 1811-9.

148. Mi, S., J. Lu, M. Sun, Z. Li, H. Zhang, M.B. Neilly, Y. Wang, Z. Qian, J. Jin, Y. Zhang, S.K. Bohlander, M.M. Le Beau, R.A. Larson, T.R. Golub, J.D. Rowley, and J. Chen, *MicroRNA expression signatures accurately discriminate acute lymphoblastic leukemia from acute myeloid leukemia.* Proc Natl Acad Sci U S A, 2007. **104**(50): p. 19971-6.

149. Wang, Y., Z. Li, C. He, D. Wang, X. Yuan, J. Chen, and J. Jin, *MicroRNAs expression signatures are associated with lineage and survival in acute leukemias.* Blood Cells Mol Dis, 2010. **44**(3): p. 191-7.

150. Zanette, D.L., F. Rivadavia, G.A. Molfetta, F.G. Barbuzano, R. Proto-Siqueira, W.A. Silva-Jr, R.P. Falcao, and M.A. Zago, *miRNA expression profiles in chronic*

lymphocytic and acute lymphocytic leukemia. Braz J Med Biol Res, 2007. **40**(11): p. 1435-40.

151.   Schotte, D., J.C. Chau, G. Sylvester, G. Liu, C. Chen, V.H. van der Velden, M.J. Broekhuis, T.C. Peters, R. Pieters, and M.L. den Boer, *Identification of new microRNA genes and aberrant microRNA profiles in childhood acute lymphoblastic leukemia.* Leukemia, 2009. **23**(2): p. 313-22.

152.   Li, Z., J. Lu, M. Sun, S. Mi, H. Zhang, R.T. Luo, P. Chen, Y. Wang, M. Yan, Z. Qian, M.B. Neilly, J. Jin, Y. Zhang, S.K. Bohlander, D.E. Zhang, R.A. Larson, M.M. Le Beau, M.J. Thirman, T.R. Golub, J.D. Rowley, and J. Chen, *Distinct microRNA expression profiles in acute myeloid leukemia with common translocations.* Proc Natl Acad Sci U S A, 2008. **105**(40): p. 15535-40.

153.   Jongen-Lavrencic, M., S.M. Sun, M.K. Dijkstra, P.J. Valk, and B. Lowenberg, *MicroRNA expression profiling in relation to the genetic heterogeneity of acute myeloid leukemia.* Blood, 2008. **111**(10): p. 5078-85.

154.   Dixon-McIver, A., P. East, C.A. Mein, J.B. Cazier, G. Molloy, T. Chaplin, T. Andrew Lister, B.D. Young, and S. Debernardi, *Distinctive patterns of microRNA expression associated with karyotype in acute myeloid leukaemia.* PLoS One, 2008. **3**(5): p. e2141.

155.   Garzon, R., S. Volinia, C.G. Liu, C. Fernandez-Cymering, T. Palumbo, F. Pichiorri, M. Fabbri, K. Coombes, H. Alder, T. Nakamura, N. Flomenberg, G. Marcucci, G.A. Calin, S.M. Kornblau, H. Kantarjian, C.D. Bloomfield, M. Andreeff, and C.M. Croce, *MicroRNA signatures associated with cytogenetics and prognosis in acute myeloid leukemia.* Blood, 2008. **111**(6): p. 3183-9.

156.   Daschkey, S., S. Rottgers, A. Giri, J. Bradtke, A. Teigler-Schlegel, G. Meister, A. Borkhardt, and P. Landgraf, *MicroRNAs distinguish cytogenetic subgroups in pediatric AML and contribute to complex regulatory networks in AML-relevant pathways.* PLoS One, 2013. **8**(2): p. e56334.

157.   Marcucci, G., K. Maharry, M.D. Radmacher, K. Mrozek, T. Vukosavljevic, P. Paschka, S.P. Whitman, C. Langer, C.D. Baldus, C.G. Liu, A.S. Ruppert, B.L. Powell, A.J. Carroll, M.A. Caligiuri, J.E. Kolitz, R.A. Larson, and C.D. Bloomfield, *Prognostic significance of, and gene and microRNA expression signatures associated with, CEBPA mutations in cytogenetically normal acute myeloid leukemia with high-risk molecular features: a Cancer and Leukemia Group B Study.* J Clin Oncol, 2008. **26**(31): p. 5078-87.

158.   Marcucci, G., M.D. Radmacher, K. Maharry, K. Mrozek, A.S. Ruppert, P. Paschka, T. Vukosavljevic, S.P. Whitman, C.D. Baldus, C. Langer, C.G. Liu, A.J.

Carroll, B.L. Powell, R. Garzon, C.M. Croce, J.E. Kolitz, M.A. Caligiuri, R.A. Larson, and C.D. Bloomfield, *MicroRNA expression in cytogenetically normal acute myeloid leukemia.* N Engl J Med, 2008. **358**(18): p. 1919-28.

159.   Garzon, R., M. Garofalo, M.P. Martelli, R. Briesewitz, L. Wang, C. Fernandez-Cymering, S. Volinia, C.G. Liu, S. Schnittger, T. Haferlach, A. Liso, D. Diverio, M. Mancini, G. Meloni, R. Foa, M.F. Martelli, C. Mecucci, C.M. Croce, and B. Falini, *Distinctive microRNA signature of acute myeloid leukemia bearing cytoplasmic mutated nucleophosmin.* Proc Natl Acad Sci U S A, 2008. **105**(10): p. 3945-50.

160.   Yekta, S., C.J. Tabin, and D.P. Bartel, *MicroRNAs in the Hox network: an apparent link to posterior prevalence.* Nat Rev Genet, 2008. **9**(10): p. 789-96.

161.   Yekta, S., I.H. Shih, and D.P. Bartel, *MicroRNA-directed cleavage of HOXB8 mRNA.* Science, 2004. **304**(5670): p. 594-6.

162.   Schotte, D., E.A. Lange-Turenhout, D.J. Stumpel, R.W. Stam, J.G. Buijs-Gladdines, J.P. Meijerink, R. Pieters, and M.L. Den Boer, *Expression of miR-196b is not exclusively MLL-driven but is especially linked to activation of HOXA genes in pediatric acute lymphoblastic leukemia.* Haematologica, 2010. **95**(10): p. 1675-82.

163.   Li, Z., H. Huang, P. Chen, M. He, Y. Li, S. Arnovitz, X. Jiang, C. He, E. Hyjek, J. Zhang, Z. Zhang, A. Elkahloun, D. Cao, C. Shen, M. Wunderlich, Y. Wang, M.B. Neilly, J. Jin, M. Wei, J. Lu, P.J. Valk, R. Delwel, B. Lowenberg, M.M. Le Beau, J. Vardiman, J.C. Mulloy, N.J. Zeleznik-Le, P.P. Liu, J. Zhang, and J. Chen, *miR-196b directly targets both HOXA9/MEIS1 oncogenes and FAS tumour suppressor in MLL-rearranged leukaemia.* Nat Commun, 2012. **3**: p. 688.

164.   Hornstein, E., J.H. Mansfield, S. Yekta, J.K. Hu, B.D. Harfe, M.T. McManus, S. Baskerville, D.P. Bartel, and C.J. Tabin, *The microRNA miR-196 acts upstream of Hoxb8 and Shh in limb development.* Nature, 2005. **438**(7068): p. 671-4.

165.   McGlinn, E., S. Yekta, J.H. Mansfield, J. Soutschek, D.P. Bartel, and C.J. Tabin, *In ovo application of antagomiRs indicates a role for miR-196 in patterning the chick axial skeleton through Hox gene regulation.* Proc Natl Acad Sci U S A, 2009. **106**(44): p. 18610-5.

166.   Ma, R., W. Yan, G. Zhang, H. Lv, Z. Liu, F. Fang, W. Zhang, J. Zhang, T. Tao, Y. You, T. Jiang, and X. Kang, *Upregulation of miR-196b confers a poor prognosis in glioblastoma patients via inducing a proliferative phenotype.* PLoS One, 2012. **7**(6): p. e38096.

167. How, C., A.B. Hui, N.M. Alajez, W. Shi, P.C. Boutros, B.A. Clarke, R. Yan, M. Pintilie, A. Fyles, D.W. Hedley, R.P. Hill, M. Milosevic, and F.F. Liu, *MicroRNA-196b regulates the homeobox B7-vascular endothelial growth factor axis in cervical cancer.* PLoS One, 2013. **8**(7): p. e67846.

168. Liu, Y., W. Zheng, Y. Song, W. Ma, and H. Yin, *Low expression of miR-196b enhances the expression of BCR-ABL1 and HOXA9 oncogenes in chronic myeloid leukemogenesis.* PLoS One, 2013. **8**(7): p. e68442.

169. Lund, A.H., *miR-10 in development and cancer.* Cell Death Differ, 2010. **17**(2): p. 209-14.

170. Ma, L., J. Teruya-Feldstein, and R.A. Weinberg, *Tumour invasion and metastasis initiated by microRNA-10b in breast cancer.* Nature, 2007. **449**(7163): p. 682-8.

171. Meyuhas, O., *Synthesis of the translational apparatus is regulated at the translational level.* Eur J Biochem, 2000. **267**(21): p. 6321-30.

172. He, L., J.M. Thomson, M.T. Hemann, E. Hernando-Monge, D. Mu, S. Goodson, S. Powers, C. Cordon-Cardo, S.W. Lowe, G.J. Hannon, and S.M. Hammond, *A microRNA polycistron as a potential human oncogene.* Nature, 2005. **435**(7043): p. 828-33.

173. Mogilyansky, E. and I. Rigoutsos, *The miR-17/92 cluster: a comprehensive update on its genomics, genetics, functions and increasingly important and numerous roles in health and disease.* Cell Death Differ, 2013. **20**(12): p. 1603-14.

174. Mendell, J.T., *miRiad roles for the miR-17-92 cluster in development and disease.* Cell, 2008. **133**(2): p. 217-22.

175. Olive, V., I. Jiang, and L. He, *mir-17-92, a cluster of miRNAs in the midst of the cancer network.* Int J Biochem Cell Biol, 2010. **42**(8): p. 1348-54.

176. Ventura, A., A.G. Young, M.M. Winslow, L. Lintault, A. Meissner, S.J. Erkeland, J. Newman, R.T. Bronson, D. Crowley, J.R. Stone, R. Jaenisch, P.A. Sharp, and T. Jacks, *Targeted deletion reveals essential and overlapping functions of the miR-17 through 92 family of miRNA clusters.* Cell, 2008. **132**(5): p. 875-86.

177. O'Donnell, K.A., E.A. Wentzel, K.I. Zeller, C.V. Dang, and J.T. Mendell, *c-Myc-regulated microRNAs modulate E2F1 expression.* Nature, 2005. **435**(7043): p. 839-43.

178. Sylvestre, Y., V. De Guire, E. Querido, U.K. Mukhopadhyay, V. Bourdeau, F. Major, G. Ferbeyre, and P. Chartrand, *An E2F/miR-20a autoregulatory feedback loop.* J Biol Chem, 2007. **282**(4): p. 2135-43.

179. Yan, H.L., G. Xue, Q. Mei, Y.Z. Wang, F.X. Ding, M.F. Liu, M.H. Lu, Y. Tang, H.Y. Yu, and S.H. Sun, *Repression of the miR-17-92 cluster by p53 has an important function in hypoxia-induced apoptosis.* EMBO J, 2009. **28**(18): p. 2719-32.

180. Hossain, A., M.T. Kuo, and G.F. Saunders, *Mir-17-5p regulates breast cancer cell proliferation by inhibiting translation of AIB1 mRNA.* Mol Cell Biol, 2006. **26**(21): p. 8191-201.

181. Yang, F., Y. Yin, F. Wang, Y. Wang, L. Zhang, Y. Tang, and S. Sun, *miR-17-5p Promotes migration of human hepatocellular carcinoma cells through the p38 mitogen-activated protein kinase-heat shock protein 27 pathway.* Hepatology, 2010. **51**(5): p. 1614-23.

182. Dews, M., J.L. Fox, S. Hultine, P. Sundaram, W. Wang, Y.Y. Liu, E. Furth, G.H. Enders, W. El-Deiry, J.M. Schelter, M.A. Cleary, and A. Thomas-Tikhonenko, *The myc-miR-17~92 axis blunts TGF{beta} signaling and production of multiple TGF{beta}-dependent antiangiogenic factors.* Cancer Res, 2010. **70**(20): p. 8233-46.

183. Wong, P., M. Iwasaki, T.C. Somervaille, F. Ficara, C. Carico, C. Arnold, C.Z. Chen, and M.L. Cleary, *The miR-17-92 microRNA polycistron regulates MLL leukemia stem cell potential by modulating p21 expression.* Cancer Res, 2010. **70**(9): p. 3833-42.

184. Ivanovska, I., A.S. Ball, R.L. Diaz, J.F. Magnus, M. Kibukawa, J.M. Schelter, S.V. Kobayashi, L. Lim, J. Burchard, A.L. Jackson, P.S. Linsley, and M.A. Cleary, *MicroRNAs in the miR-106b family regulate p21/CDKN1A and promote cell cycle progression.* Mol Cell Biol, 2008. **28**(7): p. 2167-74.

185. Pickering, M.T., B.M. Stadler, and T.F. Kowalik, *miR-17 and miR-20a temper an E2F1-induced G1 checkpoint to regulate cell cycle progression.* Oncogene, 2009. **28**(1): p. 140-5.

186. Fontana, L., E. Pelosi, P. Greco, S. Racanicchi, U. Testa, F. Liuzzi, C.M. Croce, E. Brunetti, F. Grignani, and C. Peschle, *MicroRNAs 17-5p-20a-106a control monocytopoiesis through AML1 targeting and M-CSF receptor upregulation.* Nat Cell Biol, 2007. **9**(7): p. 775-87.

187. Chen, B., S. She, D. Li, Z. Liu, X. Yang, Z. Zeng, and F. Liu, *Role of miR-19a targeting TNF-alpha in mediating ulcerative colitis.* Scand J Gastroenterol, 2013. **48**(7): p. 815-24.

188. Liu, M., Z. Wang, S. Yang, W. Zhang, S. He, C. Hu, H. Zhu, L. Quan, J. Bai, and N. Xu, *TNF-alpha is a novel target of miR-19a.* Int J Oncol, 2011. **38**(4): p. 1013-22.

189. Mavrakis, K.J., A.L. Wolfe, E. Oricchio, T. Palomero, K. de Keersmaecker, K. McJunkin, J. Zuber, T. James, A.A. Khan, C.S. Leslie, J.S. Parker, P.J. Paddison, W. Tam, A. Ferrando, and H.G. Wendel, *Genome-wide RNA-mediated interference screen identifies miR-19 targets in Notch-induced T-cell acute lymphoblastic leukaemia.* Nat Cell Biol, 2010. **12**(4): p. 372-9.

190. Olive, V., M.J. Bennett, J.C. Walker, C. Ma, I. Jiang, C. Cordon-Cardo, Q.J. Li, S.W. Lowe, G.J. Hannon, and L. He, *miR-19 is a key oncogenic component of mir-17-92.* Genes Dev, 2009. **23**(24): p. 2839-49.

191. Brock, M., M. Trenkmann, R.E. Gay, S. Gay, R. Speich, and L.C. Huber, *MicroRNA-18a enhances the interleukin-6-mediated production of the acute-phase proteins fibrinogen and haptoglobin in human hepatocytes.* J Biol Chem, 2011. **286**(46): p. 40142-50.

192. van Almen, G.C., W. Verhesen, R.E. van Leeuwen, M. van de Vrie, C. Eurlings, M.W. Schellings, M. Swinnen, J.P. Cleutjens, M.A. van Zandvoort, S. Heymans, and B. Schroen, *MicroRNA-18 and microRNA-19 regulate CTGF and TSP-1 expression in age-related heart failure.* Aging Cell, 2011. **10**(5): p. 769-79.

193. Luo, Z., Y. Dai, L. Zhang, C. Jiang, Z. Li, J. Yang, J.B. McCarthy, X. She, W. Zhang, J. Ma, W. Xiong, M. Wu, J. Lu, X. Li, X. Li, J. Xiang, and G. Li, *miR-18a promotes malignant progression by impairing microRNA biogenesis in nasopharyngeal carcinoma.* Carcinogenesis, 2013. **34**(2): p. 415-25.

194. Ohyagi-Hara, C., K. Sawada, S. Kamiura, Y. Tomita, A. Isobe, K. Hashimoto, Y. Kinose, S. Mabuchi, T. Hisamatsu, T. Takahashi, K. Kumasawa, S. Nagata, K. Morishige, E. Lengyel, H. Kurachi, and T. Kimura, *miR-92a inhibits peritoneal dissemination of ovarian cancer cells by inhibiting integrin alpha5 expression.* Am J Pathol, 2013. **182**(5): p. 1876-89.

195. Ghosh, A.K., T.D. Shanafelt, A. Cimmino, C. Taccioli, S. Volinia, C.G. Liu, G.A. Calin, C.M. Croce, D.A. Chan, A.J. Giaccia, C. Secreto, L.E. Wellik, Y.K. Lee, D. Mukhopadhyay, and N.E. Kay, *Aberrant regulation of pVHL levels by microRNA promotes the HIF/VEGF axis in CLL B cells.* Blood, 2009. **113**(22): p. 5568-74.

196. Rao, E., C. Jiang, M. Ji, X. Huang, J. Iqbal, G. Lenz, G. Wright, L.M. Staudt, Y. Zhao, T.W. McKeithan, W.C. Chan, and K. Fu, *The miRNA-17 approximately 92 cluster mediates chemoresistance and enhances tumor growth in mantle cell lymphoma via PI3K/AKT pathway activation.* Leukemia, 2012. **26**(5): p. 1064-72.

197. Niu, H., K. Wang, A. Zhang, S. Yang, Z. Song, W. Wang, C. Qian, X. Li, Y. Zhu, and Y. Wang, *miR-92a is a critical regulator of the apoptosis pathway in glioblastoma with inverse expression of BCL2L11.* Oncol Rep, 2012. **28**(5): p. 1771-7.

198. Li, H. and B.B. Yang, *Stress response of glioblastoma cells mediated by miR-17-5p targeting PTEN and the passenger strand miR-17-3p targeting MDM2.* Oncotarget, 2012. **3**(12): p. 1653-68.

199. Mouw, J.K., Y. Yui, L. Damiano, R.O. Bainer, J.N. Lakins, I. Acerbi, G. Ou, A.C. Wijekoon, K.R. Levental, P.M. Gilbert, E.S. Hwang, Y.Y. Chen, and V.M. Weaver, *Tissue mechanics modulate microRNA-dependent PTEN expression to regulate malignant progression.* Nat Med, 2014. **20**(4): p. 360-7.

200. Kurreck, J., *Antisense technologies. Improvement through novel chemical modifications.* Eur J Biochem, 2003. **270**(8): p. 1628-44.

201. Zhang, Y., Z. Wang, and R.A. Gemeinhart, *Progress in microRNA delivery.* J Control Release, 2013. **172**(3): p. 962-74.

202. Torres, A.G., M.M. Fabani, E. Vigorito, and M.J. Gait, *MicroRNA fate upon targeting with anti-miRNA oligonucleotides as revealed by an improved Northern-blot-based method for miRNA detection.* RNA, 2011. **17**(5): p. 933-43.

203. Deleavey, G.F. and M.J. Damha, *Designing chemically modified oligonucleotides for targeted gene silencing.* Chem Biol, 2012. **19**(8): p. 937-54.

204. Braasch, D.A., Z. Paroo, A. Constantinescu, G. Ren, O.K. Oz, R.P. Mason, and D.R. Corey, *Biodistribution of phosphodiester and phosphorothioate siRNA.* Bioorg Med Chem Lett, 2004. **14**(5): p. 1139-43.

205. DeVos, S.L. and T.M. Miller, *Antisense oligonucleotides: treating neurodegeneration at the level of RNA.* Neurotherapeutics, 2013. **10**(3): p. 486-97.

206. Altona, C. and M. Sundaralingam, *Conformational analysis of the sugar ring in nucleosides and nucleotides. A new description using the concept of pseudorotation.* J Am Chem Soc, 1972. **94**(23): p. 8205-12.

207.   Gelbin, A., B. Schneider, L. Clowney, S.-H. Hsieh, W.K. Olson, and H.M. Berman, *Geometric Parameters in Nucleic Acids: Sugar and Phosphate Constituents.* Journal of the American Chemical Society, 1996. **118**(3): p. 519-529.

208.   Judge, A.D., G. Bola, A.C. Lee, and I. MacLachlan, *Design of noninflammatory synthetic siRNA mediating potent gene silencing in vivo.* Mol Ther, 2006. **13**(3): p. 494-505.

209.   Hutvagner, G., M.J. Simard, C.C. Mello, and P.D. Zamore, *Sequence-specific inhibition of small RNA function.* PLoS Biol, 2004. **2**(4): p. E98.

210.   Meister, G., M. Landthaler, Y. Dorsett, and T. Tuschl, *Sequence-specific inhibition of microRNA- and siRNA-induced RNA silencing.* RNA, 2004. **10**(3): p. 544-50.

211.   Obika, S., D. Nanbu, Y. Hari, J.-i. Andoh, K.-i. Morio, T. Doi, and T. Imanishi, *Stability and structural features of the duplexes containing nucleoside analogues with a fixed N-type conformation, 2'-O,4'-C-methyleneribonucleosides.* Tetrahedron Letters, 1998. **39**(30): p. 5401-5404.

212.   K. Singh, S., A. A. Koshkin, J. Wengel, and P. Nielsen, *LNA (locked nucleic acids): synthesis and high-affinity nucleic acid recognition.* Chemical Communications, 1998(4): p. 455-456.

213.   Frieden, M. and H. Orum, *Locked nucleic acid holds promise in the treatment of cancer.* Curr Pharm Des, 2008. **14**(11): p. 1138-42.

214.   Vester, B. and J. Wengel, *LNA (locked nucleic acid): high-affinity targeting of complementary RNA and DNA.* Biochemistry, 2004. **43**(42): p. 13233-41.

215.   Petersen, M., C.B. Nielsen, K.E. Nielsen, G.A. Jensen, K. Bondensgaard, S.K. Singh, V.K. Rajwanshi, A.A. Koshkin, B.M. Dahl, J. Wengel, and J.P. Jacobsen, *The conformations of locked nucleic acids (LNA).* J Mol Recognit, 2000. **13**(1): p. 44-53.

216.   McTigue, P.M., R.J. Peterson, and J.D. Kahn, *Sequence-dependent thermodynamic parameters for locked nucleic acid (LNA)-DNA duplex formation.* Biochemistry, 2004. **43**(18): p. 5388-405.

217.   SantaLucia, J., Jr., *A unified view of polymer, dumbbell, and oligonucleotide DNA nearest-neighbor thermodynamics.* Proc Natl Acad Sci U S A, 1998. **95**(4): p. 1460-5.

218. Crinelli, R., M. Bianchi, L. Gentilini, and M. Magnani, *Design and characterization of decoy oligonucleotides containing locked nucleic acids.* Nucleic Acids Res, 2002. **30**(11): p. 2435-43.

219. Elmen, J., H. Thonberg, K. Ljungberg, M. Frieden, M. Westergaard, Y. Xu, B. Wahren, Z. Liang, H. Orum, T. Koch, and C. Wahlestedt, *Locked nucleic acid (LNA) mediated improvements in siRNA stability and functionality.* Nucleic Acids Res, 2005. **33**(1): p. 439-47.

220. Swayze, E.E., A.M. Siwkowski, E.V. Wancewicz, M.T. Migawa, T.K. Wyrzykiewicz, G. Hung, B.P. Monia, and C.F. Bennett, *Antisense oligonucleotides containing locked nucleic acid improve potency but cause significant hepatotoxicity in animals.* Nucleic Acids Res, 2007. **35**(2): p. 687-700.

221. Soutschek, J., A. Akinc, B. Bramlage, K. Charisse, R. Constien, M. Donoghue, S. Elbashir, A. Geick, P. Hadwiger, J. Harborth, M. John, V. Kesavan, G. Lavine, R.K. Pandey, T. Racie, K.G. Rajeev, I. Rohl, I. Toudjarska, G. Wang, S. Wuschko, D. Bumcrot, V. Koteliansky, S. Limmer, M. Manoharan, and H.P. Vornlocher, *Therapeutic silencing of an endogenous gene by systemic administration of modified siRNAs.* Nature, 2004. **432**(7014): p. 173-8.

222. Peng, L., H. Minbo, C. Fang, L. Xi, and Z. Chaocan, *The interaction between cholesterol and human serum albumin.* Protein Pept Lett, 2008. **15**(4): p. 360-4.

223. Brown, M.S. and J.L. Goldstein, *The receptor model for transport of cholesterol in plasma.* Ann N Y Acad Sci, 1985. **454**: p. 178-82.

224. Wolfrum, C., S. Shi, K.N. Jayaprakash, M. Jayaraman, G. Wang, R.K. Pandey, K.G. Rajeev, T. Nakayama, K. Charrise, E.M. Ndungo, T. Zimmermann, V. Koteliansky, M. Manoharan, and M. Stoffel, *Mechanisms and optimization of in vivo delivery of lipophilic siRNAs.* Nat Biotechnol, 2007. **25**(10): p. 1149-57.

225. Esau, C., X. Kang, E. Peralta, E. Hanson, E.G. Marcusson, L.V. Ravichandran, Y. Sun, S. Koo, R.J. Perera, R. Jain, N.M. Dean, S.M. Freier, C.F. Bennett, B. Lollo, and R. Griffey, *MicroRNA-143 regulates adipocyte differentiation.* J Biol Chem, 2004. **279**(50): p. 52361-5.

226. Davis, S., B. Lollo, S. Freier, and C. Esau, *Improved targeting of miRNA with antisense oligonucleotides.* Nucleic Acids Res, 2006. **34**(8): p. 2294-304.

227. Lennox, K.A. and M.A. Behlke, *A direct comparison of anti-microRNA oligonucleotide potency.* Pharm Res, 2010. **27**(9): p. 1788-99.

228. Fabani, M.M. and M.J. Gait, *miR-122 targeting with LNA/2'-O-methyl oligonucleotide mixmers, peptide nucleic acids (PNA), and PNA-peptide conjugates.* RNA, 2008. **14**(2): p. 336-46.

229. Davis, S., S. Propp, S.M. Freier, L.E. Jones, M.J. Serra, G. Kinberger, B. Bhat, E.E. Swayze, C.F. Bennett, and C. Esau, *Potent inhibition of microRNA in vivo without degradation.* Nucleic Acids Res, 2009. **37**(1): p. 70-7.

230. Obad, S., C.O. dos Santos, A. Petri, M. Heidenblad, O. Broom, C. Ruse, C. Fu, M. Lindow, J. Stenvang, E.M. Straarup, H.F. Hansen, T. Koch, D. Pappin, G.J. Hannon, and S. Kauppinen, *Silencing of microRNA families by seed-targeting tiny LNAs.* Nat Genet, 2011. **43**(4): p. 371-8.

231. Rottiers, V., S. Obad, A. Petri, R. McGarrah, M.W. Lindholm, J.C. Black, S. Sinha, R.J. Goody, M.S. Lawrence, A.S. deLemos, H.F. Hansen, S. Whittaker, S. Henry, R. Brookes, S.H. Najafi-Shoushtari, R.T. Chung, J.R. Whetstine, R.E. Gerszten, S. Kauppinen, and A.M. Naar, *Pharmacological inhibition of a microRNA family in nonhuman primates by a seed-targeting 8-mer antimiR.* Sci Transl Med, 2013. **5**(212): p. 212ra162.

232. Krutzfeldt, J., S. Kuwajima, R. Braich, K.G. Rajeev, J. Pena, T. Tuschl, M. Manoharan, and M. Stoffel, *Specificity, duplex degradation and subcellular localization of antagomirs.* Nucleic Acids Res, 2007. **35**(9): p. 2885-92.

233. Krutzfeldt, J., N. Rajewsky, R. Braich, K.G. Rajeev, T. Tuschl, M. Manoharan, and M. Stoffel, *Silencing of microRNAs in vivo with 'antagomirs'.* Nature, 2005. **438**(7068): p. 685-9.

234. Velu, C.S., A. Chaubey, J.D. Phelan, S.R. Horman, M. Wunderlich, M.L. Guzman, A.G. Jegga, N.J. Zeleznik-Le, J. Chen, J.C. Mulloy, J.A. Cancelas, C.T. Jordan, B.J. Aronow, G. Marcucci, B. Bhat, B. Gebelein, and H.L. Grimes, *Therapeutic antagonists of microRNAs deplete leukemia-initiating cell activity.* J Clin Invest, 2014. **124**(1): p. 222-36.

235. Velu, C.S. and H.L. Grimes, *Utilizing antagomiR (antisense microRNA) to knock down microRNA in murine bone marrow cells.* Methods Mol Biol, 2012. **928**: p. 185-95.

236. Matsuo, Y., R.A. MacLeod, C.C. Uphoff, H.G. Drexler, C. Nishizaki, Y. Katayama, G. Kimura, N. Fujii, E. Omoto, M. Harada, and K. Orita, *Two acute monocytic leukemia (AML-M5a) cell lines (MOLM-13 and MOLM-14) with interclonal phenotypic heterogeneity showing MLL-AF9 fusion resulting from an occult chromosome insertion, ins(11;9)(q23;p22p23).* Leukemia, 1997. **11**(9): p. 1469-77.

237. Tsuchiya, S., M. Yamabe, Y. Yamaguchi, Y. Kobayashi, T. Konno, and K. Tada, *Establishment and characterization of a human acute monocytic leukemia cell line (THP-1).* Int J Cancer, 1980. **26**(2): p. 171-6.

238. Stong, R.C., S.J. Korsmeyer, J.L. Parkin, D.C. Arthur, and J.H. Kersey, *Human acute leukemia cell line with the t(4;11) chromosomal rearrangement exhibits B lineage and monocytic characteristics.* Blood, 1985. **65**(1): p. 21-31.

239. Lange, B., M. Valtieri, D. Santoli, D. Caracciolo, F. Mavilio, I. Gemperlein, C. Griffin, B. Emanuel, J. Finan, P. Nowell, and et al., *Growth factor requirements of childhood acute leukemia: establishment of GM-CSF-dependent cell lines.* Blood, 1987. **70**(1): p. 192-9.

240. Sundstrom, C. and K. Nilsson, *Establishment and characterization of a human histiocytic lymphoma cell line (U-937).* Int J Cancer, 1976. **17**(5): p. 565-77.

241. Birnie, G.D., *The HL60 cell line: a model system for studying human myeloid cell differentiation.* Br J Cancer Suppl, 1988. **9**: p. 41-5.

242. Graham, F.L., J. Smiley, W.C. Russell, and R. Nairn, *Characteristics of a human cell line transformed by DNA from human adenovirus type 5.* J Gen Virol, 1977. **36**(1): p. 59-74.

243. Deneault, E., S. Cellot, A. Faubert, J.P. Laverdure, M. Frechette, J. Chagraoui, N. Mayotte, M. Sauvageau, S.B. Ting, and G. Sauvageau, *A functional screen to identify novel effectors of hematopoietic stem cell activity.* Cell, 2009. **137**(2): p. 369-79.

244. Risner, L.E., A. Kuntimaddi, A.A. Lokken, N.J. Achille, N.W. Birch, K. Schoenfelt, J.H. Bushweller, and N.J. Zeleznik-Le, *Functional specificity of CpG DNA-binding CXXC domains in mixed lineage leukemia.* J Biol Chem, 2013. **288**(41): p. 29901-10.

245. Schmittgen, T.D. and K.J. Livak, *Analyzing real-time PCR data by the comparative C(T) method.* Nat Protoc, 2008. **3**(6): p. 1101-8.

246. Chen, P., C. Price, Z. Li, Y. Li, D. Cao, A. Wiley, C. He, S. Gurbuxani, R.B. Kunjamma, H. Huang, X. Jiang, S. Arnovitz, M. Xu, G.M. Hong, A.G. Elkahloun, M.B. Neilly, M. Wunderlich, R.A. Larson, M.M. Le Beau, J.C. Mulloy, P.P. Liu, J.D. Rowley, and J. Chen, *miR-9 is an essential oncogenic microRNA specifically overexpressed in mixed lineage leukemia-rearranged leukemia.* Proc Natl Acad Sci U S A, 2013. **110**(28): p. 11511-6.

247. Velu, C.S., A.M. Baktula, and H.L. Grimes, *Gfi1 regulates miR-21 and miR-196b to control myelopoiesis.* Blood, 2009. **113**(19): p. 4720-8.

248. Jiang, X., H. Huang, Z. Li, C. He, Y. Li, P. Chen, S. Gurbuxani, S. Arnovitz, G.M. Hong, C. Price, H. Ren, R.B. Kunjamma, M.B. Neilly, J. Salat, M. Wunderlich, R.K. Slany, Y. Zhang, R.A. Larson, M.M. Le Beau, J.C. Mulloy, J.D. Rowley, and J. Chen, *MiR-495 is a tumor-suppressor microRNA down-regulated in MLL-rearranged leukemia.* Proc Natl Acad Sci U S A, 2012. **109**(47): p. 19397-402.

249. Jiang, X., H. Huang, Z. Li, Y. Li, X. Wang, S. Gurbuxani, P. Chen, C. He, D. You, S. Zhang, J. Wang, S. Arnovitz, A. Elkahloun, C. Price, G.M. Hong, H. Ren, R.B. Kunjamma, M.B. Neilly, J.M. Matthews, M. Xu, R.A. Larson, M.M. Le Beau, R.K. Slany, P.P. Liu, J. Lu, J. Zhang, C. He, and J. Chen, *Blockade of miR-150 maturation by MLL-fusion/MYC/LIN-28 is required for MLL-associated leukemia.* Cancer Cell, 2012. **22**(4): p. 524-35.

250. Bousquet, M., G. Zhuang, C. Meng, W. Ying, P.S. Cheruku, A.T. Shie, S. Wang, G. Ge, P. Wong, G. Wang, S. Safe, and B. Zhou, *miR-150 blocks MLL-AF9-associated leukemia through oncogene repression.* Mol Cancer Res, 2013. **11**(8): p. 912-22.

251. Broderick, J.A., W.E. Salomon, S.P. Ryder, N. Aronin, and P.D. Zamore, *Argonaute protein identity and pairing geometry determine cooperativity in mammalian RNA silencing.* RNA, 2011. **17**(10): p. 1858-69.

252. Saetrom, P., B.S. Heale, O. Snove, Jr., L. Aagaard, J. Alluin, and J.J. Rossi, *Distance constraints between microRNA target sites dictate efficacy and cooperativity.* Nucleic Acids Res, 2007. **35**(7): p. 2333-42.

253. Rinck, A., M. Preusse, B. Laggerbauer, H. Lickert, S. Engelhardt, and F.J. Theis, *The human transcriptome is enriched for miRNA-binding sites located in cooperativity-permitting distance.* RNA Biol, 2013. **10**(7): p. 1125-35.

254. Nicoloso, M.S., H. Sun, R. Spizzo, H. Kim, P. Wickramasinghe, M. Shimizu, S.E. Wojcik, J. Ferdin, T. Kunej, L. Xiao, S. Manoukian, G. Secreto, F. Ravagnani, X. Wang, P. Radice, C.M. Croce, R.V. Davuluri, and G.A. Calin, *Single-nucleotide polymorphisms inside microRNA target sites influence tumor susceptibility.* Cancer Res, 2010. **70**(7): p. 2789-98.

255. Jazdzewski, K., E.L. Murray, K. Franssila, B. Jarzab, D.R. Schoenberg, and A. de la Chapelle, *Common SNP in pre-miR-146a decreases mature miR expression and predisposes to papillary thyroid carcinoma.* Proc Natl Acad Sci U S A, 2008. **105**(20): p. 7269-74.

256.   Chin, L.J., E. Ratner, S. Leng, R. Zhai, S. Nallur, I. Babar, R.U. Muller, E. Straka, L. Su, E.A. Burki, R.E. Crowell, R. Patel, T. Kulkarni, R. Homer, D. Zelterman, K.K. Kidd, Y. Zhu, D.C. Christiani, S.A. Belinsky, F.J. Slack, and J.B. Weidhaas, *A SNP in a let-7 microRNA complementary site in the KRAS 3' untranslated region increases non-small cell lung cancer risk.* Cancer Res, 2008. **68**(20): p. 8535-40.

257.   Xiao, C., L. Srinivasan, D.P. Calado, H.C. Patterson, B. Zhang, J. Wang, J.M. Henderson, J.L. Kutok, and K. Rajewsky, *Lymphoproliferative disease and autoimmunity in mice with increased miR-17-92 expression in lymphocytes.* Nat Immunol, 2008. **9**(4): p. 405-14.

258.   Brockway, S. and N.J. Zeleznik-Le, *WEE1 is a validated target of the microRNA miR-17-92 cluster in leukemia.* Cancer Genet, 2015. **208**(5): p. 279-87.

259.   Zhuang, G., C. Meng, X. Guo, P.S. Cheruku, L. Shi, H. Xu, H. Li, G. Wang, A.R. Evans, S. Safe, C. Wu, and B. Zhou, *A novel regulator of macrophage activation: miR-223 in obesity-associated adipose tissue inflammation.* Circulation, 2012. **125**(23): p. 2892-903.

260.   Johnnidis, J.B., M.H. Harris, R.T. Wheeler, S. Stehling-Sun, M.H. Lam, O. Kirak, T.R. Brummelkamp, M.D. Fleming, and F.D. Camargo, *Regulation of progenitor cell proliferation and granulocyte function by microRNA-223.* Nature, 2008. **451**(7182): p. 1125-9.

261.   Fazi, F., A. Rosa, A. Fatica, V. Gelmetti, M.L. De Marchis, C. Nervi, and I. Bozzoni, *A minicircuitry comprised of microRNA-223 and transcription factors NFI-A and C/EBPalpha regulates human granulopoiesis.* Cell, 2005. **123**(5): p. 819-31.

262.   Eyholzer, M., S. Schmid, J.A. Schardt, S. Haefliger, B.U. Mueller, and T. Pabst, *Complexity of miR-223 regulation by CEBPA in human AML.* Leuk Res, 2010. **34**(5): p. 672-6.

263.   Harris, A.W., C.A. Pinkert, M. Crawford, W.Y. Langdon, R.L. Brinster, and J.M. Adams, *The E mu-myc transgenic mouse. A model for high-incidence spontaneous lymphoma and leukemia of early B cells.* J Exp Med, 1988. **167**(2): p. 353-71.

264.   Iotti, G., S. Mejetta, L. Modica, D. Penkov, M. Ponzoni, and F. Blasi, *Reduction of Prep1 levels affects differentiation of normal and malignant B cells and accelerates Myc driven lymphomagenesis.* PLoS One, 2012. **7**(10): p. e48353.

265.   Fantini, S., V. Salsi, A. Vitobello, F.M. Rijli, and V. Zappavigna, *MicroRNA-196b is transcribed from an autonomous promoter and is directly regulated by Cdx2 and by posterior Hox proteins during embryogenesis.* Biochim Biophys Acta, 2015. **1849**(8): p. 1066-80.

266.   Morgan, R., P.M. Pirard, L. Shears, J. Sohal, R. Pettengell, and H.S. Pandha, *Antagonism of HOX/PBX dimer formation blocks the in vivo proliferation of melanoma.* Cancer Res, 2007. **67**(12): p. 5806-13.

267.   Daniels, T.R., Neacato, II, J.A. Rodriguez, H.S. Pandha, R. Morgan, and M.L. Penichet, *Disruption of HOX activity leads to cell death that can be enhanced by the interference of iron uptake in malignant B cells.* Leukemia, 2010. **24**(9): p. 1555-65.

268.   Seita, J., D. Sahoo, D.J. Rossi, D. Bhattacharya, T. Serwold, M.A. Inlay, L.I. Ehrlich, J.W. Fathman, D.L. Dill, and I.L. Weissman, *Gene Expression Commons: an open platform for absolute gene expression profiling.* PLoS One, 2012. **7**(7): p. e40321.

VITA

Yousaf Anwar Mian was born on August 14,1982 in Elgin, IL to Vera and Muhammad Mian. He was raised in Roselle, IL and attended Lake Park High School, graduating in 2000. Yousaf attended Loyola University Chicago on a Presidential Scholarship for his undergraduate degrees, earning a BS in Biology and BA in History, as well as a minor in Chemistry, graduating as part of the class of 2004. As an undergraduate, Yousaf was a member of the Historical Honors Society and studied abroad at the University of Birmingham in Birmingham, UK.

After graduation, Yousaf joined the lab of Dr. Hamid Band, M.D., Ph.D. at Evanston Northwestern Healthcare in Evanston, IL as a Research assistant, studying the Notch signalling under Dr. Aharon Solomon, Ph.D. in a *C. elegans* model. Upon the close of this project, Yousaf joined the lab of Dr. Vimla Band, Ph.D., studying the role ADA3 in breast cancer development through the generation and phenotyping of ADA3 knockout mice, under the guidance of Dr. Alo Nag, Ph.D. As the lab moved to the University of Nebraska Medical Center in Omaha, Nebraska, Yousaf continued to work on the ADA3 project under the guidance of Dr. Chanabasavaiah Gurumurthy, D.V.M., Ph.D.

In August 2008, Yousaf matriculated to Loyola University Chicago to continue his studies with the goal of earning a PhD. He entered Loyola University Chicago as a student within the Integrated Program in Biomedical Science (IPBS). Yousaf joined the

185

lab of Dr. Nancy Zeleznik-Le, Ph.D. and joined the Program in Molecular Biology.

Yousaf currently lives in the West Loop of Chicago, IL with his dog Hudson Theodore Puppington, III. Upon graduation, Yousaf intends on seeking a post-doctoral fellowship to continue his scientific training.